The study of senescent cells using the single cell RNA sequencing

Yuta Doshida

Department of Biological Sciences

Tokyo Metropolitan University

2022

Table of contents

Abstract

Aging is the passage of physical time from birth to death. Senescence is the decline in physiological functions with age. The biological mechanisms of senescence remain to be explained. It is predicted that senescent cells with lower physiological functions will appear and increase in animal tissues and organs with age. Analyses of senescent cells are expected to contribute to a better understanding of the biological mechanisms of senescence. The property of observations about senescent cells is still unclear such as tissue distributions on an aged animal and how many kinds of senescent cells exist. As for characteristics of senescent cells, Richard G. Cutler proposed a hypothesis that the decline in physiological functions of organs and cells is due to the age-associated destabilization of strict regulations of gene expressions in cells [1]. A phenomenon explaining this hypothesis is predicted to be an age-associated change of epigenetics, which is the regulatory mechanisms of gene expression without alterations in DNA sequence.

Adipose-derived stem cells (ASCs) are mesenchymal stem cells in adipose tissue and are expected to be applied to regenerative therapies due to their multipotency. It was unclear whether ASCs derived from an aged animal had the same level of differentiation potential as ASCs derived from young animals. The stromal vascular fraction (SVF) is a cell population containing ASCs, adipocytes, and lymphocytes and can be obtained from the enzymic digestion of adipose tissue. ASCs used in regenerative therapies are isolated by subcultures of SVFs obtained from the adipose tissue of a patient. However, because properties of ASCs are easily changed depending on the culture medium components, gene expressions of ASCs may be significantly altered during a few days of subculture. Single cell RNA sequencing (scRNA-seq), which can comprehensively quantify transcripts of individual cells, is a valuable method to analyze and identify senescent cells specifically from a cell population. In this study, to examine age-associated changes in gene

expression of non-cultured ASCs, scRNA-seq was performed using SVFs which were obtained from 6-month-old (young) and 29-month-old (old) C57BL/6 male mice without subcultures, were compared between young and old.

Comprehensive gene expression on individual SVFs of young and old mice was analyzed using Seurat, software to analyze scRNA-seq data. The cell populations consisting of 1,286 cells obtained from both young and old mice were then classified into eleven groups (Group 0 to 10) based on their gene expression patterns. Three groups (Group 1, 3, and 5) of eleven groups were specified as ASCs because of the high expression levels of typical ASC marker genes. Based on gene expression patterns, it was estimated that three ASC groups were at different stages of differentiation. To validate this estimation, I extracted the gene expression data of Group 3 and 5 that differed significantly in expression and re-analyzed them using Monocle3, an analysis software like Seurat. Then, genes that showed the most difference in expression levels between Group 3 and Group5, were identified and subjected to the gene ontology analysis to extract characteristic annotation information. As the result of gene ontology analysis, negative regulator genes for differentiation, *Adamts7*, *Snai2,* and *Tgfbr1*, were found. *Adamts7* is a metalloprotease that inhibits differentiation into chondrocytes via inactivation of the growth factor progranulin. *Snai2* is a transcription factor involved in maintaining the differential potential of stem cells. *Tgfbr1* is a receptor of TGF-β and inhibits the differentiation of rat bone marrow stromal cells into osteoblasts. Next, I performed the pseudotime analysis, which represents gene expression changes as the lapse of time. The gene expression of *Adamts7*, *Snai2*, and *Tgfbr1* decreased with pseudotime course, suggesting that Group 3 is at the earliest differentiation stage of ASCs, while Group 5 is at the most advanced differentiation stage of ASCs. Moreover, the pattern of gene expression changes of *Adamts7* with pseudotime course was different between young and old mouse ASCs. This suggests that old mouse ASCs have less stringency of the regulation of the

expression of some genes involved in ASCs differentiation than young mouse ASCs and may have difficulty to progress differentiation as needed. This suggestion is consistent with the hypothesis proposed by Richard G. Cutler. Because it is the function of ASCs to differentiate as needed correctly, it is considered that ASCs that have less stringency of the regulation of some gene expressions involved in differentiation are senescent cells.

Results obtained from this study suggested that the differentiation potential of old mouse ASCs is less than that of young mouse ASCs. Additional studies are needed to conclude whether the differentiation potential of elderly people declines with age similar to that of mice. However, the observations obtained from this study could contribute to understanding age-associated changes of ASCs. In developed countries with a high percentage of the elderly population, it is hoped to extend the healthy life expectancy, which is the period when a person can live independently without limitations in daily life due to health problems. Recently, many researchers have been trying to develop senolytic drugs, which specifically induce apoptosis in senescent cells. It is expected to extend healthy life expectancy using senolytic drugs. Based on this background, I would like to develop senolytic drugs targeting senescent cells of ASCs. However, it is unsuitable to use *Adamts7* as the target of senolytic drugs because both young and old mouse ASCs express *Adamts7*. The age-associated changes of epigenetics are supposed to be one of the factors that destabilize the regulation of gene expression. Therefore, I focus on epigenetics as candidates for the target of senolytic drugs. In the future, I would like to identify the epigenetics characteristics of senescent cells of ASCs and develop senolytic drugs targeting identified those. I hope that the development of senolytic drugs would contribute to the extension of healthy life expectancy and the elucidation of biological mechanisms of senescence.

Abbreviations

Adamts7, disintegrin-like and metallopeptidase (reprolysin type) with thrombospondin type 1 motif, 7; Agt, angiotensinogen (serpin peptidase inhibitor, clade A, member 8); Bgn, biglycan; Ccl3, chemokine (C-C motif) ligand 3; Ccl4, chemokine (C-C motif) ligand 4; Ccl6, chemokine (C-C motif) ligand 6; Ccl11, chemokine (C-C motif) ligand 11; CCND1, cyclin D1; cDNA, complementary deoxyribonucleic acid; Cdkn1a, cyclin dependent kinase inhibitor 1A; Cdkn2a, cyclin dependent kinase inhibitor 2A; CDK2, cyclin-dependent kinase 2; CDK6, cyclin-dependent kinase 6; Cd14, CD14 antigen; Cd74, CD74 antigen (invariant polypeptide of major histocompatibility complex, class II antigen-associated); Cd79a, CD79A antigen (immunoglobulin-associated alpha); Cd79b, CD79B antigen; C/ebpα , CCAAT/enhancer-binding protein (C/EBP), alpha; CEL-Seq, Cell Expression by Linear amplification and Sequencing; Clec3b, C-type lectin domain family 3, member b; Clu, clusterin; Cma1, chymase 1, mast cell; Cma2, chymase 2, mast cell; Col1a2, collagen, type I, alpha 2; Col6a1, collagen, type VI, alpha 1; Col6a5, collagen type VI alpha 5 chain; COPI, coat protein complex I; Cpa3, carboxypeptidase A3, mast cell; Ctsb, cathepsin B; Cxcl1 , chemokine (C-X-C motif) ligand 1; Cxcl2, chemokine (C-X-C motif) ligand 2; DAVID, Database for Annotation, Visualization, and Integrated Discovery; DNMT1, DNA methyltransferase 1; Dpep1, dipeptidase 1; Drop-seq, Droplet-sequencing; Efemp1, epidermal growth factor-containing fibulin-like extracellular matrix protein 1; Egfr, epidermal growth factor receptor; Emb, embigin; Enpp2, ectonucleotide pyrophosphatase/phosphodiesterase 2; E2F1, E2F transcription factor 1; Fabp4, fatty acid binding protein 4, adipocyte; FOXO, forkhead box O; Fstl1, follistatin-like 1; GO, gene ontology; Gpx3, glutathione peroxidase 3; GSEA, Gene set enrichment analysis; Gsn, Gelsolin; HDAC6, histone deacetylase 6; HMGA1, high mobility group AT-hook 1; Hp, haptoglobin; Htra3, HtrA serine

peptidase 3; Id2, inhibitor of DNA binding 2; Igfbp4, insulin-like growth factor binding protein 4; Igfbp6, insulin-like growth factor binding protein 6; Igfbp7, insulin-like growth factor binding protein 7; IgE, Immunoglobulin E; IL-1, interleukin 1; IL-6, interleukin 6; Inmt, indolethylamine N-methyltransferase; Ldhc, lactate dehydrogenase C; Lpl, lipoprotein lipase; LPS, lipopolysaccharide; Mmp2, matrix metallopeptidase 2; Mmp3, matrix metallopeptidase 3; Mmp14, matrix metallopeptidase 14 (membrane-inserted); mRNA, messenger ribonucleic acid ; NES, normalized enrichment score; NF-κB, nuclear factor-kappa B; Nid1, nidogen 1; Pi16, peptidase inhibitor 16; PGC1α, peroxisome proliferator-activated receptor-γ coactivator-1α; POLE3, DNA polymerase epsilon 3, accessory subunit; Ppap2b, phosphatidic acid phosphatase type 2B; Pparγ, peroxisome proliferator activated receptor gamma; Ptgs2, prostaglandin-endoperoxide synthase 2; RNA-seq, RNA sequencing; SIRT1, sirtuin 1; SIRT2, sirtuin 2; Snai2, snail family zinc finger 2; SOD2, superoxide dismutase 2; Sparcl1, SPARC-like 1; Sult1e1, sulfotransferase family 1E, member 1; Tcte3, t-complex-associated testis expressed 3; TGF-β, transforming growth factor-β; Tgfbr1, transforming growth factor, beta receptor I; Thy1, thymus cell antigen 1, theta; Timp2, tissue inhibitor of metalloproteinase 2; TNF-α, tumor necrosis factor; Trp53, transformation related protein 53; TPM, transcripts per million; Tpsb2, tryptase beta 2; t-SNE, t-distributed stochastic neighbor embedding; UMAP, uniform manifold approximation and projection

Chapter 1 General introduction

Aging and senescence

Aging is the passage of physical time from birth to death. Senescence is the decline in physiological functions with age. Lifespan, the period of physical time from an animal's birth to death, contains two concepts: maximum life span, the longest period that an animal species can live; life expectancy, the average period that an animal species can live. Aging progresses at the same rate in all animals and all animal species. However, senescence progresses at different rates in individual animals and individual animal species. In human beings, the physiological functions of organs develop until about 20 years old and then decline with age (Figure 1). Aging is a chronological risk factor for many pathologies and increases the risk of various age-related diseases such as chronic kidney disease and osteoporosis [2, 3]. When people's daily lives are absorbed due to the development of age-related diseases, they become to need support from caregivers. Recently, people are focusing on healthy life expectancy, the period when a person can live in their daily lives without any limitations due to health problems such as bedridden and dementia. In developed countries with a high percentage of the elderly population, it is hoped to extend the healthy life expectancy because the longer term of care increases the burden on caregivers and society.

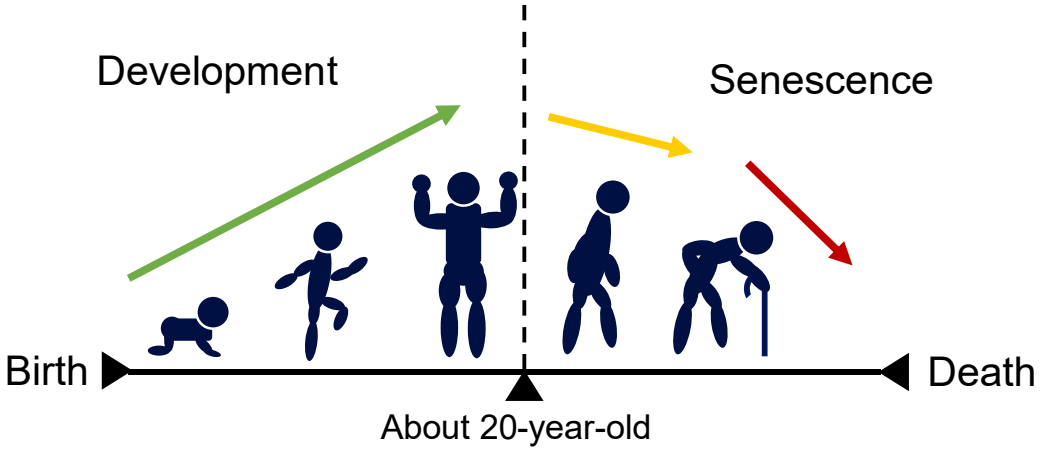

Figure 1: The physiological functions of human organs develop up to about 20 years old and then decline with age.

As the rate of development differs among individuals, the rate of senescence differs among individuals. It is considered that the progress of senescence cannot be stopped, but the rate of senescence can be slowed down by improving lifestyle or dietary habits. If the rate of senescence can be controlled through molecular approaches, the healthy life expectancy could be easily extended.

Senescence in animals and senescent cells

The physiological functions of animal tissues and organs decline with age, such as the decline of muscle strengths in skeletal muscles and cognitive decline in the brain. The biological mechanisms of senescence remain to be explained. Over 300 hypotheses about the biological mechanism of senescence have been proposed and are categorized into two: the public theory and the private theory [4, 5]. The public theory consists of hypotheses about the biological mechanism of senescence that is common to all animal species, organs, and tissues. In contrast, the private theory consists of hypotheses about the biological mechanism of senescence that is different for each animal species, organ, and tissue. The age-related occurrence and increase of senescent cells are focused on as a potent hypothesis (Figure 2) [6, 7]. Senescent cells are defined as cells whose physiological functions are declined with age. It is predicted that senescent cells are absent in young animal's bodies and occur in the bodies of animals with age. Since cells make up tissues and organs, the physiological functions of tissues are considered to decline with an increase of the number of senescent cells. However, our knowledge about the properties of senescent cells is limited.

Richard G. Cutler proposed the dysdifferentiation hypothesis of aging that aging destabilizes the stringency of regulatory mechanisms for gene expression in cells and impairs physiological functions of tissues and cells with alteration of gene expressions [1]. This hypothesis is based on the finding that expressions of globin, a globular protein constituting the hemoglobin in red blood cells, ectopically increased in brains and livers of old C57BL6 mice compared to young mice [8]. Epigenetics is a regulatory mechanism for gene expression without alterations in the DNA sequence such as DNA methylation, histone modification, and the endogenous RNA interference by microRNAs. The DNA methylation is the addition of a methyl group to the C5 position of

cytosine. The histone modification is the alteration of chromatin structures by the various post-translational modification. The patterns of DNA methylation and histone modification are reported age-associated changes and correlated with frailty and the development of various age-related diseases [9, 10]. Furthermore, studies using nematodes (*Caenorhabditis elegans*), fruit flies (*Drosophila melanogaster*), and mice (*Mus musculus*) discovered microRNAs related to the longevity and age-associated changes of microRNA expressions [11]. These age-associated changes of epigenetics can explain the idea of dysdifferentiation hypothesis of aging, in which aging destabilizes the stringency of regulatory mechanisms for gene expression.

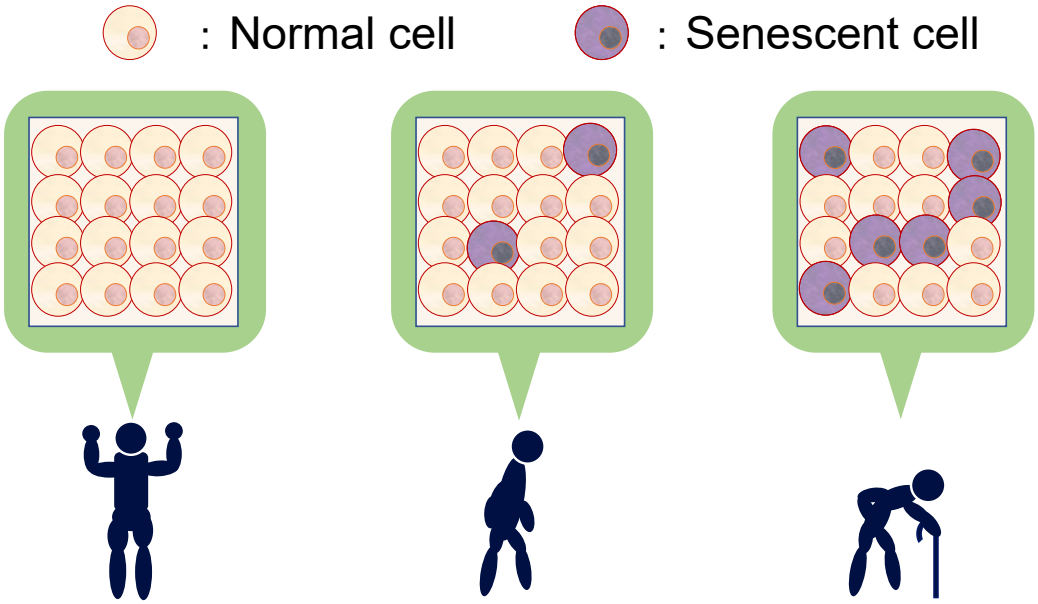

Figure 2: The number of senescent cells increases with age.

In this figure, senescent cells are colored for convenience of explanation. The distribution of senescent cells in the tissues of old animals is still unknown. Furthermore, there might be multiple types of senescent cells with entirely distinct characteristics or intermediate properties between senescent cells and normal cells (non- senescent cells).

Cellular senescence

Both the causes of senescence and the occurrence of senescent cells are still unclear, except for aging. Cellular senescence is caused by telomere shortening or severe DNA damages that exceed the capacity of DNA repair mechanisms, or both. These induce cell cycle arrest (Figure 3) [12]. This phenomenon was discovered by Leonard Hayflick in 1965 [13]. Cellular senescence could be mimicked if DNA damages were artificially induced to fibroblasts. The addition of doxorubicin, an anticancer drug that intercalates into DNA, or hydrogen peroxide, which causes oxidative damage, or irradiation of ultraviolet or ionizing radiation, are commonly used to cause DNA damage in cells or animals artificially. However, the results obtained in each study need to be carefully discussed separately for each experimental condition because observed phenotypes and various gene expressions are likely to be changed due to cells used for experiments and methods that induce DNA damage. When fibroblasts cause cellular senescence, they secrete bioactive substances such as inflammatory cytokines, chemokines, and matrix metallopeptidases. This phenomenon is called senescence-associated secretory phenotype (SASP), and secreted bioactive substances by SASP are called SASP factors (Figure 4) [14, 15]. In fibroblasts that cause cellular senescence, expressions of *cyclin dependent kinase inhibitor 2A* (*Cdkn2a*, $p16^{Ink4a}$) or *cyclin dependent kinase inhibitor 1A* (*Cdkn1a*, *p21*) increase, and $p16^{Ink4a}$ and p21 inhibit cell cycle progression (Figure 5) [16]. Inactivating gene functions associated with cellular senescence could improve physiological functions that are impaired with age and suppress SASP factors compared to untreated old mice [17]. These observations shed light on the understanding of biological mechanisms of senescence; however, many aspects of senescence are still unknown. Since cellular senescence is a phenomenon confirmed in fibroblasts, studies using senescent cells in each tissue of old animals are more important to elucidate the biological mechanisms and

phenomena of senescence. Importantly, senescent cells in the tissues of old animals are distinct from cells that caused cellular senescence.

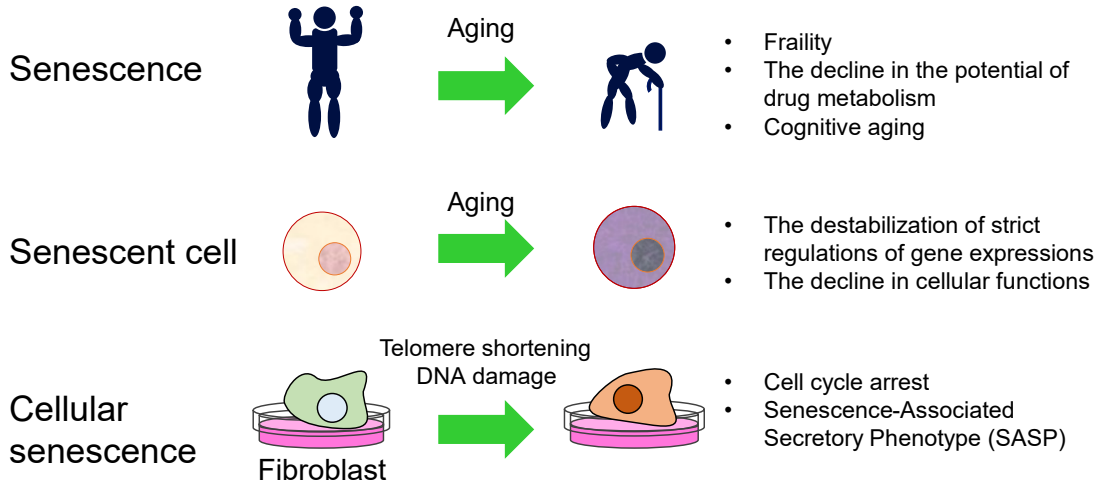

Figure 3: Differences between senescence, senescent cell, and cellular senescence.

The physiological functions of animal tissues and organs decline with age such as frailty in skeletal muscles, the decline in the potential of drug metabolism in livers, and cognitive aging in the brain. The biological mechanisms of senescence remain to be explained. Many hypotheses about the property of senescent cells have been proposed and need to be elucidated. Because cellular senescence is a phenomenon confirmed in fibroblasts, studies using senescent cells in each tissue of old animals, are more important to elucidate the biological mechanisms and phenomena of senescence than studies about cellular senescence. Importantly, senescent cells in the tissues of old animals are distinct from cells that caused cellular senescence.

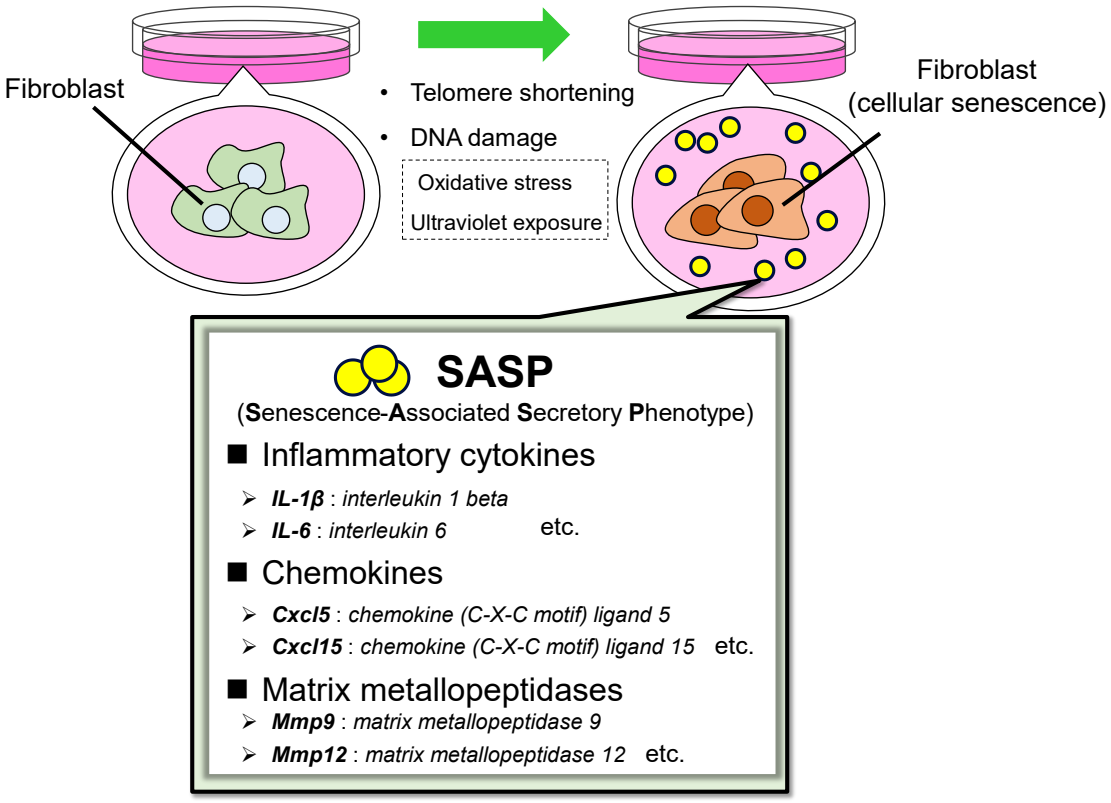

Figure 4: Senescence-associated secretory phenotype (SASP).

Fibroblasts that caused cellular senescence, secrete bioactive substances such as inflammatory cytokines, chemokines, and matrix metallopeptidases; this phenomenon is called SASP and secreted bioactive substances by SASP are called SASP factors. This figure shows representative SASP factors of inflammatory cytokines, chemokines, and matrix metallopeptidases.

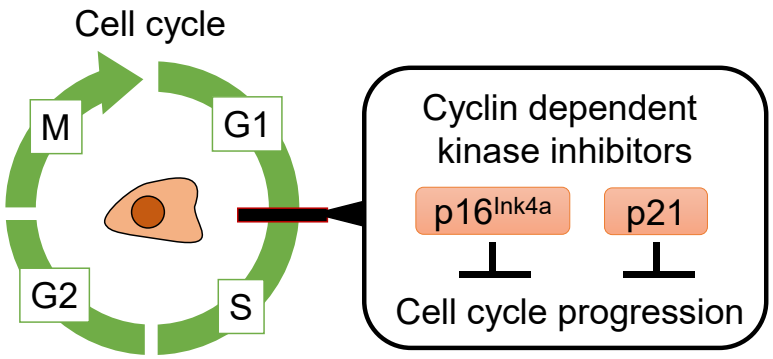

Figure 5: Cyclin dependent kinase inhibitors inhibit cell cycle progression.

In fibroblasts that cause cellular senescence, expressions of *cyclin dependent kinase inhibitor 2A* (*Cdkn2a*, *p16*^{Ink4a}) or *cyclin dependent kinase inhibitor 1A* (*Cdkn1a*, *p21*) increase, and p16^{Ink4a} and p21 inhibit cell cycle progression. *p16*^{Ink4a} is a member of splicing variants of *Cdkn2a*.

Single cell RNA sequencing (scRNA-seq)

Analyses of senescent cells are expected to contribute to understanding the biological mechanism of senescence. However, markers of senescent cells are still unknown. scRNA-seq is a method that can comprehensively determine transcripts of individual cells and is valuable to identify and specifically analyze senescent cells [18]. It is necessary to isolate dispersed cells one by one to perform scRNA-seq, which is commonly used in many studies [19]. Differences among methods of cell isolation determine the characteristics and performance of scRNA-seq. There are three main types of cell isolation methods. One of them is a method using an integrated fluidic circuit for cell isolation, and a typical example is Cell Expression by Linear amplification and Sequencing (CEL-Seq) 2 (C1) (Figure 6A) [20]. The droplet-based scRNA-seq is a method that each cell is isolated in aqueous droplets made in the oil-filled tube, and a typical example is Droplet-sequencing (Drop-seq) (Figure 6B) [21]. The microwell-based scRNA-seq is a method to isolate cells by seeding them from above into microwells with a diameter that can hold one cell (Figure 6C) [18]. Especially, the microwell-based method has three advantages compared to other methods. This method does not require large and expensive devices, this causes minimum damages to cells during isolation, this can obtain gene expression data from hundreds to thousands of cells at once [18]. Conventional methods such as microarrays and RNA-seq, which use tissue homogenates, cannot quantify gene expressions in a subset of cells from a large population [22]. In these scRNA-seq technics, the messenger ribonucleic acid (mRNA) of cells is used as a template for the synthesis of complementary deoxyribonucleic acid (cDNA), which is then used for sequence analysis.

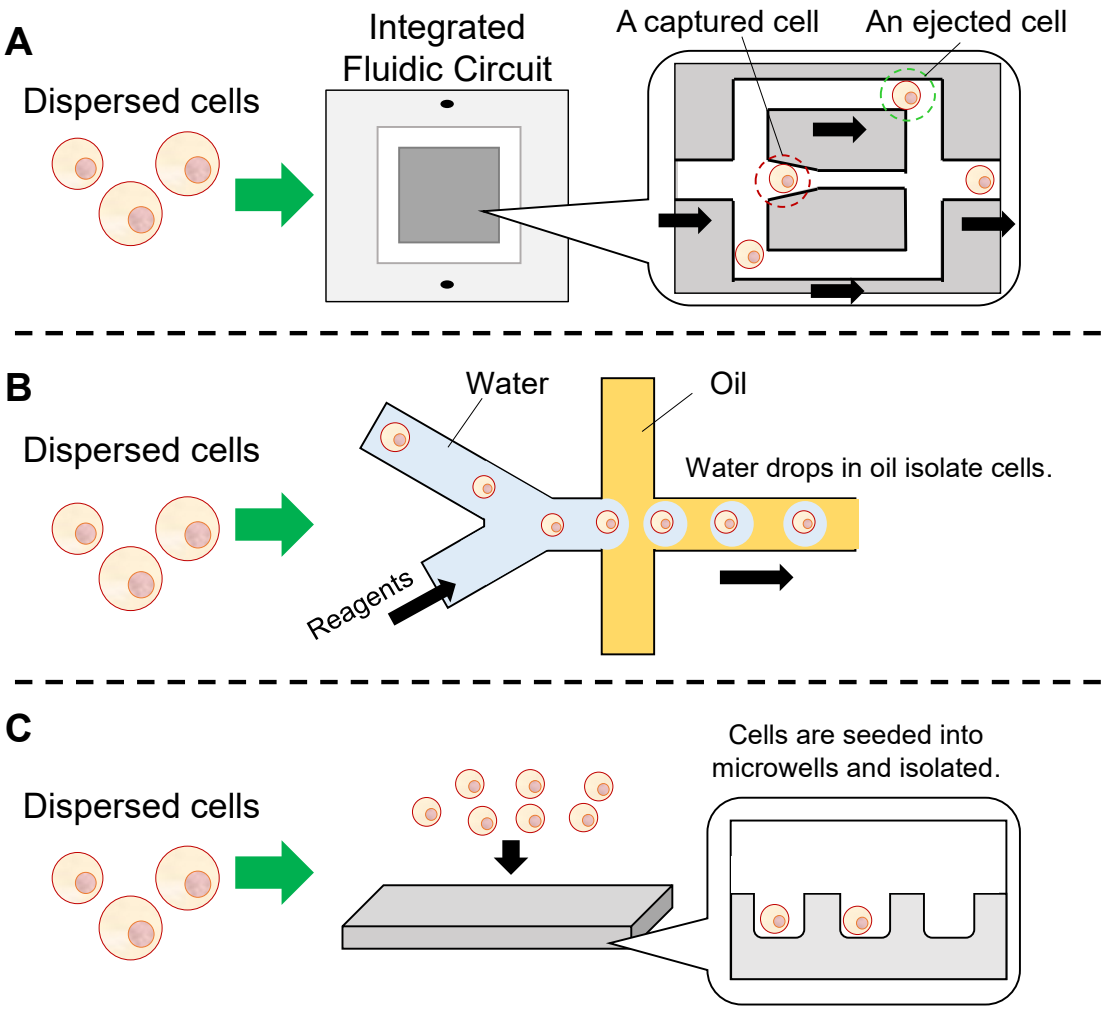

Figure 6: Three main types of cell isolation methods to perform scRNA-seq.

(A) Dispersed cells are flowed into an integrated fluid circuit to be isolated. In the integrated fluid circuit, units that capture cells are regularly aligned. When the first cell enters a unit, it is held at the central tube of a unit. Following cells cannot be held at the center tube of a unit because of the presence of the first cell and pass through the bypass tubes on both sides to move to the next unit. (B) Each cell is isolated in aqueous droplets made in the oil-filled tube. The system for the droplet-based method consists of an oil-filled tube and two aqueous tubes. The dispersed cells flow in one aqueous tube, and the reagents necessary for cDNA synthesis flow in the other aqueous tube. The flow rates of the aqueous solution and oil are strictly controlled. To process a

large number of cells in a short time, several these systems need to be simultaneously performed. (C) The microwell-based scRNA-seq is a method to isolate cells by seeding them from above into microwells with a diameter that can hold one cell. Because cells are only seeded from above, more cells can be isolated in a short time with minimum damage.

Adipose-derived stem cell (ASC)

Stem cells have pluripotency, the ability to differentiate into various cells that function in various organs, and self-renewal, the ability to replicate cells with the same characteristics. Mesenchymal stem cells in animal tissues differentiate in response to the necessity to maintain homeostasis in the body and play an essential role in supplying new cells to tissues. Adipose-derived stem cells (ASCs) are mesenchymal stem cells found in adipose tissue (Figure 7). ASCs are expected to be applied to regenerative therapies. They are being studied for clinical use because adipose tissue can be obtained from donors with minimally invasive procedures such as liposuction and surgery, and isolation of ASCs from donor's adipose tissue is easy and convenient [23-26]. In addition, ASCs can be artificially induced to differentiate into various cells such as adipocytes, chondrocytes, and osteoblasts [25, 27]. A method for isolating ASCs from adipose tissue is outlined in Figure 8 [26]. First, the intercellular adhesion of adipose tissue obtained from a donor is digested using type I collagenase. After centrifugation, adipocytes, which accumulate fat intracellularly, and fatty components move to the supernatant while other cells precipitate. This precipitate is a cell population called the stromal vascular fraction (SVF), which contains ASCs, lymphocytes, and adipocyte progenitors called preadipocytes. After the SVF cells are cultured for two to three days, only ASCs adhere to the bottom of the culture dish. Finally, isolated ASCs can be obtained.

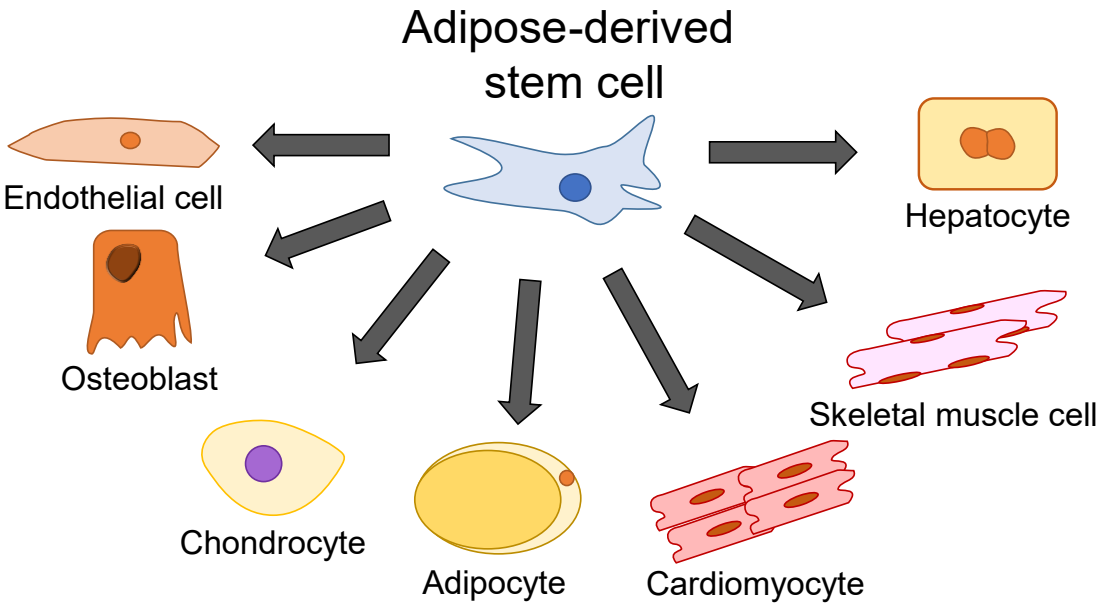

Figure 7: Adipose-derived stem cells (ASCs) are mesenchymal stem cells in adipose tissue and are expected to be applied to regenerative therapies due to their multipotency.

ASCs have multipotency, which can differentiate into endothelial cells, osteoblasts, chondrocytes, adipocytes, cardiomyocytes, skeletal muscle cells, and hepatocytes. For example, in regenerative medicine applications, stromal vascular fraction (SVF) cells obtained from a patient have been injected into damaged cartilage tissue to differentiate ASCs into chondrocytes and regenerate cartilage tissue.

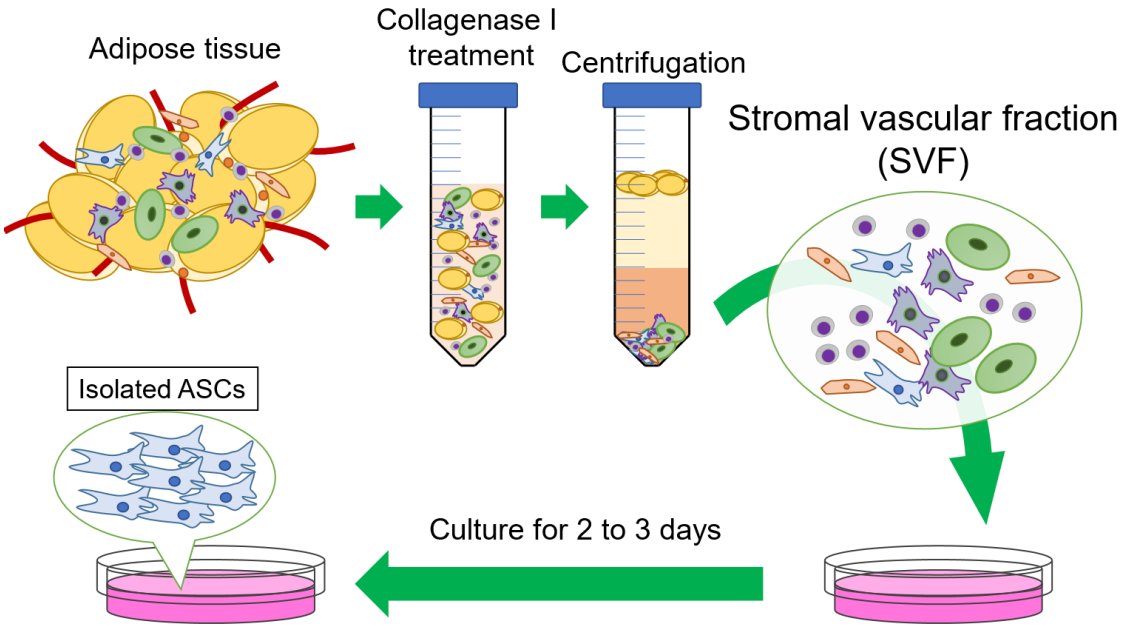

Figure 8: Isolation of ASCs from adipose tissue.

Adipose tissue obtained by liposuction or surgery from donors is mainly composed of ASCs, red blood cells, lymphocytes, endothelial cells, preadipocytes, and adipocytes [28]. First, the intercellular adhesion of adipose tissue is enzymatically digested using type I collagenase. After centrifugation, adipocytes, which accumulate fat intracellularly, and fatty components move to the supernatant while other cells precipitate. This precipitate is a cell population called the stromal vascular fraction (SVF), which contains ASCs, lymphocytes, and adipocyte progenitors called preadipocytes. After the SVF cells are cultured for two to three days, only ASCs adhere to the bottom of the culture dish. Finally, isolated ASCs can be obtained. This method is developed by Sugii *et al.* [26].

Chapter 2 Introduction

Studies using subcultured ASCs

Several studies have already been reported comparing ASCs from the elderly with those from the young [27, 29-31]. Liu *et al.* compared ASCs from three different age groups: child (6 to 12 years), young adult (22 to 27 years), elderly (60 to 73years) [27]. They reported that the differentiation and self-renewal potentials of ASCs from an age group of the elderly were reduced compared to ASCs from two age groups of the child and young adult. Maredziak *et al.* reported that proliferative efficiency and the ability to differentiate into chondrocytes and osteoblasts were reduced in ASCs from three elderly groups (57.5 ± 0.7 years, 67.0 ± 1.4 years, and 75 ± 2.8 years) compared to those from a younger group (24 ± 1.4 years) [30]. These findings indicate that the differentiation and self-renewal potentials of ASCs from the elderly are declined compared to ASCs from the young. However, these reports use ASCs that have been obtained by several times subcultures. ASCs can be artificially induced to differentiate into specific cells by culturing them in a differentiation medium (Figure 9) [25, 27]. Differentiation medium contains growth factors such as vascular endothelial growth factor and small molecules such as vitamin C and valproic acid. The culture medium components are selected according to the cells to be artificially differentiated [32]. Since properties of ASCs are easily changed depending on the culture medium components, gene expressions of ASCs may be significantly altered for a few days of subculture.

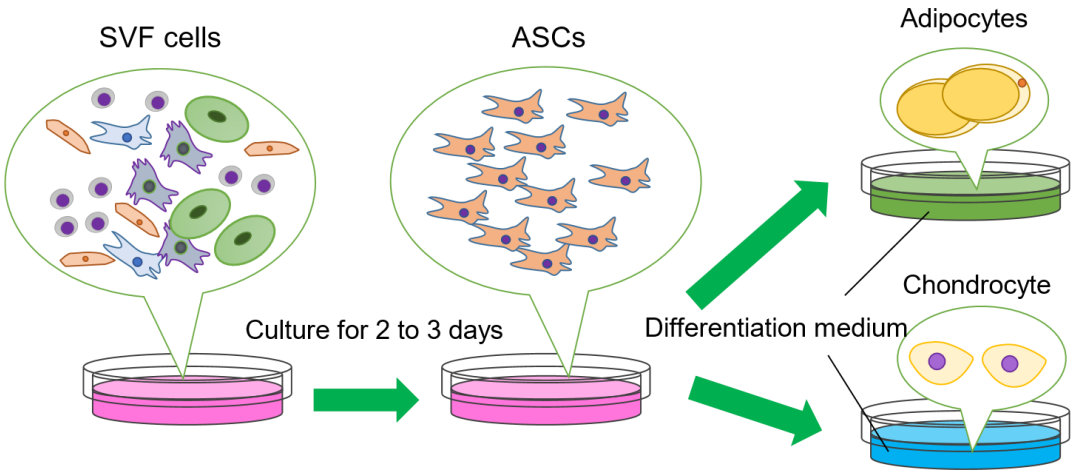

Figure 9: The properties of ASCs are easily changed by the culture medium components and culture conditions.

ASCs isolated by cultures can be artificially differentiated into specific cells by culturing them in a differentiation medium. This differentiation medium contains growth factors such as vascular endothelial growth factor and small molecules such as vitamin C and valproic acid. The culture medium components are selected according to the cells to be artificially differentiated.

Objectives in this study

Clinical studies using ASCs obtained from healthy donors to transplant to other patients are underway, but they have not yet been put to clinical use. On the other hand, the clinical use of ASCs obtained from patients for their regenerative therapies can avoid side effects such as allergy, rejection, and infection. The donors of ASCs are generally elderly because most patients who undergo regenerative therapies are also elderly. Therefore, it is important to observe whether ASCs from the elderly have the same level of differentiation and self-renewal potentials as those from the young in determining the guidelines for selecting donors for regenerative therapy. The preceding studies cannot exclude the effects that the culture has already altered gene expression in ASCs for isolation. To avoid this problem, this study examined gene expressions in the uncultured SVF cells using the microwell-based scRNA-seq to observe how the differentiation potential of ASCs alters with age (Figure 10) [33].

This study examined gene expression in the SVF cells obtained from the epididymal fat of 6- and 29-month-old male mice. The epididymal fat, a member of the visceral fat, can be obtained stably even from low weight mice, while the subcutaneous fat is difficult to be obtained from them. Sex-dependent differences in the transcriptome of visceral fat have been confirmed [34]. Therefore, this study used epididymal fat in experiments. Mice (*Mus musculus*) have been used to study senescence and gerontology, as have other model organisms, such as nematodes (*C. elegans*) and fruit flies (*Drosophila melanogaster*). Because most mice younger than 6 months are still in the process of sexual maturation and development, 6-month-old mice, which are in the first stage of aging and have completed sexual maturation and development, are considered to be suitable as young controls in aging studies using mice [35]. On the other hand, mice have a life expectancy of about 32 months [36]. Therefore, this study used healthy 29-month-old mice, which

corresponds to approximately 73-year-old in humans, and 6-month-old mice, which corresponds to approximately 15-year-old in humans, to maximize the effect of aging on ASC differentiation potential as much as possible.

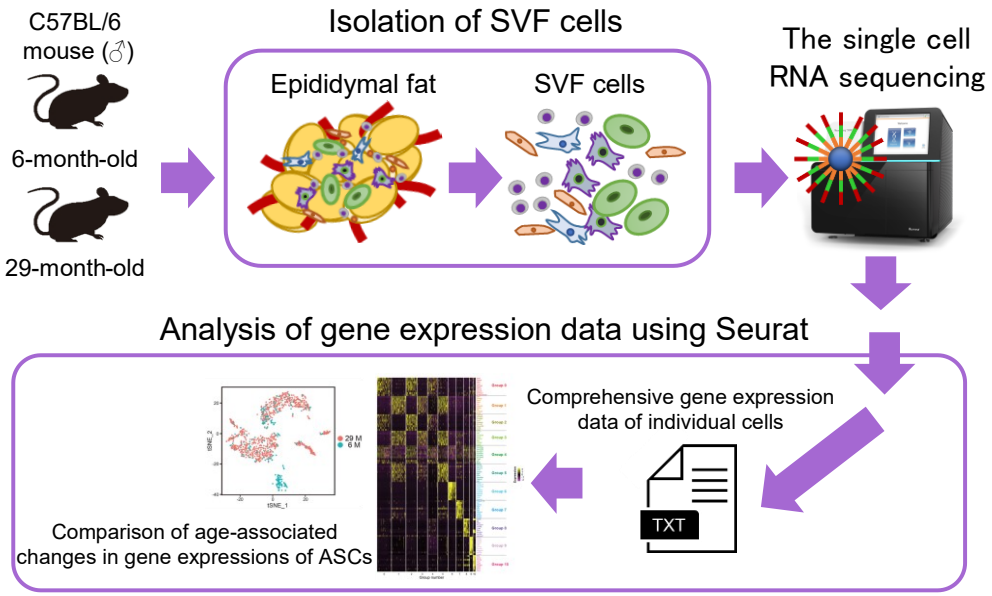

Figure 10: The workflow of comparing the gene expression in ASCs between young and old mice.

6-month-old (young) and 29-month-old (old) C57BL/6NCr male mice were sacrificed, and epididymal fat was collected. The cells were dispersed using type I collagenase and were centrifuged to obtain the SVF. The gene expression of SVF cells was examined using the microwell-based scRNA-seq. The comprehensive gene expression data obtained from individual cells were compared between young and old ASCs using the analysis software Seurat, which is commonly used to analyze data obtained by the scRNA-seq. The detailed procedures of scRNA-seq performed in this study are described in Chapter 2.

Chapter 3 Materials and methods

Animals

Animal experiments were performed in accordance with the animal care and use protocol approved by the Institutional Animal Care and Use Committee of the Tokyo Metropolitan Institute of Gerontology (TMIG, Tokyo, Japan) (Permit Number: 18028) and the Guidelines for the Care and Use of Laboratory Animals of TMIG. All male mice of the C57BL/6Ncr strain were bred in an environment with free access to low-dose radiation (6 kGy) irradiated CRF-1 (Oriental Yeast Ltd., Tokyo, Japan) [37] as food and 5 μm filtered tap water containing 2 ppm chlorine as drinking water. The breeding environment was maintained at a room temperature of 22 ± 1°C and humidity of 55 ± 5% under a 12-hour light/dark cycle (light period: 8:00 - 20:00, dark period: 20:00 - 8:00) to keep animals comfortable. The number of animals used in the experiment was kept to the minimum necessary for interpretation of the data, and animal discomfort was kept to a minimum.

Isolation of SVF cells

6- and 29-month-old male mice were anesthetized using pentobarbital (Nembutal, Dainippon Sumitomo Pharma, Osaka, Japan) and isoflurane (Pfizer Inc., New York, NY, USA) and were sacrificed after confirmation of unconsciousness. Blood was removed by perfusion with phosphate-buffered saline from the left ventricle, and epididymal fat was collected. Intercellular adhesions of epididymal fat were enzymatically digested by gently agitating at 37°C for 1 hour in Hank's balanced salt solution (Gibco, Thermo Fisher Scientific, Waltham, MA, USA) containing 2 mg/ml type I collagenase (Gibco, Thermo Fisher Scientific, Waltham, MA, USA), 1% bovine serum albumin (Sigma-Aldrich, St. Louis, MO, USA), 200 nM adenosine (Sigma-Aldrich, St. Louis, MO, USA), and 50 μg/ml glucose (VWR International, Radnor, PA, USA).

After centrifugation at 1,450 rpm for 5 min, the supernatant containing fat components and adipocytes was removed. The cell pellet was suspended in Hank's balanced salt solution, followed by filtration through a 100 μm nylon mesh filter (Corning, Corning, NY, USA) and centrifuged at 1,450 rpm for 5 min. To remove residual erythrocytes, the precipitate was suspended in ammonium-chloride-potassium lysing buffer (Lonza, Alpharetta, GA, USA). After centrifugation at 1,450 rpm for 5 min, the precipitated SVF cells were washed with phosphate-buffered saline and then performed the scRNA-seq. Trypan blue (Thermo Fisher Scientific, Waltham, MA, USA) was mixed with the cell suspension at a ratio of 3:1, and the cell density and cell viability were calculated. Purification of the SVF with enzymatic digestion was performed based on the method developed by Sugii *et al.* [26].

scRNA-seq

This study performed the scRNA-seq developed by Hashimoto *et al.* (Figure 11) [18]. The scRNA-seq is a technique to quantify the transcripts of individual cells comprehensively. A microwell slide made of dimethylsiloxane contains 1.6 x 10^5 microwells of 20 pl volumes per 2 mm square, and each microwell contains one barcode bead. The barcode bead is bonded with a single-stranded nucleotide containing two characteristic sequences: an oligo dT sequence and a barcode sequence. The oligo dT sequence consists of 25 bases of thymine, which allows it to hybridize specifically to mRNA. The barcode sequence consists of 12 randomly arranged bases of four types of bases: adenine, thymine, guanine, and cytosine. The SVF cells suspended in phosphate-buffered saline were seeded into a microwell slide from above and entered into the microwells in free fall by incubating at room temperature for 8 min. Then, cell lysis solution (500 mM lithium chloride, 100 mM Tris-HCl (pH 7.5), 1% lithium dodecyl sulfate, 10 mM ethylenediaminetetraacetic acid, and 5 mM dithiothreitol) was added to lyse the cell membrane

and exposed the mRNA in the microwells. The oligo dT sequence of a barcode bead specifically hybridizes to the mRNA of a cell. The barcode beads were collected by centrifuging the microwell slide at 12,000 rpm for 10 seconds at 4°C. After centrifugation again, the precipitated beads were suspended in buffer (1x SSIV buffer (Invitrogen, Carlsbad, CA, USA), 1 mM dNTPs (Invitrogen, Carlsbad, CA, USA), 20% betaine, 6 mM $MgCl_2$, 1.65 units/µl RNasin (Promega, Madison, WI, USA), 5 mM dithiothreitol). The cDNA synthesis was performed using SuperScript IV reverse transcriptase (Invitrogen, Carlsbad, CA, USA) under the following conditions at 35°C for 5 min, 50°C for 10 min, and then 55°C for 10 min. cDNA was stored at -30°C until use.

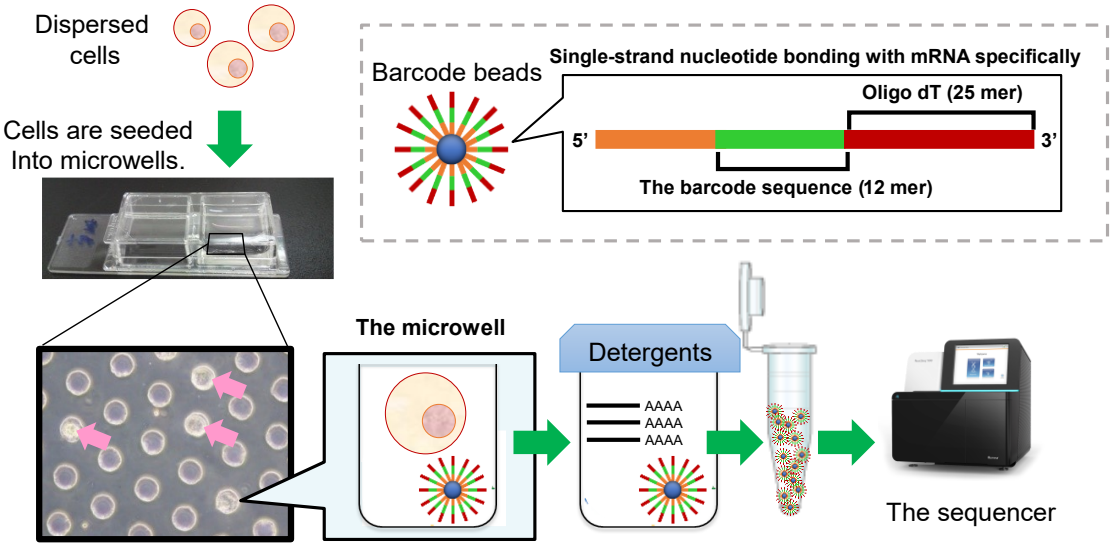

Figure 11: The overview of scRNA-seq performed in this study.

This study performed the scRNA-seq developed by Hashimoto *et al.* [18]. The microwell slide made of dimethylsiloxane has 1.6 x 10^5 microwells of 20 pl volumes per 2 mm square, and each microwell contains one barcode bead. The barcode bead is bonded with a single-stranded nucleotide containing two characteristic sequences: an oligo dT sequence and a barcode sequence. The oligo dT sequence consists of 25 bases of thymine, which allows it to hybridize specifically to mRNA. The barcode sequence consists of 12 randomly arranged bases of four types of bases: adenine, thymine, guanine, and cytosine. The sequence of the barcode sequence is different for each barcode bead. When cells are seeded into a microwell slide from above, one cell enters into a microwell containing one barcode bead. The oligo dT sequence hybridizes to the cell-derived mRNA when the cell is lysed. Analyses of the barcode sequence in synthesized cDNA with a sequencer, transcripts of individual cells can be quantified.

Preparation of the sequencing library

The cDNA was fragmented using the M220 Focused-ultrasonicator (Covaris Inc., Woburn, MS, USA), and then a sequence library was produced by following the instructions of the Illumina TruSeq™ library prep kit (Illumina, San Diego, CA, USA). The quality and quantity of the sequencing libraries were confirmed using an Agilent 4200 TapeStation (Agilent, Santa Clara, CA, USA) and Roche® KAPA Library Quantification Kits (Merck KGaA, Darmstadt, (Merck KGaA, Darmstadt, Germany). Sequence libraries were sequenced for 25 bases from the side of the barcode sequence and 60 bases from the side of the mRNA using the paired-end sequencing mode of the NextSeq 500/550 High Output v2 Kit (Illumina).

Read alignment and gene expression quantification

Sequence data, 60 bases from the side of the mRNA, obtained using scRNA-seq was aligned to Refseq transcript sequences using bowtie 2.2.6 [38]. Then, the aligned reads were linked to their paired extracted barcode sequences. By counting mapped reads per barcode, the gene count data in individual cells were obtained and the transcripts per million (TPM) of each gene were calculated in each cell.

Analysis of gene expression data obtained by scRNA-seq

The comprehensive gene expression data of individual cells in the SVF was analyzed using Seurat 2.4, the software for analyses of data obtained by scRNA-seq [39]. Before comparing the gene expression, the quality check of the gene expression data was performed as following procedures. First, genes expressed by less than 3 cells at less than 3 TPM were excluded as noise. Next, the cells with more than 400 and less than 8,000 expressed genes and less than 5% expression of mitochondrial genes were employed in the analysis, and other cells were excluded

from the analysis. Finally, 1,286 cells and 19,936 genes passed the quality check and were used for subsequent analysis. The cells were then classified into eleven groups by non-hierarchical clustering analysis, and t-distributed stochastic neighbor embedding (t-SNE) plots were generated using Seurat [40].

Pseudotime analysis

Pseudotime analysis was performed using the R package Monocle 3 version 0.2.0 under R version 3.6.1 [41]. After normalizing the data, dimensionality reduction and clustering were performed to create uniform manifold approximation and projection (UMAP) plots [42]. Monocle 3 provided a path in the UMAP space using a principal graph-embedding procedure based on the SimplePPT algorithm [43, 44]. Pseudotime was calculated based on Euclidean distance in the UMAP space after artificially setting the start and endpoints of the pseudotime course [45]. Genes whose expression significantly changed with the pseudotime course were extracted using spatial autocorrelation analysis with Moran's I test [46]. The genes with similar expression patterns were classified into 19 modules. The expression levels of each module were visualized by heat mapping and hierarchical clustering analysis.

Gene ontology (GO) analysis

GO Term is one of the annotation information of genes, and GO analysis is an analysis to search for characteristic GO Terms in multiple gene groups using statistical methods. In this study, GO Terms were searched using functional annotation of the Database for Annotation, Visualization, and Integrated Discovery (DAVID) version 6.8 [47, 48]. The gene sets assigned GO Term with p-values less than 0.050 in the GOTERM_BP_DIRECT category were extracted.

Gene set enrichment analysis (GSEA)

GSEA is a computational method that determines which of two groups a defined gene set is enriched to be expressed. Two datasets, GO (c5.all) and REACTOME (c2.all) involved the Molecular Signatures Database provided by the BROAD Institute in the USA, and GSEA version 4.0.2 were used for the analysis [49, 50]. Gene symbols in gene expression data were converted to the Mouse Genome Informatics (MGI) ID [51], which is provided by the Jackson Laboratory (Bar Harbor, ME, USA), based on the GRCm38 dataset in the Ensembl Gene 98 database using BioMart provided by the European Bioinformatics Institute (EMBL-EBI). After ranking and rearranging the genes based on expression data using the Signal2Noise metric, the enrichment scores of the gene sets were calculated using a weighted scoring scheme. The normalized enrichment score (NES) was calculated with 1,000 permutations. Gene sets with nominal p-values less than 0.05 were selected.

Protein-protein interaction (PPI) analysis

STRING version 11.0 was used to analyze protein-protein association networks with high confidence (more than 7.0 confidence score) [52]. Four evidence data, such as (i) co-expression, (ii) text-mining, (iii) biochemical/genetic data (“experiments”), and (iv) previously curated pathway, and protein-complex knowledge (“databases”) of STRING, were used to calculate the interaction scores of each network edge.

Chapter 4 Results

The gene expression analysis of mouse SVF cells by scRNA-seq

To compare the gene expression of ASCs between young and old, SVF cells were isolated from young (6-month-old) and old (29-month-old) C57BL/6NCr male mice. The cell viability was 83.3% in the young SVF and 80.7% in the old SVF. The scRNA-seq provided gene expression data of 271 cells from young SVF cells and 1015 cells from old SVF cells. To identify the cell population of ASCs in SVF, a non-hierarchical clustering analysis was performed using combined young and old single-cell gene expression data to classify a total of 1286 SVF cell populations into 11 groups (Group 0 to 10): 193 cells in Group 0, 191 cells in Group 1, 146 cells in Group 2, 136 cells in Group 3, 136 cells in Group 4, 134 cells in Group 5, 103 cells in Group 6, 94 cells in Group 7, 78 cells in Group 8, 42 cells in Group 9, and 33 cells in Group 10. Seurat identified the top 10 genes that were characteristically expressed in each group and provided a heat map showing expression levels of these genes (Figure 12). This heat map showed that the expression patterns of Group 0, 2, and 4 (Groups 0-2-4) and Group 1, 3, and 5 (Groups 1-3-5) were similar, although they were divided into three groups, respectively. Patterns of gene expression in each cell were visualized by t-SNE plots, which is one of the dimension reduction methods like principal component analysis (Figure 13).

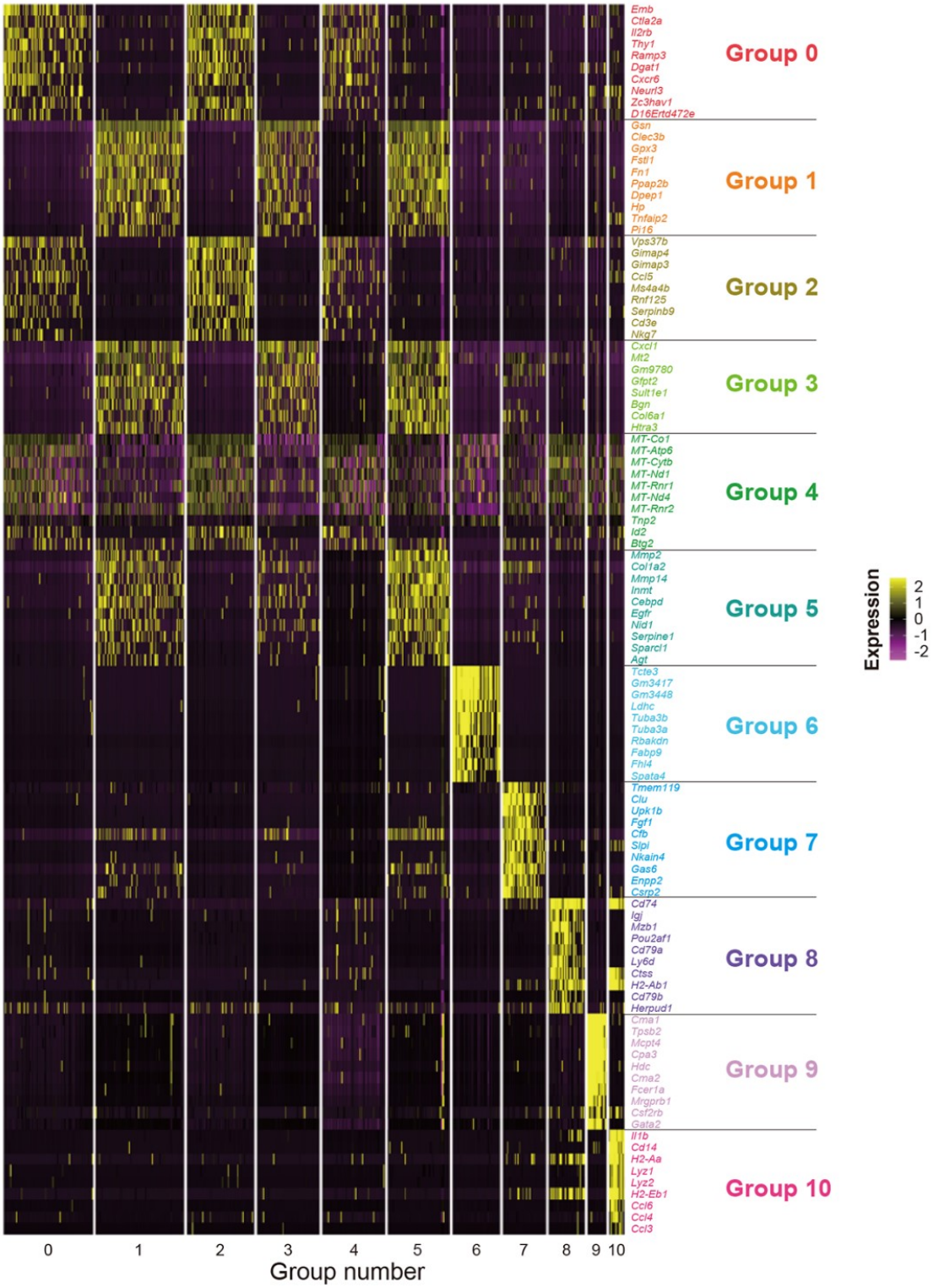
Emb
Ctla2a
Il2rb
Thy1
Ramp3
Dgat1
Cxcr6
Neurl3
Zc3hav1
D16Ertd472e
Group 0
Gsn
Ciec3b
Gpx3
Fstl1
Fn1
Ppap2b
Dpep1
Hp
Tnfaip2
Pi16
Group 1
Vps37b
Gimap4
Gimap3
Ccl5
Ms4a4b
Rnf125
Serpinb9
Cd3e
Nkg7
Group 2
Cxcl1
Mt2
Gm9780
Gfpt2
Sult1e1
Bgn
Col6a1
Htra3
Group 3
MT-Co1
MT-Atp6
MT-Cytb
MT-Nd1
MT-Rnr1
MT-Nd4
MT-Rnr2
Tnp2
Id2
Btg2
Group 4
Mmp2
Col1a2
Mmp14
Inmt
Cebpd
Egfr
Nid1
Serpine1
Sparcl1
Agt
Group 5
Tcte3
Gm3417
Gm3448
Ldhc
Tuba3b
Tuba3a
Rbakdn
Fabp9
Fhl4
Spata4
Group 6
Tmem119
Clu
Upk1b
Fgf1
Cfb
Slpi
Nkain4
Gas6
Enpp2
Csrp2
Group 7
Cd74
Igj
Mzb1
Pou2af1
Cd79a
Ly6d
Ctss
H2-Ab1
Cd79b
Herpud1
Group 8
Cma1
Tpsb2
Mcpt4
Cpa3
Hdc
Cma2
Fcer1a
Mrgprb1
Csf2rb
Gata2
Group 9
Il1b
Cd14
H2-Aa
Lyz1
Lyz2
H2-Eb1
Ccl6
Ccl4
Ccl3
Group 10
0 1 2 3 4 5 6 7 8 9 10
Group number
Expression
2
1
0
-1
-2

Figure 12: Non-hierarchical clustering analysis of gene expression data from young (6-month-old) and old (29-month-old) mice.

SVF cells of young (cell number, n = 271) and old (cell number, n = 1015) mice were classified into 11 groups (Group 0 to 10) using Seurat version 2.4. This heat map shows the expression levels of the top 10 genes characteristically expressed in each of the 11 groups. Gene names of the top 10 genes characteristically expressed in each group are listed in Supplemental table 1.

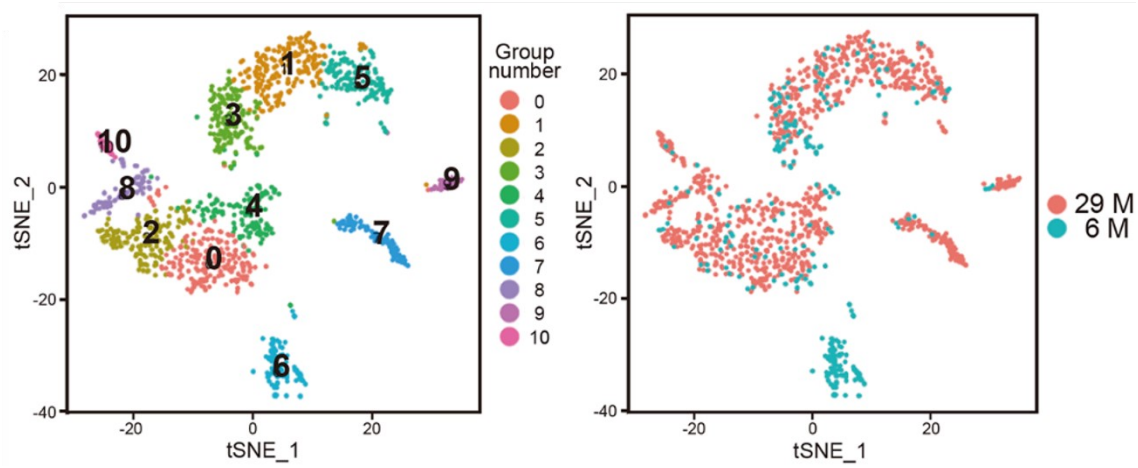

Figure 13: The t-SNE plots generated from gene expression data obtained from young and old mice.

The t-distributed stochastic neighbor embedding (t-SNE) plots were generated from gene expression data of SVF cells of young (cell number, n = 271) and old (cell number, n = 1015) mice. The plots of cells are colored according to group number (left) and age (right): 29-month-old (29 M) and 6-month-old (6 M).

Identification of cell populations in the SVF

GO analysis was performed using the annotation information of the top 10 genes characteristically expressed in each group to determine the cell types of each group in the SVF (Supplemental table 1). Groups 0-2-4 and Groups 1-3-5 were considered to have similar expression patterns based on the result of a t-SNE plot and were analyzed as one group, respectively (Figure 13). Then, the cell types of each group were predicted from the top 10 genes characteristically expressed (Supplemental table 2).

Among the genes characteristically expressed in Groups 0-2-4, I focused on *embigin* (*Emb*), *thymus cell antigen 1, theta* (*Thy1*), and *inhibitor of DNA binding 2* (*Id2*). *Emb* is an intercellular adhesion molecule that maintains hematopoietic stem cells (HSCs) in quiescence [53]. *Thy1* is a marker gene of HSCs [54], and *Id2* is involved in maintaining the self-renewal potentials of HSCs [55]. Based on the above, Groups 0-2-4 was predicted to be the cell population of HSCs.

Among the genes characteristically expressed in Group 6, I focused on *lactate dehydrogenase C* (*Ldhc*) and *t-complex-associated testis expressed 3* (*Tcte3*). *Ldhc*, a member of the lactate dehydrogenase family, is highly expressed in spermatocytes, sperms, and oocytes; male and female *Ldhc* transgenic (knockout) mice have significantly low reproductive efficiencies [56]. *Tcte3*, which is highly expressed in the testis, regulates the motility in sperms [57]. Based on the above, Group 6 was predicted to be the cell population of sperms. Originally, the SVF does not contain sperms. In addition, Group 6 was composed only of cells from a young mouse (Figure 13). This suggests that sperm may have been contaminated during the collection of the young mouse SVF.

Among the genes characteristically expressed in Group 7, I focused on *clusterin* (*Clu*) and *ectonucleotide pyrophos-phatase/phosphodiesterase 2* (*Enpp2*). *Clu* is highly expressed in Sertoli

cells and is involved in intercellular adhesion [58, 59]. *Enpp2* is also highly expressed in Sertoli cells [60]. Based on the above, Group 7 was predicted to be the cell population of Sertoli cells.

Among the genes that are characteristically expressed in Group 8, I focused on *CD74 antigen (invariant polypeptide of major histocompatibility complex, class II antigen-associated)* (*Cd74*), *CD79A antigen (immunoglobulin-associated alpha) (Cd79a*), and *CD79B antigen* (*Cd79b*). *Cd74* is involved in B cell maturation through the signaling pathway of nuclear factor-kappa B (NF-κB) [61, 62]. *Cd79a* and *Cd79b* are components of a complex of receptors that recognize antigens on the cell surface of B cells [63]. Based on the above, Group 8 was predicted to be the cell population of B cells.

Among the genes that are characteristically expressed in Group 9, I focused on *carboxypeptidase A3, mast cell* (*Cpa3*), *chymase 1, mast cell* (*Cma1*), *chymase 2, mast cell* (*Cma2*), and *tryptase beta 2* (*Tpsb2*). *Cpa3* is one of the major components of the granules of mast cells [64]. *Cma1* and *Cma2* are chymotrypsin-like serine proteases, called chymase, present in the granules of mast cells, *Tpsb2* is a neutral serine protease present in the granules of mast cells, and these have been confirmed to be highly expressed in mast cells [65-67]. Based on the above, Group 9 was predicted to be the cell population of mast cells.

Among the genes characteristically expressed in Group 10, I focused on *CD14 antigen* (*Cd14*), *chemokine (C-C motif) ligand 3* (*Ccl3*), *chemokine (C-C motif) ligand 4* (*Ccl4*), and *chemokine (C-C motif) ligand 6* (*Ccl6*). *Cd14* is a membrane protein present in the cell membranes of monocytes and macrophages. It induces inflammatory responses through binding to lipopolysaccharide (LPS), a major component of the cell wall of Gram-negative bacteria [68]. *Ccl3*, *Ccl4*, and *Ccl6* are chemokines that induce lymphocyte migration to inflammatory sites and are highly expressed in macrophages [69-71]. Based on the above, Group 10 was predicted to be the cell population of macrophages.

Among the genes that are characteristically expressed in Groups 1-3-5, seventeen genes (*gelsolin* (*Gsn*), *C-type lectin domain family 3, member b* (*Clec3b*), *glutathione peroxidase 3* (*Gpx3*) *follistatin-like 1* (*Fstl1*), *phosphatidic acid phosphatase type 2B* (*Ppap2b*), *dipeptidase 1* (*Dpep1*), *haptoglobin* (*Hp*), *peptidase inhibitor 16* (*Pi16*), *chemokine (C-X-C motif) ligand 1* (*Cxcl1*), *sulfotransferase family 1E, member 1* (*Sult1e1*), *biglycan* (*Bgn*), *HtrA serine peptidase 3* (*Htra3*), *matrix metallopeptidase 2* (*Mmp2*), *indolethylamine N-methyltransferase* (*Inmt*), *nidogen 1* (*Nid1*), *SPARC-like 1* (*Sparcl1*), and *angiotensinogen (serpin peptidase inhibitor, clade A, member 8)* (*Agt*)) were reported to be highly expressed genes in ASCs [72]. Moreover, six typical ASC marker genes such as *Gsn*, *Cxcl1*, *collagen, type I, alpha 2* (*Col1a2*), *collagen, type VI, alpha 1* (*Col6a1*), *Mmp2*, and *matrix metallopeptidase 14 (membrane-inserted)* (*Mmp14*) [73], were highly expressed in Groups 1-3-5 (Figure 14A). Furthermore, the expression levels of these genes were higher in Group 1-3-5 (indicated by X in Figure 14B) than in the other eight groups (indicated by Y in Figure 14B). Based on these results, Groups 1-3-5 was identified as the cell population of ASCs.

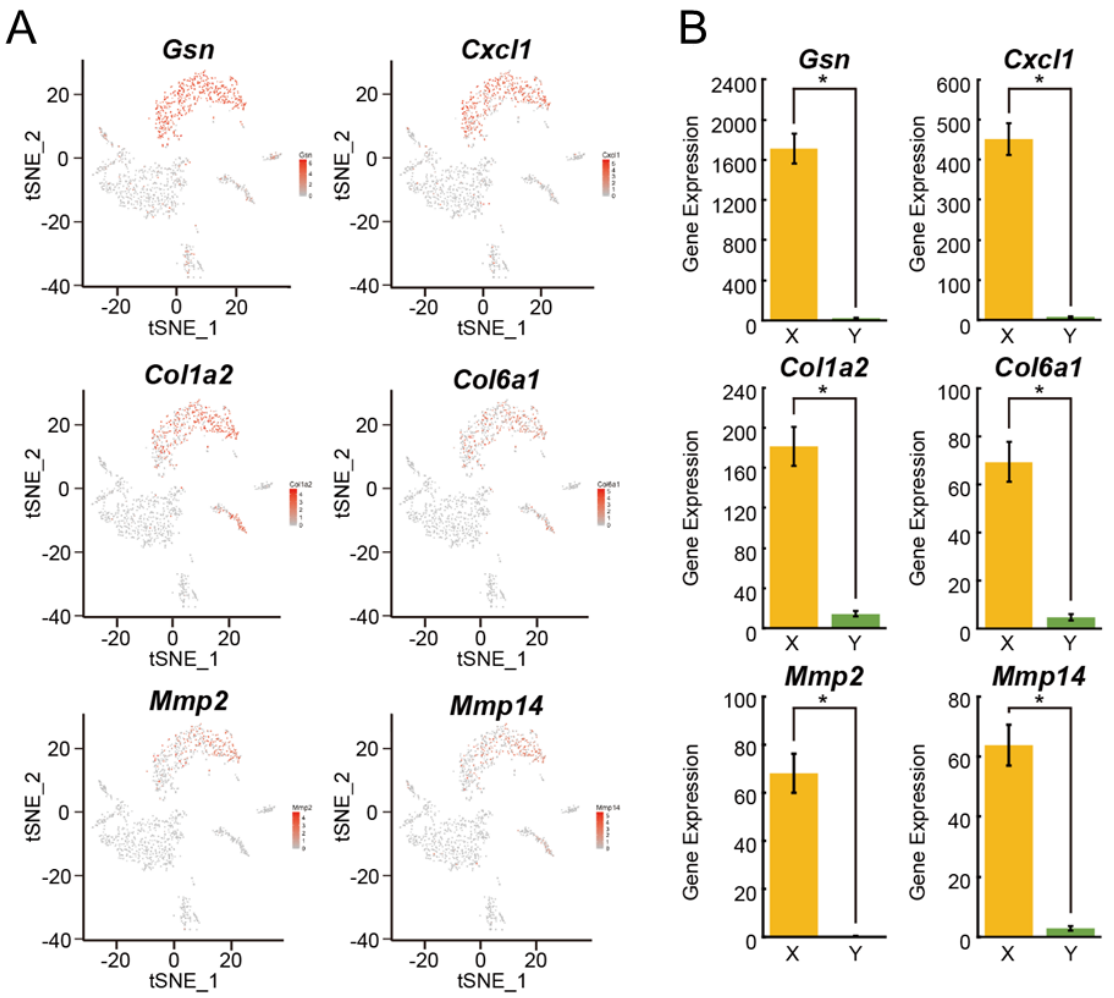

Figure 14: The expression of six typical ASC marker genes.

(A) Heatmaps indicating the expression levels of *Gsn*, *Cxcl1*, *Col1a2*, *Col6a1*, *Mmp2*, and *Mmp14* in t-SNE plots. (B) Gene expression levels (transcripts per million, TPM) of *Gsn*, *Cxcl1*, *Col1a2*, *Col6a1*, *Mmp2*, and *Mmp14* in Groups 1-3-5 (X) (cell number, n = 461) and the other eight groups (Y) (cell number, n = 825). Values are indicated as mean ± standard error. Statistical analysis was performed using a two-tailed Welch's t-test. *p<0.001.

The expression levels of stem cell marker proteins in the SVF

Stem cell antigen-1 (Sca1; Ly6A/E) is a marker protein for stem cells, including ASCs [74]. Sca1 is encoded by the *Ly6a* gene, a representative member of the lymphocyte antigen 6 (Ly6) superfamily, and the *Ly6a* gene has two alleles, Ly6a and Ly6e [75, 76]. Then, the expression levels of *Ly6a* and *Ly6e* were examined in Groups 1-3-5 and the other eight groups (Figure 15). The expression levels of *Ly6a* were high in Groups 1-3-5 (indicated by X in Figure 15). On the other hand, the expression levels of *Ly6e* were high in the other eight groups (indicated by Y in Figure 15). In addition, both *Ly6a* and *Ly6e* were not listed in the top 10 genes characteristically expressed in each group (Supplemental table 1).

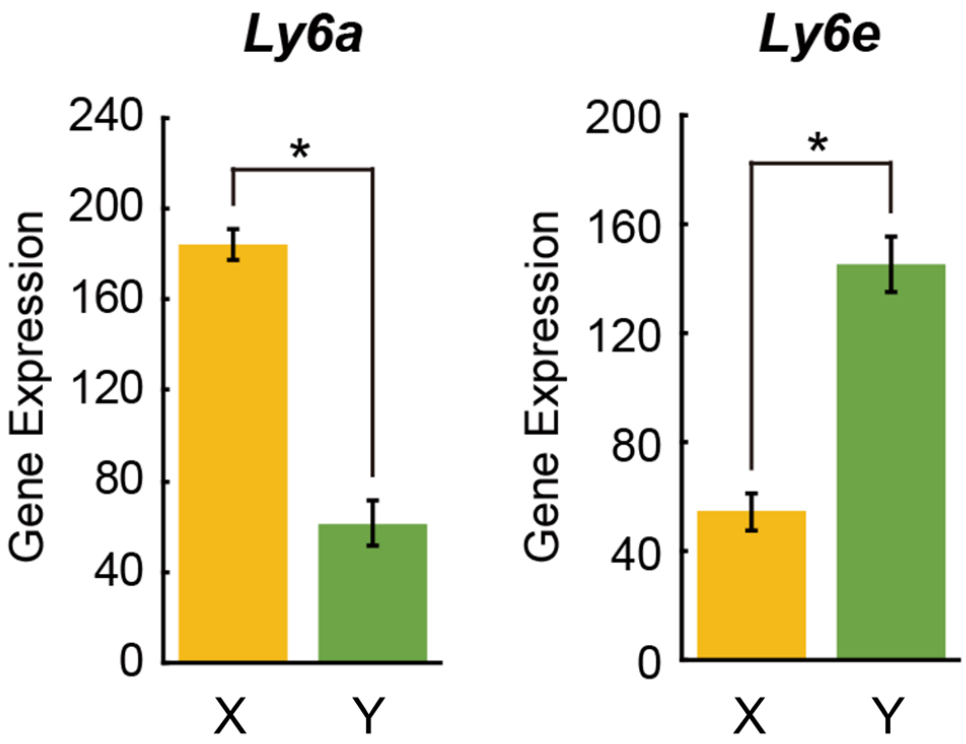

Figure 15: Gene expression levels of stem cell marker protein in the SVF.

Gene expression levels (TPM) of *Ly6a* and *Ly6e* in Groups 1-3-5 (X) (cell number, n = 461) and the other eight groups (Y) (cell number, n = 825) are shown. Values are indicated as mean ± standard error. Statistical analysis was performed using a two-tailed Welch's t-test. *p<0.001.

Age-associated changes in ASCs

The total number of cells in Groups 1-3-5 of young (cell number, n = 84) and old (cell number, n = 377) mice accounted for 50.0% and 37.1% of the SVF that exclude Group 6, respectively, and showed a lower percentage of ASCs in the old mouse SVF compared to young mouse SVF (Table 1). On the other hand, the total number of cells in Groups 0-2-4 of young (cell number, n = 70) and old (cell number, n = 405) mice accounted for 41.7% and 40.0% of the SVF that exclude Group 6, respectively, and no significant difference was observed between young and old. The percentage of cells in each group among the ASCs of young and old mice was calculated (Table 2). Group 3 was the most abundant group in young, accounting for 58.3% of young mouse ASCs, while Group 3 was the smallest group in old, accounting for 23.1% of old mouse ASCs. Young mouse ASCs were more in the order of Group 3, Group 1, and Group 5, while old mouse ASCs were more in the order of Group 1, Group 5, and Group 3.

Next, the percentages of cells expressing *Gsn*, *Cxcl1*, *Col1a2*, *Col6a1*, *Mmp2*, and *Mmp14* in Group 1, Group 3, and Group 5 were calculated, respectively, and were compared between young and old (Figure 16). Henceforth, the percentage of cells expressing genes will be indicated as "positive cell rate" in this study. In Group 1, the positive cell rates for *Cxcl1* and *Mmp2* were higher in old mouse ASCs than in young mouse ASCs. In Group 3, the positive cell rate for *Mmp14* was higher in old mouse ASCs than in young mouse ASCs. In Group 5, the positive cell rates for *Gsn* and *Cxcl1* were higher, and that of *Col6a1* was lower in old mouse ASCs than young mouse ASCs. However, the positive cell rate for *Col1a2* was not significantly different between young and old mice in any groups.

Although cellular senescence is a phenomenon found in studies using fibroblasts, it is interesting to know whether the expression of genes associated with cellular senescence is

enhanced in the tissues of old animals. In fibroblasts that caused cellular senescence, secretion of SASP factors and cell cycle arrest are observed. In this study, the positive cell rates for nine SASP factors such *interleukin 6* (*IL-6*), *chemokine (C-X-C motif) ligand 2* (*Cxcl2*), *chemokine (C-C motif) ligand 11* (*Ccl11*), *insulin-like growth factor binding protein 4* (*Igfbp4*), *insulin-like growth factor binding protein 6* (*Igfbp6*), *insulin-like growth factor binding protein 7* (*Igfbp7*), *matrix metallopeptidase 3* (*Mmp3*), *tissue inhibitor of metalloproteinase 2* (*Timp2*), and *cathepsin B* (*Ctsb*) [15], and three genes involved in the cell cycle arrest such *Cdkn1a*, *transformation-related protein 53* (*Trp53*), and *Cdkn2a* [16], were calculated and compared between young and old (Figure 17). In Group 1, the positive cell rate for *Timp2* was lower in old mouse ASCs than in young mouse ASCs. In Group 3, the positive cell rates for *Cxcl2*, *Igfbp4*, *Timp2*, and *Ctsb* were higher, and that of *Mmp3* was lower in old mouse ASCs than in young mouse ASCs. In Group 5, the positive cell rates for *Ccl11*, *Ctsb*, and *Cdkn1a* were higher, and those of *Igfbp4*, *Igfbp6*, and *Mmp3* were lower in old mouse ASCs than in young mouse ASCs. There was no significant difference in the positive cell rate for *IL-6*, *Igfbp7*, and *Trp53* between old and young mice in any group. The expression of *Cdkn2a* was too low to be detected in this study.

	Young	Old
Group 0	30 cells (17.9%)	163 cells (16.1%)
Group 1	23 cells (13.7%)	168 cells (16.6%)
Group 2	19 cells (11.3%)	127 cells (12.5%)
Group 3	49 cells (29.2%)	87 cells (8.6%)
Group 4	21 cells (12.5%)	115 cells (11.3%)
Group 5	12 cells (7.1%)	122 cells (12.0%)
Group 6	103 cells	0 cells
Group 7	5 cells (3.0%)	89 cells (8.8%)
Group 8	5 cells (3.0%)	73 cells (7.2%)
Group 9	2 cells (1.2%)	40 cells (3.9%)
Group 10	2 cells (1.2%)	31 cells (3.1%)
Groups 0-2-4	70 cells (41.7%)	405 cells (40.0%)
Groups 1-3-5	84 cells (50.0%)	377 cells (37.1%)

Table 1: The numbers of cells in each group of the SVF in young and old mice.

The numbers of cells in each group, Groups 0-2-4, and Groups 1-3-5 of the SVF in young and old mice, are shown. The percentage of cells in each group out of 168 cells in the young mouse SVF, excluding Group 6, and 1015 cells in the SVF of old are shown in parentheses.

	Young	Old
Group 1	23 cells (27.4%)	168 cells (44.6%)
Group 3	49 cells (58.3%)	87 cells (23.1%)
Group 5	12 cells (14.3%)	122 cells (32.3%)

Table 2: Differences of cells involved in Group 1, Group 3, and Group 5 between young and old.

The number of cells in Group 1, Group 3, and Group 5 of young and old mice, respectively. The percentages of cells in each group out of 84 cells in Groups 1-3-5 of young and 377 cells in Groups 1-3-5 of old are shown in parentheses.

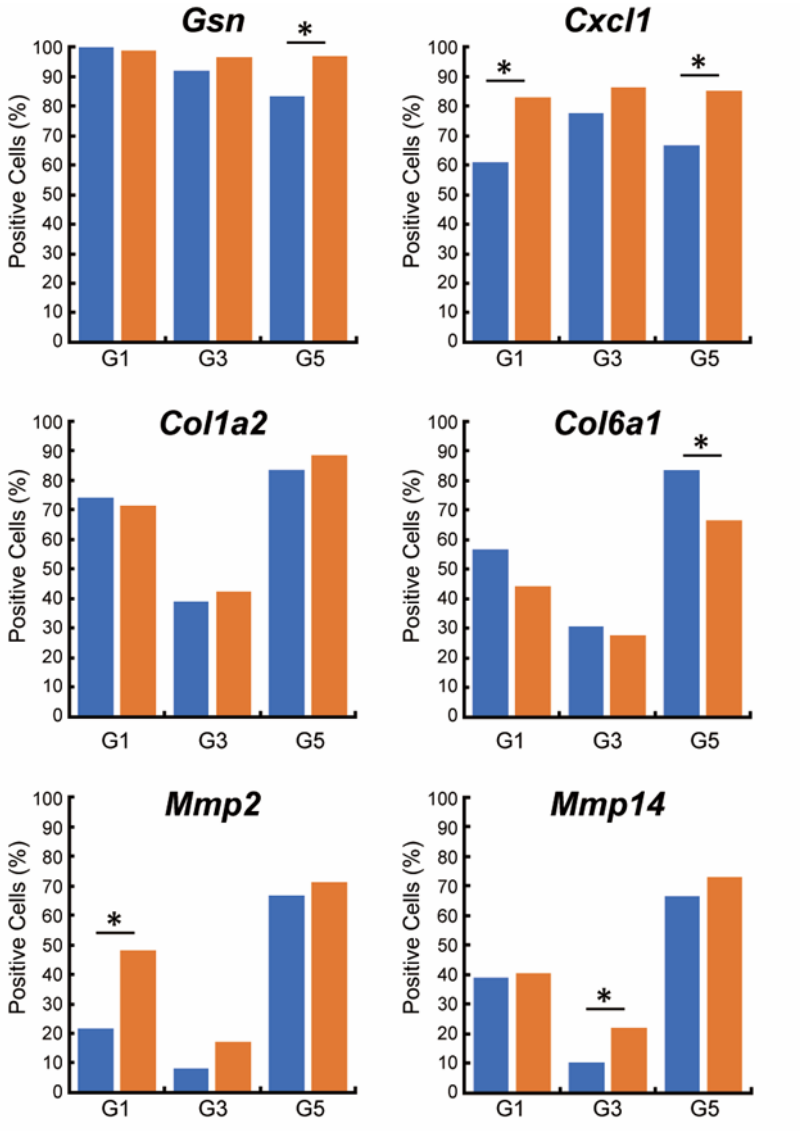

Figure 16: Differences in the positive cell rates of genes highly expressed in ASCs between young and old.

Positive cells (%) are the positive cell rates for *Gsn*, *Cxcl1*, *Col1a2*, *Col6a1*, *Mmp2*, and *Mmp14* in Group 1, Group 3, and Group 5 of young (blue) and old (orange). A cell expressing more than 1 TPM of one gene was counted as the positive cell. G1: Group 1 (cell number, n = 191), G3: Group 3 (cell number, n = 136), G5: Group 5 (cell number, n = 134). Statistical analysis was performed using a two-tailed chi-square test. *p<0.05.

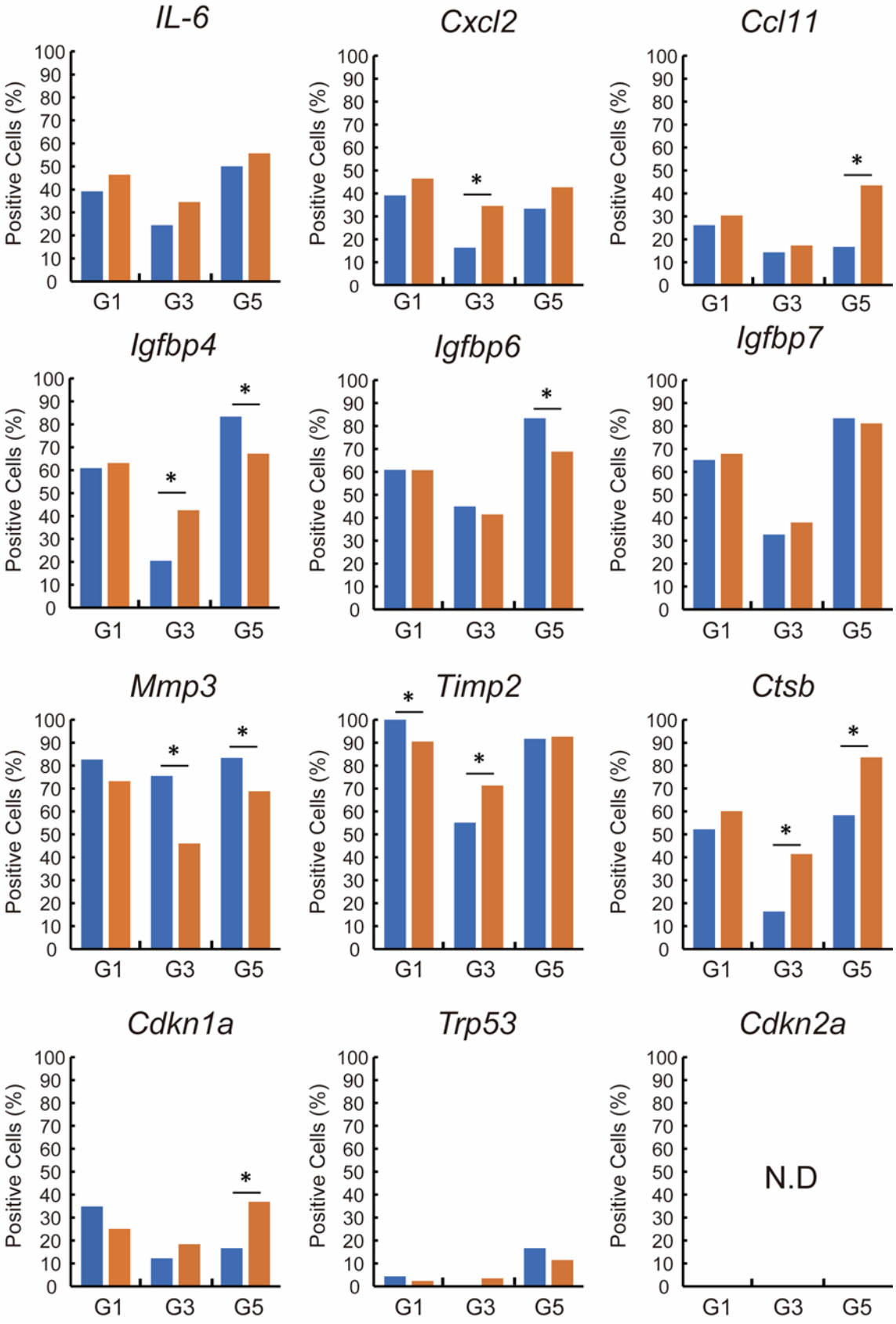
IL-6
Cxcl2
Ccl11
Igfbp4
Igfbp6
Igfbp7
Mmp3
Timp2
Ctsb
Cdkn1a
Trp53
Cdkn2a
Positive Cells (%)
0
10
20
30
40
50
60
70
80
90
100
G1
G3
G5
*
N.D

Figure 17: Differences in the positive cell rates of genes associated with cellular senescence between young and old.

Positive cells (%) is the positive cell rates for *IL-6*, *Cxcl2*, *Ccl11*, *Igfbp4*, *Igfbp6*, *Igfbp7*, *Mmp3*, *Timp2*, *Ctsb*, *Cdkn1a*, *Trp53*, and *Cdkn2a* in Group 1, Group 3, and Group 5 of young (blue) and old (orange). A cell expressing more than 1 TPM of one gene was counted as the positive cell. G1: Group 1 (cell number, n = 191), G3: Group 3 (cell number, n = 136), G5: Group 5 (cell number, n = 134). N.D: not detected. Statistical analysis was performed using a two-tailed chi-square test. *p<0.05.

The differentiation stage of ASCs

Most ASCs in adipose tissue differentiate into preadipocytes and then adipocytes. Based on the results of t-SNE plots, I hypothesized that Groups 1-3-5 are ASCs in different stages of differentiation. To validate the differentiation stages of Groups 1-3-5, the expression levels of highly expressed genes in preadipocytes and adipocytes were examined (Figure 18). Genes such as *epidermal growth factor receptor* (*Egfr*), *epidermal growth factor-containing fibulin-like extra-cellular matrix protein 1* (*Efemp1*), and *Igfbp4*, are highly expressed in preadipocytes, while genes such *fatty acid binding protein 4, adipocyte* (*Fabp4*), *CCAAT/enhancer-binding protein (C/EBP), alpha* (*C/ebpα*) are highly expressed in adipocytes, and genes that are highly expressed in both preadipocytes and adipocytes include *lipoprotein lipase* (*Lpl*) and *peroxisome proliferator activated receptor gamma* (*Pparγ*) (Figure 19) [74]. The expression levels of *Egfr*, *Efemp1* and *Igfbp4* in Group 1 were lower than those in Group 5, and the expression levels of *Lpl*, *Egfr*, *Efemp1,* and *Igfbp4* in Group 3 were lower than those in Group 5. However, there was no significant difference in any genes between Group 1 and Group 3. Furthermore, the expression levels of *Pparγ*, *Fabp4*, and *C/ebpα* in Group 3 were the lowest compared to those in Group 1 and Group 5, but significant differences were not found (Figure 19). The expression of *Pparγ* could not be confirmed in Group 3. Based on these results, it was considered that Group 5 are close to preadipocytes and are in the most advanced stage of differentiation, Group 3 are highly undifferentiated and in the earliest stage of differentiation, and Group 1 are intermediate ASCs between Group 5 and Group 3.

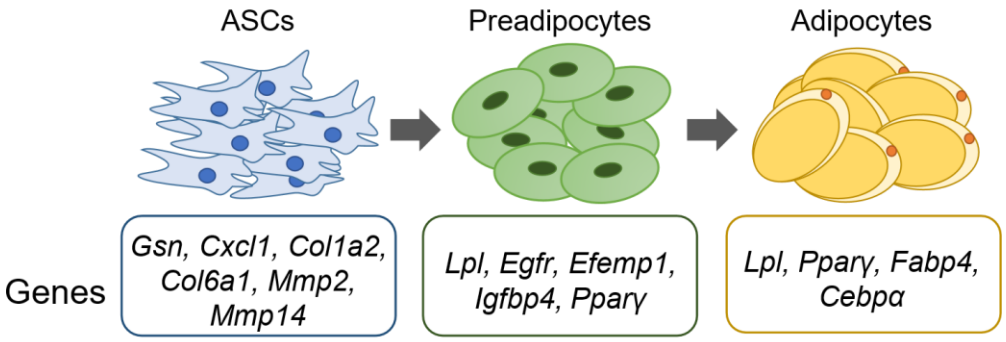

Figure 18: Genes highly expressed in ASCs, preadipocytes, and adipocytes, respectively.

Most ASCs in adipose tissue are considered to differentiate into preadipocytes and then adipocytes that accumulate fat. Several genes have been highly expressed in ASCs, preadipocytes, and adipocytes, respectively [73, 74]. The expression of genes involved in differentiation is thought to vary continuously during differentiation.

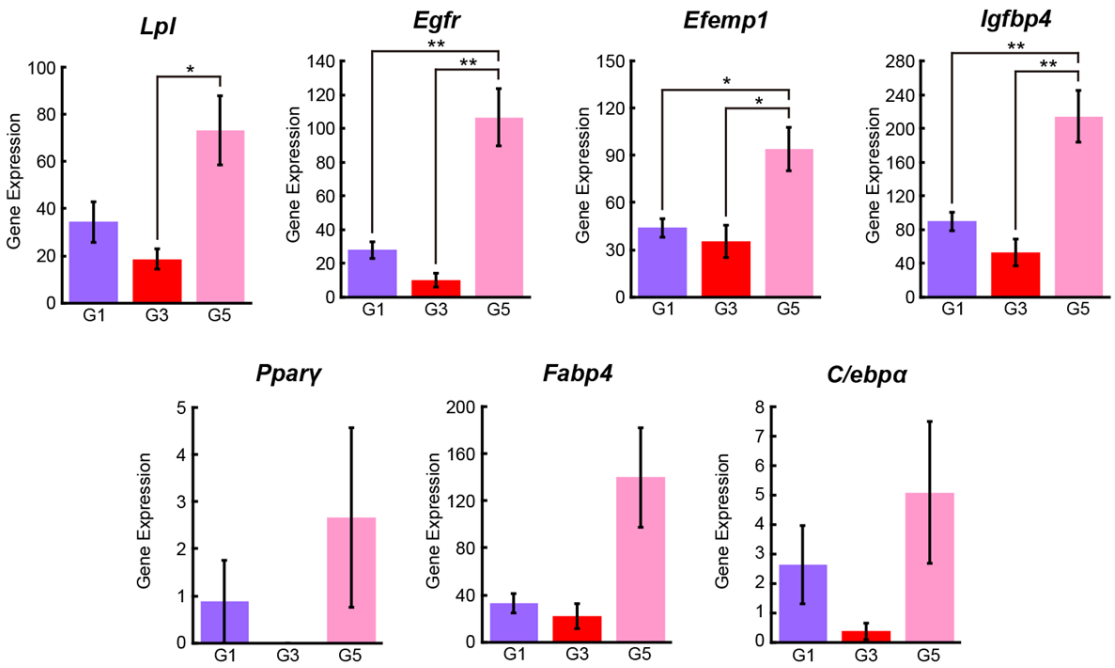

Figure 19: The expression levels of genes highly expressed in preadipocytes and adipocytes. Gene expression levels (TPM) of *Lpl*, *Egfr*, *Efemp1*, *Igfbp4*, *Pparγ*, *Fabp4*, and *C/ebpα* in Group 1 (purple), Group 3 (red), and Group 5 (peach) are shown. G1: Group 1 (cell number, n = 191), G3: Group 3 (cell number, n = 136), G5: Group 5 (cell number, n = 134). Values are indicated as mean ± standard error. Statistical analysis was performed using Tukey's post hoc test. *p<0.05, **p<0.01.

Pseudotime analysis

To examine the differentiation stages of Groups 1-3-5 in more detail, gene expression data of only Group 3 that predicted to be highly undifferentiated ASCs, and Group 5 that predicted to be ASCs close to preadipocytes were extracted and reanalyzed using Monocle 3 [41]. Based on the gene expression data, Monocle 3 generated UMAP plots of Group 3 and Group 5 cells [42]. UMAP is one of the methods of dimension reduction like t-SNE. The heatmaps of genes highly expressed in preadipocytes such as *lpl*, *Egfr*, *Efemp1*, and *Igfbp4* showed higher expression levels in Group 5 than in Group 3 (Figure 20). The same results obtained using Seurat were also confirmed by the analysis using Monocle3. Based on the hypothesis that Group 3 is highly undifferentiated ASCs and Group 5 is ASCs close to preadipocytes, I set the starting point of the pseudotime to Group 3 and the endpoint of the pseudotime to Group 5 on the UMAP plot (Figure 21).

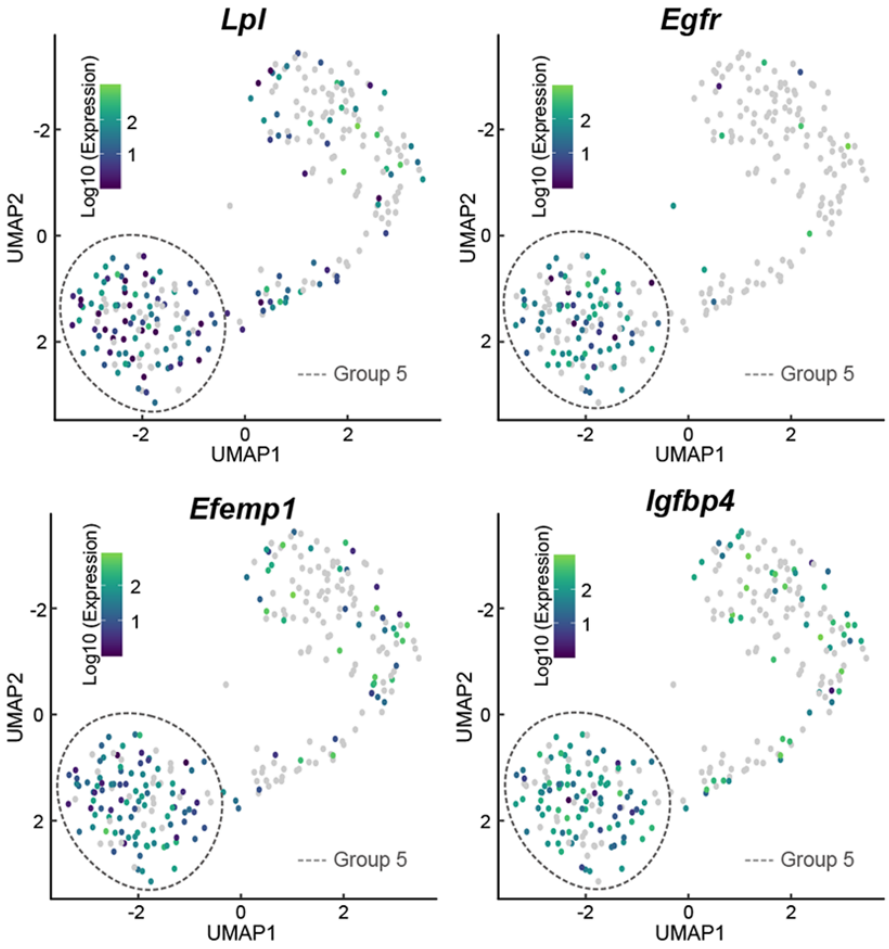

Figure 20: Expression levels of genes highly expressed in preadipocytes in reanalysis using Monocle 3.

The data from Group 3 (cell number, n = 136) and Group 5 (cell number, n = 134) of young and old mice were reanalyzed using Monocle 3. Heatmaps show the expression levels of *Lpl*, *Egfr*, *Efemp1*, *Igfbp4* in the uniform manifold approximation and projection (UMAP) plots. The gray dotted circles indicate the region of Group 5 in the UMAP plot.

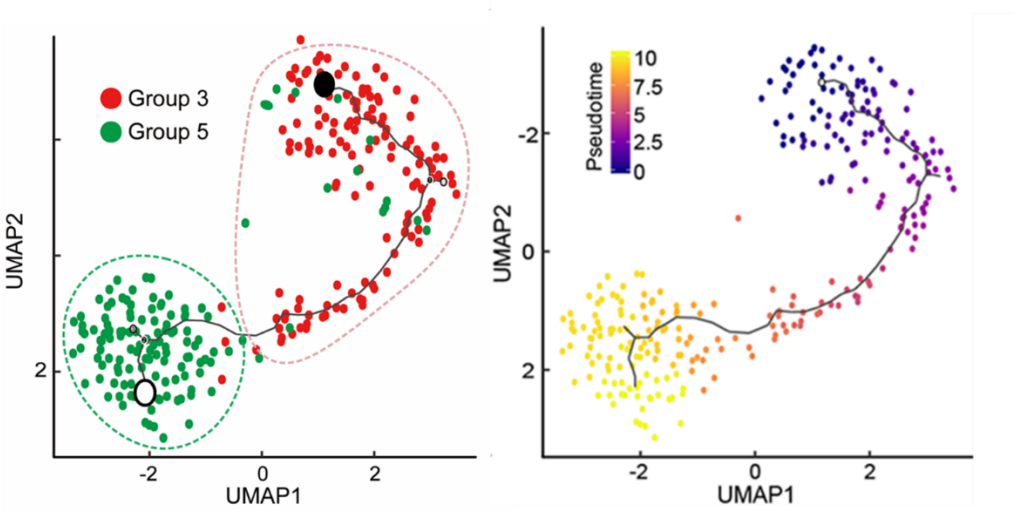

Figure 21: Setting up pseudotime and generating of a pseudotime course with Monocle3.

The black lines in the UMAP plots indicate the path of the pseudotime course. The UMAP plot on the left is colored by Group (red: Group 3, green: Group 5). The black dot indicates the starting point of the pseudotime course, and the white dot indicates the endpoint of the pseudotime course. The right figure is a heat map showing the pseudotime course.

Identification of genes whose expression levels change with the pseudotime course

Genes whose expression significantly changed with the pseudotime course were extracted using spatial autocorrelation analysis called Moran's I test [46]. Extracted genes with similar expression patterns were classified into 19 modules (module 1 to 19) using Monocle3. The expression levels of each module were visualized in the heatmap, and hierarchical clustering analysis was performed (Figure 22). Especially, module 6 showed a significantly higher expression level in Group 3 than in Group 5. Genes included in module 6 are shown in Table 3. Moreover, GO terms abundant in module 6 were searched using the functional annotation in DAVID version 6.8 [47, 48]. GO Term, negative regulation of chondrocyte differentiation, was discovered in module 6 and consisted of three genes associated with the differentiation, *disintegrin-like and metallopeptidase (reprolysin type) with thrombospondin type 1 motif, 7* (*Adamts7*), *snail family zinc finger 2* (*Snai2*), and *transforming growth factor, beta receptor I* (*Tgfbr1*) (Table 4). *Adamts7* is a metalloproteinase that inhibits chondrocyte differentiation by inactivating growth factor progranulin [77]. *Snai2* is a transcription factor that represses the differentiation of human epidermal progenitor cells and adipocytes [78, 79]. *Tgfbr1* is a receptor of transforming growth factor-β (TGF-β) and inhibits the differentiation of rat bone marrow-derived mesenchymal stem cells into osteoblasts [80]. The gene expression of *Adamts7*, *Snai2*, and *Tgfbr1* was high in the early half of the pseudotime and then decreased with the pseudotime course (Figure 23). This suggested that expressions of *Adamts7*, *Snai2*, and *Tgfbr1* are characteristically high in the early differentiation stage of ASCs.

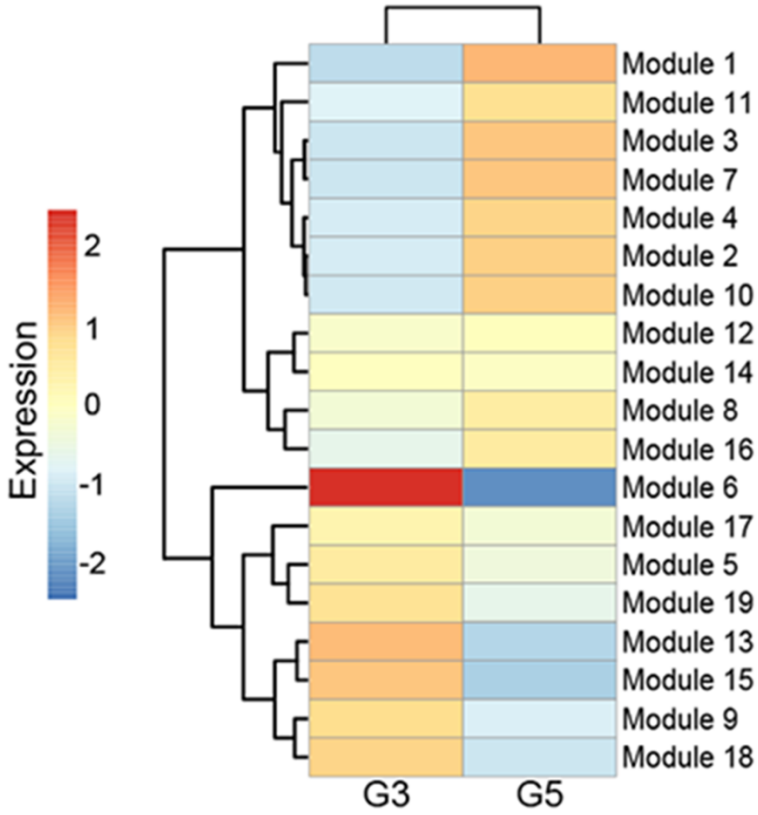

Figure 22: Expressions of groups of genes whose expression change with the pseudotime course in Groups 3 and Group 5.

The Heatmap shows the expression levels of the modules and is a result of hierarchical cluster analysis between Group 3 (G3) and Group 5 (G5). The modules consisted of genes with similar expression patterns with the pseudotime course. Genes whose expression changed significantly with the pseudotime course were extracted using spatial autocorrelation analysis of Moran's I test. $q<0.05$.

Module 6						
1700020D05Rik	*Ccne1*	*Fbxo45*	*Lhfpl1*	*Odf4*	*Samd10*	*Tmem151a*
1700023E05Rik	*Cd9*	*Fgf5*	*Lman2l*	*Olfr1426*	*Samt2*	*Tmem184b*
1700026L06Rik	*Cdhr1*	*Fgf8*	*LOC100045026*	*Olfr536*	*Scn1b*	*Tmem191c*
1700030C10Rik	*Cdt1*	*Fkbp11*	*LOC105245480*	*Olfr70*	*Sebox*	*Tmem204*
1700048O20Rik	*Cenpb*	*Fkbp14*	*Lonp2*	*Olfr722*	*Serinc5*	*Tmem26*
2410089E03Rik	*Cggbp1*	*Fscn3*	*Lppr2*	*Olfr947-ps1*	*Sertad3*	*Tmem261*
2610318N02Rik	*Chrna4*	*G6pc3*	*Lrrc27*	*Omp*	*Shcbp1*	*Tmem35*
2610507B11Rik	*Chrnb3*	*Gata3*	*Lrrc28*	*Otos*	*Shisa7*	*Tmem98*
2810021J22Rik	*Chst7*	*Gja5*	*Lrrc34*	*Otud6b*	*Slc16a8*	*Tmx1*
6430706D22Rik	*Clasp1*	*Gm11696*	*Lrrc75a*	*Parp12*	*Slc17a7*	*Tnp2*
A330069E16Rik	*Clstn2*	*Gm13139*	*Lrrn3*	*Parp2*	*Slc22a16*	*Top1mt*
Abca5	*Cnnm3*	*Gm20736*	*Lsg1*	*Pcdhgb2*	*Slc23a2*	*Tppp2*
Abhd1	*Comt*	*Gm20741*	*Lta*	*Pcyt2*	*Slc29a4*	*Ttc9b*
Acap3	*Csrp3*	*Gm3002*	*Lyzl4*	*Pdia4*	*Slit1*	*Ttll4*
Actn2	*Cxcl16*	*Gm5478*	*Mafg*	*Pdik1l*	*Smad1*	*Tuba1b*
Adamts7	*Cypt15*	*Gm5941*	*Map3k11*	*Pfdn2*	*Smg7*	*Tubb6*
Adgrb2	*D5Ertd579e*	*Gng2*	*Mapk4*	*Phactr1*	*Smim20*	*Ubr2*
Ahdc1	*Dak*	*Got1l1*	*Meig1*	*Pik3c2g*	*Snai2*	*Ugt2a2*
Alkbh2	*Dctn1*	*Gstm2*	*Mfsd10*	*Pinc*	*Snhg5*	*Uhrf2*
Armc6	*Decr1*	*Gtpbp1*	*Mfsd11*	*Pld3*	*Snrpf*	*Umodl1*
Armcx1	*Dennd6b*	*H1fx*	*Mkl2*	*Plk3*	*Snx24*	*Unc45b*
Arrdc5	*Dhx37*	*H2afx*	*Mmd*	*Plvap*	*Snx32*	*Usp32*
Atg4c	*Dnpep*	*Hap1*	*Mmp15*	*Pnmal1*	*Socs5*	*Wdr46*
Atp2a1	*Doc2g*	*Hmga2*	*Mmp3*	*Polr2f*	*Spaca3*	*Wdr6*
Atp2a2	*Dpysl5*	*Hmgxb4*	*Morc3*	*Proser3*	*Spire2*	*Wdr76*
Atp5k	*Dtx3*	*Hspb2*	*Mov10*	*Prr15l*	*Stard5*	*Wdr81*
AU015836	*E030002O03Rik*	*Hspb6*	*Mpp4*	*Prrc2a*	*Stk36*	*Wdr83os*
B3gat1	*Eapp*	*Ifnk*	*Mrpl14*	*Psg27*	*Stx3*	*Wdr91*
Batf2	*Eftud2*	*Ikzf5*	*Mrpl27*	*Pskh1*	*Sult1a1*	*Wfdc12*
Bbs1	*Ehmt2*	*Impg2*	*Mrpl46*	*Ptger3*	*Sult1c1*	*Whsc1l1*
BC017643	*Elavl2*	*Inadl*	*Mta2*	*Rab19*	*Sult4a1*	*Zbtb22*
BC027072	*Ell3*	*Ino80e*	*Mtss1l*	*Rab30*	*Suz12*	*Zc3h4*
BC051019	*Emp1*	*Iqcc*	*Mybbp1a*	*Rasgrp3*	*Syk*	*Zcchc5*
Blvra	*Enox1*	*Iqcf4*	*Myeov2*	*Rasl11b*	*Tab1*	*Zcwpw1*
Bpifb9a	*Eps8l3*	*Itpa*	*Naip5*	*Rbm17*	*Tagln3*	*Zfand2a*
Brd9	*Esm1*	*Kctd15*	*Ncbp1*	*Rbm19*	*Tbl2*	*Zfp235*
Bst2	*Fam120aos*	*Khdrbs3*	*Ncoa5*	*Rexo4*	*Tcea1*	*Zfp260*
C1ql2	*Fam151a*	*Kif18a*	*Ndfip1*	*Rhbdf2*	*Tcof1*	*Zfp513*
Calca	*Fam183b*	*Krcc1*	*Nif3l1*	*Ric8b*	*Tgfbr1*	*Zfp654*
Cbx3	*Fam195b*	*Krt19*	*Nradd*	*Rnf170*	*Tgs1*	*Zfp664*
Ccdc148	*Fam20a*	*Lce1f*	*Nrsn2*	*Ropn1*	*Them6*	*Zscan20*
Ccdc3	*Fam43a*	*Lce3a*	*Ntf5*	*Rp1l1*	*Thumpd3*	
Ccdc34	*Fam53b*	*Ldoc1*	*Nts*	*Rpl10l*	*Tm2d1*	
Ccl20	*Fank1*	*Lefty2*	*Nudt2*	*Rps29*	*Tmed2*	

Table 3: The list of all genes in module 6.

Three genes associated with the differentiation, *disintegrin-like and metallopeptidase (reprolysin type) with thrombospondin type 1 motif, 7* (*Adamts7*), *snail family zinc finger 2* (*Snai2*), and *transforming growth factor, beta receptor I* (*Tgfbr1*), are indicated in red.

GO term	PValue	Genes
regulation of epithelial to mesenchymal transition	5.42E-04	*TGFBR1, CLASP1, ELL3, FAM195B*
chaperone-mediated protein folding	7.16E-04	*TTC9B, FKBP14, PDIA4, FKBP11, UNC45B*
sulfur compound metabolic process	0.02	*SULT4A1, CHST7, SULT1C1*
pharyngeal system development	0.02	*FGF8, GATA3, TGFBR1*
negative regulation of chondrocyte differentiation	0.02	*ADAMTS7, SNAI2, TGFBR1*
protein folding	0.02	*TMX1, PFDN2, FKBP14, PDIA4, FKBP11, TUBA1B*
positive regulation of endoplasmic reticulum calcium ion concentration	0.03	*ATP2A2, ATP2A1*
regulation of muscle contraction	0.03	*HSPB6, ATP2A2, ATP2A1*
positive regulation of cell cycle arrest	0.04	*UHRF2, HMGA2, MYBBP1A*
multicellular organismal reproductive process	0.04	*UMODL1, COMT*

Table 4: GO Terms searched using DAVID based on genes in module 6.

The functional annotation of DAVID version 6.8 was used to search for GO Terms in module 6, and GO Terms with *p*-values less than 0.050 in the GOTERM_BP_DIRECT category were extracted. From left to right, the table shows GO Term, p-value, and genes in Module 6 corresponding to the GO Term.

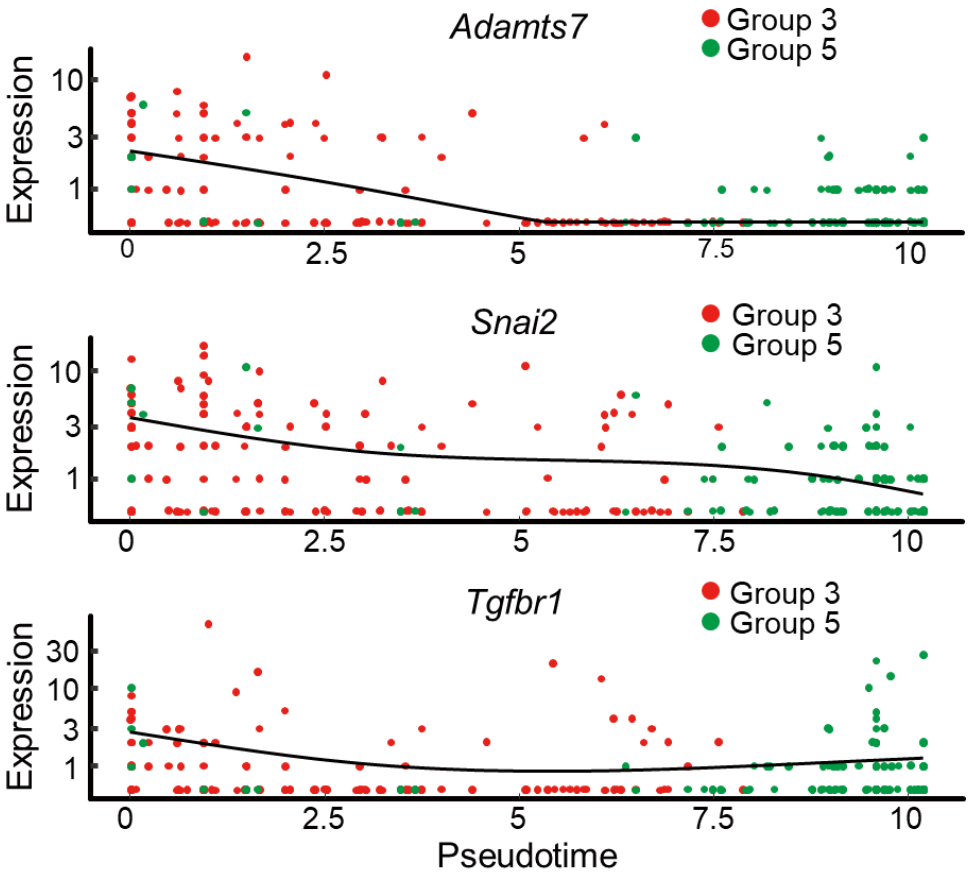

Figure 23: Gene expression patterns with pseudotime course.

The horizontal axis shows the pseudotime course, and the vertical axis shows the gene expression. The black line shows the gene expression pattern of *Adamts7*, *Snai2*, and *Tgfbr1* with the pseudotime course. The red dots represent cells in Group 3 (cell number, n = 136), and the green dots represent cells in Group 5 (cell number, n = 134).

Age-associated changes with pseudotime course

The gene expression patterns of *Adamts7*, *Snai2*, and *Tgfbr1*, which associate with negative regulation of differentiation, and *Lpl*, *Efemp1*, *Egfr*, and *Igfbp4*, which are highly expressed in preadipocytes, were examined in young and old mice (Figure 24). There were differences in the expression pattern of *Adamts7*, *Egfr*, and *Igfbp4* with the pseudotime course between young and old mice, At the same time, there were no significant differences in the expression pattern of *Snai2*, *Tgfbr1*, *Lpl*, and *Efemp1* with the pseudotime course between young and old mice.

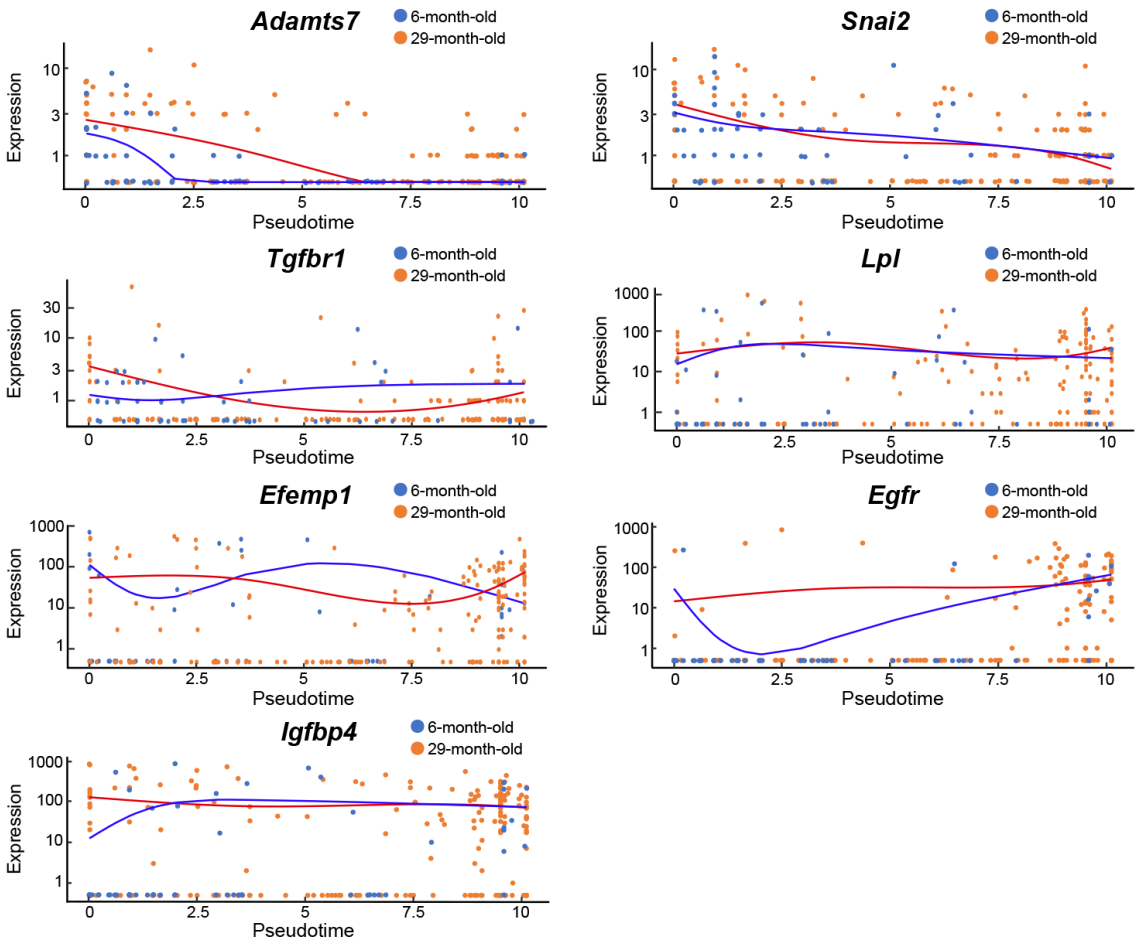

Figure 24: Age-associated changes in gene expression patterns with pseudotime course.

These show the gene expression patterns of *Adamts7*, *Snai2*, *Tgfbr1*, *Lpl*, *Efemp1*, *Egfr*, and *Igfbp4* with pseudotime course in 6-month-old (blue line) and 29-month-old (red line). Blue dots indicate young cells (cell number, n = 61), and orange dots indicate old cells (cell number, n = 209).

Examination of age-associated changes in ASCs using GSEA and PPI analysis

Because Group 3 cells are highly undifferentiated among ASCs, Group 3 were focused on and examined the changes in gene expression in young and old mice using GSEA [49, 50]. The GSEA compared gene expression data of Group 3 between young and old and found that genes included in four gene sets such "heterochromatin organization", "coat protein complex I (COPI)-coated vesicle membrane", "histone H3 deacetylation", and "forkhead box O (FOXO) -mediated transcription of oxidative stress metabolic and neuronal genes" were more frequently enriched in old mouse Group 3 than in young mouse Group 3. The corresponding NESs were 1.68, 1.52, 1.48, and 1.54, respectively (Figure 25A-D, Supplemental table 3-6). On the other hand, genes included in the three gene sets such "the structural constituents of ribosomes", "cytosolic ribosomes", and "extracellular matrix structural constituents conferring tensile strength" were more frequently enriched in young mouse Group 3 than in the old mouse Group 3. The corresponding NESs were -2.04, -2.00, and -1.93, respectively. (Figure 25E-G, Supplemental tables 7-9). Finally, the genes that contributed to the increase in absolute enrichment score in each gene set were extracted and used to perform the PPI analysis using STRING (Figure 25) [52].

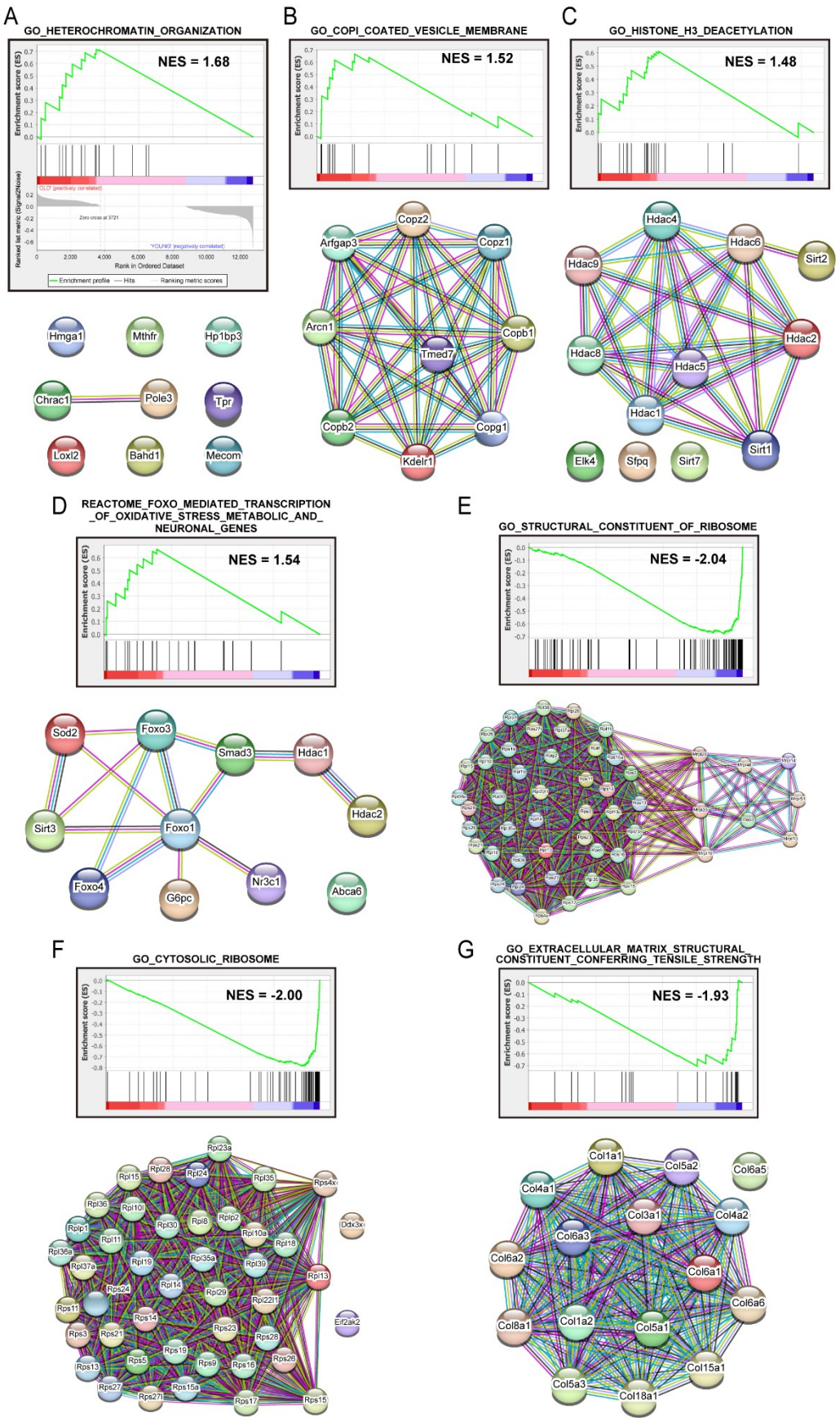
A
GO_HETEROCHROMATIN_ORGANIZATION
NES = 1.68
Enrichment score (ES)
Ranked list metric (Signal2Noise)
Rank in Ordered Dataset
Enrichment profile
Hits
Ranking metric scores
Hmga1
Mthfr
Hp1bp3
Chrac1
Pole3
Tpr
Loxl2
Bahd1
Mecom
B
GO_COPI_COATED_VESICLE_MEMBRANE
NES = 1.52
Copz2
Arfgap3
Copz1
Arcn1
Copb1
Tmed7
Copb2
Copg1
Kdelr1
C
GO_HISTONE_H3_DEACETYLATION
NES = 1.48
Hdac4
Hdac6
Hdac9
Sirt2
Hdac2
Hdac8
Hdac5
Hdac1
Sirt1
Elk4
Sfpq
Sirt7
D
REACTOME_FOXO_MEDIATED_TRANSCRIPTION_OF_OXIDATIVE_STRESS_METABOLIC_AND_NEURONAL_GENES
NES = 1.54
Sod2
Foxo3
Smad3
Hdac1
Hdac2
Sirt3
Foxo1
Foxo4
G6pc
Nr3c1
Abca6
E
GO_STRUCTURAL_CONSTITUENT_OF_RIBOSOME
NES = -2.04
F
GO_CYTOSOLIC_RIBOSOME
NES = -2.00
Rpl23a
Rpl28
Rpl15
Rpl24
Rpl35
Rps4x
Rpl36
Rpl10l
Rplp1
Rpl30
Rpl8
Rplp2
Ddx3x
Rpl11
Rpl10a
Rpl18
Rpl36a
Rpl37a
Rpl19
Rpl35a
Rpl39
Rpl13
Rps24
Rpl14
Rpl29
Rpl22l1
Rps11
Rps14
Eif2ak2
Rps3
Rps21
Rps23
Rps28
Rps19
Rps5
Rps9
Rps16
Rps26
Rps13
Rps27
Rps15a
Rps27l
Rps17
Rps15
G
GO_EXTRACELLULAR_MATRIX_STRUCTURAL_CONSTITUENT_CONFERRING_TENSILE_STRENGTH
NES = -1.93
Col1a1
Col5a2
Col6a5
Col4a1
Col3a1
Col4a2
Col6a3
Col6a2
Col6a1
Col6a6
Col8a1
Col1a2
Col5a1
Col15a1
Col5a3
Col18a1

Figure 25: Examination of age-associated changes in ASCs using GSEA and PPI analysis. GSEA results show the enrichment score (green line) and gene distributions (black line) among 12,729 genes rearranged according to the relative expression levels in Group 3 between young and old mice. Bars colored according to the gene distribution between the young (blue) and old (red) groups are shown. (A-C), (E-G) Results were obtained using the GO public database (c5.all). (D) Results were obtained using a curated public database (c2.all). All figures' nominal p-values are lower than 0.05. (A–G) PPI among core enrichment genes of each gene set was analyzed using STRING. The confidence score cutoff for showing edges was set to 'high' (confidence score > 7.0). Edge colors indicated the type of evidence such as (i) co-expression (black), (ii) text-mining (yellow), (iii) biochemical/genetic data ("experiments") (magenta), and (iv) previously curated pathway and protein-complex knowledge ("databases") (cyan) of STRING. All genes included in each gene set are listed in Supplemental tables 3-9.

Chapter 5 Discussion

This study performed the scRNA-seq to compare ASCs in the uncultured SVF between young and old. Bioinformatic approaches such as Seurat, Monocle 3, GSEA, and STRING were used to examine the age-associated changes in gene expression of ASCs. As a result, Groups 1-3-5 was identified as ASCs among 11 groups of the SVF. Pseudotime analysis suggested that Group 3 was more undifferentiated than Group 5 and revealed age-associated high gene expression levels of *Adamts7*, *Egfr*, and *Igfbp4* in the earliest differentiation stage of ASCs. Furthermore, GSEA was performed on Group 3, highly undifferentiated ASCs, and revealed that genes included in four gene sets such as "heterochromatin organization", "coat protein complex I (COPI)-coated vesicle membrane", "histone H3 deacetylation", and "forkhead box O (FOXO) -mediated transcription of oxidative stress metabolic and neuronal genes", were more frequently enriched in old mouse ASCs compared to young mouse ASCs, while genes included in three gene sets such as "the structural constituents of ribosomes", "cytosolic ribosomes", and "extracellular matrix structural constituents conferring tensile strength", were more frequently enriched in young mouse ASCs compared to old mouse ASCs.

Identification of the cell populations in the SVF

The SVF cells were classified into 11 groups based on the comprehensive gene expression data of the SVF cells. Then, the top 10 genes that were characteristically expressed in each group were used to predict that Groups 0-2-4 was HSC, Groups 1-3-5 was ASC, Group 6 was sperm, Group 7 was Sertoli cell, Group 8 was B cell, Group 9 was mast cell, and Group 10 was macrophage.

Groups 0-2-4 was predicted to be the cell population of HSCs. HSC is a member of the somatic stem cells that can differentiate into hematopoietic cells such as neutrophils, red blood cells, mast cells, and macrophages. Most HSCs are distributed in the bone marrow. A few HSCs are thought to exist in adipose tissue, but it is unclear whether HSCs in adipose tissue are homogeneous with HSCs in bone marrow [81]. Therefore, it is considered that HSCs were included in the analysis of this study to be reasonable.

Group 6 was predicted to be the cell population of sperms. However, the SVF does not usually contain sperms. Group 6 was composed only of cells from a young mouse. These suggest that sperms may have been contaminated during the collection of the SVF. Therefore, Group 6 was excepted from further analyses.

Group 7 was predicted to be the cell population of Sertoli cells. Because Sertoli cells are cells that assist and promote spermatogenesis in the testis, it is unlikely that Sertoli cells were included in the SVF. However, unlike the sperms, composed only of cells from a young mouse, Group 7 consisted of 5 and 89 cells from young and old SVF, respectively. These suggested that the cell population of Group 7 may have properties similar to those of Sertoli cells, although additional validation is needed for the more accurate prediction.

Group 8 was predicted to be the cell population of B cells. B cells play a central role in the humoral immunity of the body by producing antibodies. Immunoglobulins on the cell surface of

a B cell recognize antigens such LPS, a major component of the cell wall of Gram-negative bacteria, and import the antigens into the B cell to generate antibodies against the antigens [82].

Group 9 was predicted to be the cell population of mast cells. Mast cells have a receptor (high-affinity receptor for IgE) that recognizes Immunoglobulin E (IgE), a type of immunoglobulin. When the IgE that recognized antigens binds to the receptor, mast cells secrete histamine and neutral serine proteases into the extracellular space [65-67]. Mast cells are widely distributed in animal tissues, including adipose tissue, and are considered contained in the SVF.

Group 10 was predicted to be the cell population of macrophages. Macrophages are cells that phagocytose and digest dead cells and bacteria that invade from outside the body. They also have functions such as secreting cytokines that activate other lymphocytes and chemokines that recruit other lymphocytes to the inflamed site [69-71]. Because it has been reported that hematopoietic cells such as B cells, mast cells, and macrophages are also included in the SVF [28], it is considered that these hematopoietic cells were included in the analysis of this study to be reasonable.

Seventeen genes highly expressed in ASCs, *Gsn*, *Clec3b*, *Gpx3*, *Fstl1*, *Ppap2b*, *Dpep1*, *Hp*, *Pi16*, *Cxcl1*, *Sult1e1*, *Bgn*, *Htra3*, *Mmp2*, *Inmt*, *Nid1*, *Sparcl1*, and *Agt*, were characteristically expressed in Groups 1-3-5. In addition, the expression levels of six typical ASC marker genes, *Gsn*, *Cxcl1*, *Col1a2*, *Col6a1*, *Mmp2*, and *Mmp14*, were higher in Groups 1-3-5 than in the other eight groups. Based on these results, Groups 1-3-5 was identified as the cell population of ASCs.

Sca1 was originally identified as a marker protein for hematopoietic stem cells [75, 83] and mesenchymal stem cells, including ASCs [84, 85]. The expression level of *Ly6a* was high in Groups 1-3-5, while the expression level of *Ly6e* was low. This result suggests that *Ly6a* may be more valuable than *Ly6e* as a marker gene to identify ASCs.

Differences between young and old in the SVF

The percentages of Groups 1-3-5 in the SVF of young and old mice was 50.0% in young, and 37.1% in old, and they were about 0.7-fold lower in old than in young. In other groups, the percentages of B cells (Group 8), mast cells (Group 9), and macrophages (Group 10) were 2.4, 3.3, and 15.5 times higher in old than in young, respectively. On the other hand, the percentages of HSCs (Groups 0-2-4) and their three constituent groups, Group 0, Group 2, and Group 4, were not significantly different between young and old. However, these data are not enough to discuss whether the number of ASCs in the adipose tissue decreases with age. It has been reported that aging increases the secretion of inflammatory cytokines in adipose tissue [86]. In another report, the expression levels of inflammatory cytokines such as *prostaglandin-endoperoxide synthase 2* (*Ptgs2*), *interleukin 1* (*IL-1*), *IL-6*, and *tumor necrosis factor* (*TNF-α*) were higher in the epididymal fat of old (22-24 months old) mice than in the epididymal fat of young (5-6 months old) mice [87]. In this analysis, the percentages of lymphocytes such as B cells, mast cells, and macrophages were higher in the old mouse SVF than in the young mouse SVF. This suggested that inflammation in adipose tissue might be more active with age and that the balance between ASCs and lymphocytes in adipose tissue may change with age.

Differentiation stages in ASCs

Based on the pattern of the t-SNE plots of Groups 1-3-5 and the expression levels of genes highly expressed in preadipocytes and adipocytes in Groups 1-3-5, it was predicted that Group 5 are close to preadipocytes and are in the most advanced stage of differentiation, Group 3 are highly undifferentiated and in the earliest stage of differentiation, and Group 1 are intermediate ASCs between Group 5 and Group3. Monocle3 and GO analysis were performed and identified three genes, *Adamts7*, *Snai2*, and *Tgfbr1*, that were more highly expressed in Group 3 than in Group 5. *Adamts7* is a metalloproteinase that belongs to the ADAMTS family and inhibits chondrocyte differentiation by inactivating the progranulin, a growth factor secreted by cultured ASCs [77, 88, 89]. However, it has not yet been validated whether *Adamts7* is involved in the differentiation of ASCs through the inactivating the progranulin. In this study, pseudotime analysis confirmed that high expression levels of *Adamts7* were observed in the early differentiation stage of ASCs, followed by a significant decrease in the advanced differentiation stage of ASCs. These results strongly suggest that *Adamts7* is involved in maintaining the undifferentiated state of ASCs through the inactivation of progranulin. *Snai2* is a transcription factor that represses the differentiation of human epidermal progenitor cells and adipocytes [78, 79]. *Tgfbr1* is a receptor for TGF-β and suppresses the differentiation of rat bone marrow-derived mesenchymal stem cells into osteoblasts [80]. However, the relationship between *Tgfbr1* and the differentiation of ASC is still unclear. It is considered that the pseudotime obtained from Monocle 3 shows the course of differentiation of ASCs because these three genes are negative regulators of differentiation and their expression decreased with pseudotime course. These supported the initial prediction.

Age-associated changes in ASCs

Based on the previous results, ASCs were examined and compared between young and old. In Young mouse ASCs, there were more cells in Group 3, Group 1, and Group 5 in that order, while in old mouse ASCs, there were more cells in Group 1, Group 5, and Group 3 in that order. Compared to young, the percentages of Group1 and Group 5 in old mouse ASCs were 1.6-fold and 2.3-fold higher, respectively, while the percentage of Group 3 was 0.4-fold lower. These results suggest that the relative number of undifferentiated ASCs might decrease with age.

Next, the positive cell rates for six typical ASC marker genes, *Gsn*, *Cxcl1*, *Col1a2*, *Col6a1*, *Mmp2*, and *Mmp14*, were examined in Groups 1, Group 3, and Group 5. Differences in the positive cell rates of *Gsn*, *Cxcl1*, *Col6a1*, *Mmp2*, and *Mmp14* were confirmed, but there were no significant differences in the positive cell rates of *Col1a2* between young and old mice in any group. However, these statistical differences are too small to consider biological differences. Therefore, these results suggest that age-associated changes in the positive cell rates for the six typical ASC marker genes are not particularly large.

To examine age-associated changes in expression of genes associated cellular senescence in ASCs, the positive cell rates of nine SASP factors, *IL-6*, *Cxcl2*, *Ccl11*, *Igfbp4*, *Igfbp6*, *Igfbp7*, *Mmp3*, *Timp2*, and *Ctsb*, and three genes associated with the cell cycle arrest, *Cdkn1a*, *Trp53*, and *Cdkn2a*, were compared between young and old. Differences in the positive cell rates of *Cxcl2*, *Ccl11*, *Igfbp4*, *Igfbp6*, *Mmp3*, *Timp2*, *Ctsb*, and *Cdkn1a* were confirmed. However, these statistical differences are too small to consider biological differences. There were no significant differences in the positive cell rates for *IL-6*, *Igfbp7*, and *Trp53* between young and old in any of the groups, and the expression of *Cdkn2a* was too low to be detected in this study. Since there were differences in the positive cell rates of seven SASP factors, these genes expressions might

have a few age-associated changes. On the other hand, these results of *Cdkn1a*, *Trp53*, and *Cdkn2a* suggest that age-related changes in the positive cell rates of the genes associated with the cell cycle arrest are also not particularly large.

Age-associated differences in the expression patterns with pseudotime course

The high expression levels of *Adamts7* were observed in the early differentiation stages of old mouse ASCs and did not decrease significantly with pseudotime course. On the other hand, the high expression levels of *Adamts7* decreased significantly with the pseudotime course. Moreover, pseudotime analysis of Monocle3 showed that the gene expression of *Egfr* and *Igfbp4* differed between young and old ASCs in the early differentiation stage. *Egfr* is a receptor for epidermal growth factor and activates intracellular signaling pathways involved in cell differentiation and proliferation [90]. When epidermal growth factor was added to the medium culturing ASCs isolated from human adipose tissue, the expression levels of genes associated with cell cycle progression, *cyclin D1* (*CCND1*), *cyclin-dependent kinase 2* (*CDK2*), *cyclin-dependent kinase 6* (*CDK6*), *E2F transcription factor 1* (*E2F1*), and *high mobility group AT-hook 1* (*HMGA1*), and genes associated with adipocyte differentiation, *PPARγ*, *peroxisome proliferator-activated receptor-γ coactivator-1α* (*PGC1α)*, and *C/EBPα*, increased in human ASCs [91]. In this study, the expression level of *Egfr* was low in the early differentiation stage of young mouse ASCs and then increased with pseudotime course. On the other hand, there was no significant change in the expression level of *Egfr* across all differentiation stages in old mouse ASCs.

Igfbp4 is also highly expressed in adipocytes and contributes to adipose tissue development [92]. In this study, the gene expression of *Igfbp4* was low in the early differentiation stage of young mouse ASCs compared to old mouse ASCs. On the other hand, there was no significant change in the expression level of *Igfbp4* across all differentiation stages in old mouse ASCs. The stem cell differentiation is strictly controlled by the balance of transcription factors such as *Pparγ*

and *Cebpα* and signaling pathways activated by bioactive substances such as the endothelial growth factor and the fibroblast growth factor [93]. Therefore, these results suggest that old mouse ASCs cannot maintain strictly the balance of the transcription factors and bioactive substances involved in ASCs differentiation with age-associated changes in regulatory mechanisms of these gene expressions compared to young mouse ASCs and may have difficulty progressing differentiation as needed. This suggestion is consistent with the idea of dysdifferentiation hypotheses of aging proposed by Richard G. Cutler [1]. One of the factors that cause instability in gene expression regulation is age-associated changes of epigenetics such as DNA methylation, histone modifications, and microRNA expression. The study examining age-related changes in epigenetics of *Adamts7*, *Egfr*, and *Igfbp4* would contribute to elucidating the mechanism of age-related decline in differentiation potential in ASCs. Because it is the function of ASCs to differentiate as needed correctly, it is also considered that ASCs that have less stringency of the regulation of the expression of some genes involved in differentiation are senescent cells.

It is interesting to see how these senescent cells are distributed in the epididymal fat of an aged animal. However, the scRNA-seq cannot provide us with information on the distribution of senescent cells in tissues of an aged animal. In the future, I would like to investigate the distribution of senescent cells in tissues using the spatial transcriptome such as sequential fluorescence *in situ* hybridization (seqFISH+) [94] and multiplexed error-robust FISH (MERFISH) [95], which can simultaneously examine the location of senescent cells in tissues in addition to comprehensive gene expression analysis. This study examines transcriptome in mouse SVFs with low damages as far as possible. However, some treatments during the collection of SVFs, such as centrifugation and incubation with type I collagenase might affect gene expression differently because of differences in sensitivity to any extrinsic stimulations between young and

old ASCs. This spatial transcriptome can examine gene expressions with less invasiveness than this study and allows us to analyze the properties of ASCs under conditions closer to those of living organisms.

Age-associated changes of gene expression in Group 3

GSEA was performed using only the gene expression data of Group 3 because it is considered Group 3 to represent the earliest differentiation stage of ASCs from young and old mice from the pseudotime analysis using Monocle3. GSEA found that genes included in four gene sets such "heterochromatin organization", "coat protein complex I (COPI)-coated vesicle membrane", "histone H3 deacetylation", and “forkhead box O (FOXO) -mediated transcription of oxidative stress metabolic and neuronal genes" were more frequently enriched in old mouse Group 3 than in young mouse Group 3 (Supplemental table 3-6). Genes in the gene set "heterochromatin organization" that contributed to the increase in absolute enrichment score included *Hmga1, DNA polymerase epsilon 3, accessory subunit* (*Pole3*), and *chromatin accessibility complex subunit 1* (*Chrac1*). The CHRAC1/POLE3 heterodimer promotes ATP-dependent chromatin remodeling and is also involved in repairing DNA double-strand breaks [96, 97]. *Hmga1* is important for forming the characteristic heterochromatin structure observed in a type of senescent cells [98]. The coat protein complex I (COPI) is a major factor in the maturation of the Golgi cis-tank and retrograde transport from the Golgi to the endoplasmic reticulum and is composed of seven subunits (α, β, β', γ, δ, ε, ζ) [99]. The "coat protein complex I (COPI)-coated vesicle membrane" gene set contained α, β, γ, ε, and ζ of the seven COPI subunits, and these subunits contributed to the increase in the absolute enrichment score. These results suggest that the structure of COPI may become unstable with age, and the function of retrograde transport may be impaired.

The "histone H3 deacetylation" gene set contained *sirtuin 1* (*Sirt1*), *sirtuin 2* (*Sirt2*), and *histone deacetylase 6* (*Hdac6*), and these genes contributed to the increase in absolute enrichment score. *SIRT1* and *SIRT2* are protein deacetylases, and their main targets are Trp53 (p53), DNA methyltransferase 1 (DNMT1), and proteins belonging to the FOXO family [100]. Knockdown

of *SIRT1* inhibits proliferation and differentiation of human ASCs [101], while knockdown of *Sirt2* promotes differentiation of mouse 3T3-L1 preadipocytes into adipocytes [102]. PPI analysis using STRING found the relationship between *Hdac6* and *Sirt1*. HDAC6/SIRT1 inhibits nucleotide excision repair via deacetylation of replication protein A1 in eukaryotic cells [103]. Because *Chrac1*, *Pole3*, *Sirt1*, and *Hdac6* are highly expressed in Group 3 of an old mouse, various DNA repair systems might be promoted in the earliest differentiation stage of ASCs from an old mouse.

The "forkhead box O (FOXO)-mediated transcription of oxidative stress metabolic and neuronal genes" gene set contained *Foxo1*, *Foxo4*, and *superoxide dismutase 2* (*Sod2*), and these genes contributed to the increase in absolute enrichment score. PPI analysis using STRING revealed two relationships, one between *Foxo1* and *Sod2* and the other between *Foxo1* and *Foxo4*. *Foxo1* and *Sod2* regulate differentiation into adipocytes [104, 105]. On the other hand, Foxo4, which inhibits apoptosis by directly binding to p53, is associated with cellular senescence and targets senolytic drugs, specifically inducing apoptosis in senescent cells [17, 106]. The high expression of *Foxo4* and *Hmga1* in Group 3 of the old mouse suggested that Group 3 of the old mouse is in a previous phase of cell cycle arrest.

Furthermore, GSEA found that genes included in three gene sets such "the structural constituents of ribosomes," "cytosolic ribosomes," and "extracellular matrix structural constituents conferring tensile strength" were more frequently enriched in young mouse Group 3 than in old mouse Group 3 (Supplemental table 7-8). Two gene sets, "the structural constituents of ribosomes" and "cytosolic ribosomes," contain genes that encode ribosomes responsible for protein translation. The "cytosolic ribosomes" gene set contained 52 genes encoding ribosomal proteins that function in cells. The structural constituents of ribosomes" contained 64 genes

encoding ribosomal proteins that function in mitochondria and the 52 genes included in the "cytosolic ribosomes" gene set. Among these genes, 43 ribosomal proteins that function in cells and 7 ribosomal proteins that function in mitochondria contributed to the increase in absolute enrichment score. These results suggested that ribosomal protein biosynthesis's potential to function in cells declined in old mouse ASCs in the earliest differentiation stage. Ribosome biosynthesis plays an essential role in the differentiation of mesenchymal stem cells [107]. Diamond-Blackfan anemia is a congenital heart disease caused by genetic mutations in multiple ribosomal proteins. Genetic mutations in ribosomal proteins reduce the amount of ribosomal proteins in hematopoietic stem cells and prevent the normal differentiation into red blood cells [108]. There had been no reports of age-associated changes in ribosomal proteins in ASCs.

The "extracellular matrix structural constituents conferring tensile strength" gene set contained genes belonging to the family of type VI collagen alpha (Col6a) (Supplemental table 9). PPI analysis using STRING did not find any relationships between *collagen type VI alpha 5 chain* (*Col6a5*) and other members of the Col6a family, and the role of *Col6a5* in ASCs is still unclear. Type VI collagens are major components of the extracellular matrix of adipose tissue [109, 110] and play an important role in the self-renewal potentials of ASCs and their differentiation into adipocytes [110]. The deficiency of COL6A in knockout mice induces adipocyte hypertrophy and fragility of the extracellular matrix in adipose tissue, although the total fat weight is lower than in wild-type mice [110]. Adipocytes in epididymal and subcutaneous fat of C57BL6 male mice become enlarged with age [111]. GSEA indicated that the expressions of type VI collagens decreased in old mouse ASCs in the earliest differentiation stage. These results suggested that the low expressions of type VI collagens in old mouse ASCs might be factoring in the age-related hypertrophy of adipocytes and the reduction of self-renew and differentiation potentials of ASCs.

The future of senescence studies in ASCs

This study examined the transcriptome of SVFs obtained from young and old male mouse epididymal fat. Since sex-dependent differences in the transcriptome of visceral fat have been confirmed [34], the findings of this study should be confirmed in female mouse gonadal fat in further analysis.

In the 20th century, the search for genes with life-extending effects was actively pursued using model organisms such as *C. elegans*, *Drosophila melanogaster*, and *Mus musculus* to reveal the biological mechanisms of senescence. Considering the application to humans, it is ethically difficult to edit such genes of a fetus to extend its lifespan. Recently, many researchers have been trying to develop senolytic drugs, which are drugs that specifically induce apoptosis in senescent cells. It is expected to extend healthy life expectancy using senolytic drugs. Famous senolytic drugs include Quercetin, a polyphenol found in onion peels, and Dasatinib, a molecular target drug that binds to tyrosine kinase and inhibits its activity, used in the treatment of chronic myeloid leukemia [112]. In 2017, FOXO4-DRI (forkhead box O4 peptide in a D-retro inverso conformation), a peptide synthesized from a portion of Foxo4 with D-amino acids, was developed as a senolytic drug and improved walking ability, renal function, and body fur density of old mice by administration [113]. Moreover, N, N'- [Thiobis (2,1-ethanediyl-1,3,4-thiadiazole-5,2-diyl)] bisbenzeneacetamide (BPTES), which was already known as an inhibitor of glutaminase 1 (GLS1), a glutamine-metabolizing enzyme, was found to be a senolytic drug. The administration of BPTES improved muscular endurance and renal function and decreased serum levels of inflammatory cytokines TNF-α and IL-6 in old mice [114]. Each senolytic drug that has already been developed targets a different molecule. Therefore, it is necessary to combine multiple senolytic drugs or develop more useful senolytic drugs for clinical application in humans.

However, even if senescent cells are selectively induced cell death in animal tissues using senolytic drugs, it does not necessarily mean that the physiological functions of organs will be improved, or that healthy life expectancy will be extended.

There is no senolytic drug that acts on senescent ASCs. In this study, the expression patterns of *Adamts7* with pseudotime course were different between young and old. However, it is difficult to apply *Adamts7* to a target for senolytic drugs because young mouse ASCs also express *Adamts7*. This study suggests that old mouse ASCs cannot strictly maintain the balance of the transcription factors and bioactive substances involved in ASCs differentiation with age-associated changes in regulatory mechanisms of these gene expressions compared to young mouse ASCs and may have difficulty progressing differentiation as needed. Since epigenetics, the regulatory mechanisms of gene expression, such as DNA methylation, histone protein modification, and microRNA expression, are altered during aging [9-11], epigenetics is expected to be a candidate as a target for senolytic drugs instead of *Adamts7*. In the future, I would like to identify the epigenetics that are characteristic of old animal ASCs and develop senolytic drugs targeting them. It is important to confirm whether a cell expressing a target for senolytic drugs is the senescent cell. Functional and molecular characteristics of senescent cells are still largely unknown. Since senescent cells are defined as cells whose physiological functions decline with age, physiological functions which decline with age should be different for each cell type. For example, ASCs whose differentiation and self-renewal potentials decline with age can be considered senescent cells because these are major functions of ASCs. If the differentiation potential in old mouse ASCs recovers to the same level as that in young mouse ASCs after administration of the drug under development, the drug could be considered to induce cell death in senescent cells. These senolytic drugs are expected to contribute to further improvements in the outcome of patients who have undergone regenerative medicine using ASCs.

Chapter 6 Conclusion

In this study, microwell-based scRNA-seq was performed to examine comprehensive gene expression in uncultured ASCs and compare them between young and old mice. This study suggested that old mouse ASCs have less stringency of the regulatory mechanism of some gene expressions involved in ASCs differentiation than young mouse ASCs and may have difficulty progressing differentiation as needed. This suggestion is consistent with the idea of dysdifferentiation hypotheses of aging proposed by Richard G. Cutler. Since it is the function of ASCs to differentiate as needed correctly, it is considered that ASCs that have less stringency of the regulation of the expression of some genes involved in differentiation are senescent cells. The distribution of senescent ASCs in adipose tissue is still unclear. I would like to investigate the distribution of these senescent cells in adipose tissue using spatial transcriptome techniques such as seqFISH+ [94] and MERFISH [95] in the future. Although additional studies are needed to conclude whether the differentiation potential of elderly people declines with age similar to that of mice, the observations obtained from this study could contribute to understanding age-associated changes of ASCs. However, it is necessary to experimentally validate each finding in this study in a different way. The age-associated changes of epigenetics are supposed to be one of the factors that destabilize the regulation of gene expression. Therefore, I focus on epigenetics as candidates for the target of senolytic drugs. In the future, I would like to identify the epigenetics characteristic of senescent ASCs and develop senolytic drugs targeting identified epigenetic characteristics. I hope that the development of senolytic drugs would contribute to the extension of healthy life expectancy and the elucidation of biological mechanisms of senescence.

References

[1] R.G. Cutler, Recent progress in testing the longevity determinant and dysdifferentiation hypotheses of aging, Archives of Gerontology and Geriatrics 12(2) (1991) 75-98.

[2] S. Goto, The Biological Mechanisms of Aging: A Historical and Critical Overview, Aging Mechanisms, Springer, Tokyo2015, pp. 3-27.

[3] K. Nitta, K. Okada, M. Yanai, S. Takahashi, Aging and Chronic Kidney Disease, Kidney and Blood Pressure Research 38(1) (2013) 109-120.

[4] G.M. Martin, S.N. Austad, T.E. Johnson, Genetic analysis of ageing: role of oxidative damage and environmental stresses, Nature Genetics 13(1) (1996) 25-34.

[5] Z.A. MEDVEDEV, AN ATTEMPT AT A RATIONAL CLASSIFICATION OF THEORIES OF AGEING, Biological Reviews 65(3) (1990) 375-398.

[6] M. Xu, T. Pirtskhalava, J.N. Farr, B.M. Weigand, A.K. Palmer, M.M. Weivoda, C.L. Inman, M.B. Ogrodnik, C.M. Hachfeld, D.G. Fraser, J.L. Onken, K.O. Johnson, G.C. Verzosa, L.G.P. Langhi, M. Weigl, N. Giorgadze, N.K. LeBrasseur, J.D. Miller, D. Jurk, R.J. Singh, D.B. Allison, K. Ejima, G.B. Hubbard, Y. Ikeno, H. Cubro, V.D. Garovic, X. Hou, S.J. Weroha, P.D. Robbins, L.J. Niedernhofer, S. Khosla, T. Tchkonia, J.L. Kirkland, Senolytics improve physical function and increase lifespan in old age, Nature Medicine 24(8) (2018) 1246-1256.

[7] M. Xu, T. Tchkonia, H. Ding, M. Ogrodnik, E.R. Lubbers, T. Pirtskhalava, T.A. White, K.O. Johnson, M.B. Stout, V. Mezera, N. Giorgadze, M.D. Jensen, N.K. LeBrasseur, J.L. Kirkland, JAK inhibition alleviates the cellular senescence-associated secretory phenotype and frailty in old age, Proceedings of the National Academy of Sciences 112(46) (2015) E6301.

[8] T. Ono, R.G. Cutler, Age-dependent relaxation of gene repression: increase of endogenous murine leukemia virus-related and globin-related RNA in brain and liver of mice, Proceedings of

the National Academy of Sciences 75(9) (1978) 4431-4435.

[9] B.A. Benayoun, E.A. Pollina, A. Brunet, Epigenetic regulation of ageing: linking environmental inputs to genomic stability, Nature Reviews Molecular Cell Biology 16(10) (2015) 593-610.

[10] M. Zampieri, F. Ciccarone, R. Calabrese, C. Franceschi, A. Bürkle, P. Caiafa, Reconfiguration of DNA methylation in aging, Mechanisms of Ageing and Development 151 (2015) 60-70.

[11] H.E. Kinser, Z. Pincus, MicroRNAs as modulators of longevity and the aging process, Human Genetics 139(3) (2020) 291-308.

[12] P.L. de Keizer, The Fountain of Youth by Targeting Senescent Cells?, Trends Mol Med 23(1) (2017) 6-17.

[13] L. Hayflick, The limited in vitro lifetime of human diploid cell strains, Experimental Cell Research 37(3) (1965) 614-636.

[14] J.P. Coppe, C.K. Patil, F. Rodier, Y. Sun, D.P. Munoz, J. Goldstein, P.S. Nelson, P.Y. Desprez, J. Campisi, Senescence-associated secretory phenotypes reveal cell-nonautonomous functions of oncogenic RAS and the p53 tumor suppressor, PLoS Biol 6(12) (2008) 2853-68.

[15] J.P. Coppe, P.Y. Desprez, A. Krtolica, J. Campisi, The senescence-associated secretory phenotype: the dark side of tumor suppression, Annu Rev Pathol 5 (2010) 99-118.

[16] F. Rodier, J. Campisi, Four faces of cellular senescence, Journal of Cell Biology 192(4) (2011) 547-556.

[17] M.P. Baar, R.M.C. Brandt, D.A. Putavet, J.D.D. Klein, K.W.J. Derks, B.R.M. Bourgeois, S. Stryeck, Y. Rijksen, H. van Willigenburg, D.A. Feijtel, I. van der Pluijm, J. Essers, W.A. van Cappellen, W.F. van Ijcken, A.B. Houtsmuller, J. Pothof, R.W.F. de Bruin, T. Madl, J.H.J. Hoeijmakers, J. Campisi, P.L.J. de Keizer, Targeted Apoptosis of Senescent Cells Restores Tissue

Homeostasis in Response to Chemotoxicity and Aging, Cell 169(1) (2017) 132-147.e16.

[18] S. Hashimoto, Y. Tabuchi, H. Yurino, Y. Hirohashi, S. Deshimaru, T. Asano, T. Mariya, K. Oshima, Y. Takamura, Y. Ukita, A. Ametani, N. Kondo, N. Monma, T. Takeda, S. Misu, T. Okayama, K. Ikeo, T. Saito, S. Kaneko, Y. Suzuki, M. Hattori, K. Matsushima, T. Torigoe, Comprehensive single-cell transcriptome analysis reveals heterogeneity in endometrioid adenocarcinoma tissues, Sci Rep 7(1) (2017) 14225.

[19] C. Ziegenhain, B. Vieth, S. Parekh, B. Reinius, A. Guillaumet-Adkins, M. Smets, H. Leonhardt, H. Heyn, I. Hellmann, W. Enard, Comparative Analysis of Single-Cell RNA Sequencing Methods, Molecular Cell 65(4) (2017) 631-643.e4.

[20] T. Hashimshony, N. Senderovich, G. Avital, A. Klochendler, Y. de Leeuw, L. Anavy, D. Gennert, S. Li, K.J. Livak, O. Rozenblatt-Rosen, Y. Dor, A. Regev, I. Yanai, CEL-Seq2: sensitive highly-multiplexed single-cell RNA-Seq, Genome Biology 17(1) (2016) 77.

[21] Evan Z. Macosko, A. Basu, R. Satija, J. Nemesh, K. Shekhar, M. Goldman, I. Tirosh, Allison R. Bialas, N. Kamitaki, Emily M. Martersteck, John J. Trombetta, David A. Weitz, Joshua R. Sanes, Alex K. Shalek, A. Regev, Steven A. McCarroll, Highly Parallel Genome-wide Expression Profiling of Individual Cells Using Nanoliter Droplets, Cell 161(5) (2015) 1202-1214.

[22] Y. Ye, H. Song, J. Zhang, S. Shi, Understanding the Biology and Pathogenesis of the Kidney by Single-Cell Transcriptomic Analysis, Kidney Diseases 4(4) (2018) 214-225.

[23] J.M. Gimble, A.J. Katz, B.A. Bunnell, Adipose-Derived Stem Cells for Regenerative Medicine, Circulation Research 100(9) (2007) 1249-1260.

[24] R.D. González-Cruz, E.M. Darling, Adipose-derived stem cell fate is predicted by cellular mechanical properties, Adipocyte 2(2) (2013) 87-91.

[25] H. Mizuno, M. Tobita, A.C. Uysal, Concise Review: Adipose-Derived Stem Cells as a Novel Tool for Future Regenerative Medicine, STEM CELLS 30(5) (2012) 804-810.

[26] S. Sugii, Y. Kida, W.T. Berggren, R.M. Evans, Feeder-dependent and feeder-independent iPS cell derivation from human and mouse adipose stem cells, Nature Protocols 6(3) (2011) 346-358.

[27] M. Liu, H. Lei, P. Dong, X. Fu, Z. Yang, Y. Yang, J. Ma, X. Liu, Y. Cao, R. Xiao, Adipose-Derived Mesenchymal Stem Cells from the Elderly Exhibit Decreased Migration and Differentiation Abilities with Senescent Properties, Cell Transplantation 26(9) (2017) 1505-1519.

[28] S.P. Weisberg, D. McCann, M. Desai, M. Rosenbaum, R.L. Leibel, A.W. Ferrante, Jr., Obesity is associated with macrophage accumulation in adipose tissue, The Journal of Clinical Investigation 112(12) (2003) 1796-1808.

[29] X. Shan, C. Roberts, E.J. Kim, A. Brenner, G. Grant, I. Percec, Transcriptional and Cell Cycle Alterations Mark Aging of Primary Human Adipose-Derived Stem Cells, STEM CELLS 35(5) (2017) 1392-1401.

[30] M. Marędziak, K. Marycz, K.A. Tomaszewski, K. Kornicka, B.M. Henry, The Influence of Aging on the Regenerative Potential of Human Adipose Derived Mesenchymal Stem Cells, Stem Cells International 2016 (2016) 2152435.

[31] E.U. Alt, C. Senst, S.N. Murthy, D.P. Slakey, C.L. Dupin, A.E. Chaffin, P.J. Kadowitz, R. Izadpanah, Aging alters tissue resident mesenchymal stem cell properties, Stem Cell Research 8(2) (2012) 215-225.

[32] J.M. Gimble, A.J. Katz, B.A. Bunnell, Adipose-derived stem cells for regenerative medicine, Circ Res 100(9) (2007) 1249-60.

[33] Y. Doshida, H. Sano, S. Iwabuchi, T. Aigaki, M. Yoshida, S. Hashimoto, A. Ishigami, Age-associated changes in the transcriptomes of non-cultured adipose-derived stem cells from young and old mice assessed via single-cell transcriptome analysis, PLOS ONE 15(11) (2020) e0242171.

[34] C. Savva, L.A. Helguero, M. González-Granillo, T. Melo, D. Couto, B. Buyandelger, S. Gustafsson, J. Liu, M.R. Domingues, X. Li, M. Korach-André, Maternal high-fat diet programs

white and brown adipose tissue lipidome and transcriptome in offspring in a sex- and tissue-dependent manner in mice, International Journal of Obesity (2022).

[35] S. Yanai, S. Endo, Functional Aging in Male C57BL/6J Mice Across the Life-Span: A Systematic Behavioral Analysis of Motor, Emotional, and Memory Function to Define an Aging Phenotype, Frontiers in Aging Neuroscience 13(457) (2021).

[36] K. Xie, F. Neff, A. Markert, J. Rozman, J.A. Aguilar-Pimentel, O.V. Amarie, L. Becker, R. Brommage, L. Garrett, K.S. Henzel, S.M. Hölter, D. Janik, I. Lehmann, K. Moreth, B.L. Pearson, I. Racz, B. Rathkolb, D.P. Ryan, S. Schröder, I. Treise, R. Bekeredjian, D.H. Busch, J. Graw, G. Ehninger, M. Klingenspor, T. Klopstock, M. Ollert, M. Sandholzer, C. Schmidt-Weber, M. Weiergräber, E. Wolf, W. Wurst, A. Zimmer, V. Gailus-Durner, H. Fuchs, M. Hrabě de Angelis, D. Ehninger, Every-other-day feeding extends lifespan but fails to delay many symptoms of aging in mice, Nature Communications 8(1) (2017) 155.

[37] M. Iwama, A. Amano, K. Shimokado, N. Maruyama, A. Ishigami, Ascorbic Acid Levels in Various Tissues, Plasma and Urine of Mice during Aging, Journal of Nutritional Science and Vitaminology 58(3) (2012) 169-174.

[38] H. Li, R. Durbin, Fast and accurate long-read alignment with Burrows–Wheeler transform, Bioinformatics 26(5) (2010) 589-595.

[39] T. Stuart, A. Butler, P. Hoffman, C. Hafemeister, E. Papalexi, W.M. Mauck, 3rd, Y. Hao, M. Stoeckius, P. Smibert, R. Satija, Comprehensive Integration of Single-Cell Data, Cell 177(7) (2019) 1888-1902 e21.

[40] A.R. Jamieson, M.L. Giger, K. Drukker, H. Li, Y. Yuan, N. Bhooshan, Exploring nonlinear feature space dimension reduction and data representation in breast CADx with Laplacian eigenmaps and -SNE, Medical Physics 37(1) (2010) 339-351.

[41] J. Cao, M. Spielmann, X. Qiu, X. Huang, D.M. Ibrahim, A.J. Hill, F. Zhang, S. Mundlos, L.

Christiansen, F.J. Steemers, C. Trapnell, J. Shendure, The single-cell transcriptional landscape of mammalian organogenesis, Nature 566(7745) (2019) 496-502.

[42] R.M. Parra-Hernández, J.I. Posada-Quintero, O. Acevedo-Charry, H.F. Posada-Quintero, Uniform Manifold Approximation and Projection for Clustering Taxa through Vocalizations in a Neotropical Passerine (Rough-Legged Tyrannulet, Phyllomyias burmeisteri), Animals (Basel) 10(8) (2020) 1406.

[43] Q. Mao, L. Yang, L. Wang, S. Goodison, Y. Sun, SimplePPT: A Simple Principal Tree Algorithm, Proceedings of the 2015 SIAM International Conference on Data Mining (SDM), pp. 792-800.

[44] Q. Mao, L. Wang, I.W. Tsang, Y. Sun, Principal Graph and Structure Learning Based on Reversed Graph Embedding, IEEE Transactions on Pattern Analysis and Machine Intelligence 39(11) (2017) 2227-2241.

[45] X. Qiu, Q. Mao, Y. Tang, L. Wang, R. Chawla, H.A. Pliner, C. Trapnell, Reversed graph embedding resolves complex single-cell trajectories, Nature Methods 14(10) (2017) 979-982.

[46] P.A. Moran, Notes on continuous stochastic phenomena, Biometrika 37(1-2) (1950) 17-23.

[47] D.W. Huang, B.T. Sherman, R.A. Lempicki, Systematic and integrative analysis of large gene lists using DAVID bioinformatics resources, Nature Protocols 4(1) (2009) 44-57.

[48] D.W. Huang, B.T. Sherman, R.A. Lempicki, Bioinformatics enrichment tools: paths toward the comprehensive functional analysis of large gene lists, Nucleic Acids Res 37(1) (2008) 1-13.

[49] A. Subramanian, P. Tamayo, V.K. Mootha, S. Mukherjee, B.L. Ebert, M.A. Gillette, A. Paulovich, S.L. Pomeroy, T.R. Golub, E.S. Lander, J.P. Mesirov, Gene set enrichment analysis: A knowledge-based approach for interpreting genome-wide expression profiles, Proceedings of the National Academy of Sciences 102(43) (2005) 15545.

[50] V.K. Mootha, C.M. Lindgren, K.-F. Eriksson, A. Subramanian, S. Sihag, J. Lehar, P.

Puigserver, E. Carlsson, M. Ridderstråle, E. Laurila, N. Houstis, M.J. Daly, N. Patterson, J.P. Mesirov, T.R. Golub, P. Tamayo, B. Spiegelman, E.S. Lander, J.N. Hirschhorn, D. Altshuler, L.C. Groop, PGC-1α-responsive genes involved in oxidative phosphorylation are coordinately downregulated in human diabetes, Nature Genetics 34(3) (2003) 267-273.

[51] C.J. Bult, J.A. Blake, C.L. Smith, J.A. Kadin, J.E. Richardson, t.M.G.D. Group, Mouse Genome Database (MGD) 2019, Nucleic Acids Res 47(D1) (2018) D801-D806.

[52] D. Szklarczyk, A.L. Gable, D. Lyon, A. Junge, S. Wyder, J. Huerta-Cepas, M. Simonovic, N.T. Doncheva, J.H. Morris, P. Bork, L.J. Jensen, Christian v. Mering, STRING v11: protein–protein association networks with increased coverage, supporting functional discovery in genome-wide experimental datasets, Nucleic Acids Res 47(D1) (2018) D607-D613.

[53] L. Silberstein, Kevin A. Goncalves, Peter V. Kharchenko, R. Turcotte, Y. Kfoury, F. Mercier, N. Baryawno, N. Severe, J. Bachand, Joel A. Spencer, A. Papazian, D. Lee, Brahmananda R. Chitteti, Edward F. Srour, J. Hoggatt, T. Tate, C. Lo Celso, N. Ono, S. Nutt, J. Heino, K. Sipilä, T. Shioda, M. Osawa, Charles P. Lin, G.-f. Hu, David T. Scadden, Proximity-Based Differential Single-Cell Analysis of the Niche to Identify Stem/Progenitor Cell Regulators, Cell Stem Cell 19(4) (2016) 530-543.

[54] W. Craig, R. Kay, R.L. Cutler, P.M. Lansdorp, Expression of Thy-1 on human hematopoietic progenitor cells, Journal of Experimental Medicine 177(5) (1993) 1331-1342.

[55] P. van Galen, A. Kreso, E. Wienholds, E. Laurenti, K. Eppert, Eric R. Lechman, N. Mbong, K. Hermans, S. Dobson, C. April, J.-B. Fan, John E. Dick, Reduced Lymphoid Lineage Priming Promotes Human Hematopoietic Stem Cell Expansion, Cell Stem Cell 14(1) (2014) 94-106.

[56] F. Odet, C. Duan, W.D. Willis, E.H. Goulding, A. Kung, E.M. Eddy, E. Goldberg, Expression of the Gene for Mouse Lactate Dehydrogenase C (Ldhc) Is Required for Male Fertility1, Biology of Reproduction 79(1) (2008) 26-34.

[57] M. Saberiyan, R. Mirfakhraie, M. Moghni, H. Teimori, Study of Linc00574 Regulatory Effect on the TCTE3 Expression in Sperm Motility, Reproductive Sciences 28(1) (2021) 159-165.

[58] L. Zhang, M. Chen, Q. Wen, Y. Li, Y. Wang, Y. Wang, Y. Qin, X. Cui, L. Yang, V. Huff, F. Gao, Reprogramming of Sertoli cells to fetal-like Leydig cells by Wt1 ablation, Proceedings of the National Academy of Sciences 112(13) (2015) 4003.

[59] D.D. Mruk, C.Y. Cheng, Tight junctions in the testis, Philosophical Transactions of the Royal Society of London. Series B, Biological Sciences 365 (2010) 1621-1635.

[60] H.D. Zomer, P.P. Reddi, Characterization of rodent Sertoli cell primary cultures, Molecular Reproduction and Development 87(8) (2020) 857-870.

[61] S. Becker-Herman, G. Arie, H. Medvedovsky, A. Kerem, I. Shachar, CD74 Is a Member of the Regulated Intramembrane Proteolysis-processed Protein Family, Molecular Biology of the Cell 16(11) (2005) 5061-5069.

[62] R. Stein, M.J. Mattes, T.M. Cardillo, H.J. Hansen, C.-H. Chang, J. Burton, S. Govindan, D.M. Goldenberg, CD74: A New Candidate Target for the Immunotherapy of B-Cell Neoplasms, Clinical Cancer Research 13(18) (2007) 5556s.

[63] I.A. Astsaturov, E. Matutes, R. Morilla, B.K. Seon, D.Y. Mason, N. Farahat, D. Catovsky, Differential expression of B29 (CD79b) and mb-1 (CD79a) proteins in acute lymphoblastic leukaemia, Leukemia 10(5) (1996) 769-73.

[64] S. Wernersson, G. Pejler, Mast cell secretory granules: armed for battle, Nature Reviews Immunology 14(7) (2014) 478-494.

[65] S. Carl-McGrath, I. Gräntzdörffer, U. Lendeckel, M.P. Ebert, C. Röcken, Angiotensin II-generating enzymes, angiotensin-converting enzyme (ACE) and mast cell chymase (CMA1), in gastric inflammation may be regulated by H. pylori and associated cytokines, Pathology 41(5) (2009) 419-427.

[66] V. Payne, P.C.A. Kam, Mast cell tryptase: a review of its physiology and clinical significance, Anaesthesia 59(7) (2004) 695-703.

[67] J. Kalesnikoff, S.J. Galli, New developments in mast cell biology, Nature Immunology 9(11) (2008) 1215-1223.

[68] C. Hermansson, A. Lundqvist, L.U. Magnusson, C. Ullström, G. Bergström, L.M. Hultén, Macrophage CD14 expression in human carotid plaques is associated with complicated lesions, correlates with thrombosis, and is reduced by angiotensin receptor blocker treatment, International Immunopharmacology 22(2) (2014) 318-323.

[69] T. Baba, N. Mukaida, Role of macrophage inflammatory protein (MIP)-1α/CCL3 in leukemogenesis, Molecular & Cellular Oncology 1(1) (2014) e29899.

[70] V.C. Asensio, I.L. Campbell, Chemokines in the CNS: plurifunctional mediators in diverse states, Trends in Neurosciences 22(11) (1999) 504-512.

[71] M.S. Berger, D.D. Taub, A. Orlofsky, T.R. Kleyman, B. Coupaye-Gerard, D. Eisner, S.A. Cohen, THE CHEMOKINE C10: IMMUNOLOGICAL AND FUNCTIONAL ANALYSIS OF THE SEQUENCE ENCODED BY THE NOVEL SECOND EXON, Cytokine 8(6) (1996) 439-447.

[72] R.B. Burl, V.D. Ramseyer, E.A. Rondini, R. Pique-Regi, Y.-H. Lee, J.G. Granneman, Deconstructing Adipogenesis Induced by β3-Adrenergic Receptor Activation with Single-Cell Expression Profiling, Cell Metabolism 28(2) (2018) 300-309.e4.

[73] M. Tokunaga, M. Inoue, Y. Jiang, R.H. Barnes, D.A. Buchner, T.-H. Chun, Fat depot-specific gene signature and ECM remodeling of Sca1high adipose-derived stem cells, Matrix Biology 36 (2014) 28-38.

[74] W.P. Cawthorn, E.L. Scheller, O.A. MacDougald, Adipose tissue stem cells meet preadipocyte commitment: going back to the future[S], Journal of Lipid Research 53(2) (2012)

227-246.

[75] M. van de Rijn, S. Heimfeld, G.J. Spangrude, I.L. Weissman, Mouse hematopoietic stem-cell antigen Sca-1 is a member of the Ly-6 antigen family, Proceedings of the National Academy of Sciences 86(12) (1989) 4634.

[76] R.G.E. Palfree, F.J. Dumont, U. Hammerling, Ly-6A.2 and Ly-6E.1 molecules are antithetical and identical to MALA-1, Immunogenetics 23(3) (1986) 197-207.

[77] X.-H. Bai, D.-W. Wang, L. Kong, Y. Zhang, Y. Luan, T. Kobayashi, H.M. Kronenberg, X.-P. Yu, C.-j. Liu, ADAMTS-7, a Direct Target of PTHrP, Adversely Regulates Endochondral Bone Growth by Associating with and Inactivating GEP Growth Factor, Molecular and Cellular Biology 29(15) (2009) 4201-4219.

[78] D.S. Mistry, Y. Chen, Y. Wang, K. Zhang, G.L. Sen, SNAI2 Controls the Undifferentiated State of Human Epidermal Progenitor Cells, STEM CELLS 32(12) (2014) 3209-3218.

[79] P.A. Pérez-Mancera, C. Bermejo-Rodríguez, I. González-Herrero, M. Herranz, T. Flores, R. Jiménez, I. Sánchez-García, Adipose tissue mass is modulated by SLUG (SNAI2), Human Molecular Genetics 16(23) (2007) 2972-2986.

[80] G.-Y. Shen, H. Ren, Q. Shang, W.-H. Zhao, Z.-D. Zhang, X. Yu, J.-J. Huang, J.-J. Tang, Z.-D. Yang, D. Liang, X.-B. Jiang, Let-7f-5p regulates TGFBR1 in glucocorticoid-inhibited osteoblast differentiation and ameliorates glucocorticoid-induced bone loss, International Journal of Biological Sciences 15(10) (2019) 2182-2197.

[81] A. Scherberich, N.D. Di Maggio, K.M. McNagny, A familiar stranger: CD34 expression and putative functions in SVF cells of adipose tissue, World J Stem Cells 5(1) (2013) 1-8.

[82] K. Pieper, B. Grimbacher, H. Eibel, B-cell biology and development, Journal of Allergy and Clinical Immunology 131(4) (2013) 959-971.

[83] G.J. Spangrude, S. Heimfeld, I.L. Weissman, Purification and Characterization of Mouse

Hematopoietic Stem Cells, Science 241(4861) (1988) 58-62.

[84] S. Morikawa, Y. Mabuchi, Y. Kubota, Y. Nagai, K. Niibe, E. Hiratsu, S. Suzuki, C. Miyauchi-Hara, N. Nagoshi, T. Sunabori, S. Shimmura, A. Miyawaki, T. Nakagawa, T. Suda, H. Okano, Y. Matsuzaki, Prospective identification, isolation, and systemic transplantation of multipotent mesenchymal stem cells in murine bone marrow, Journal of Experimental Medicine 206(11) (2009) 2483-2496.

[85] B.E. Welm, S.B. Tepera, T. Venezia, T.A. Graubert, J.M. Rosen, M.A. Goodell, Sca-1pos Cells in the Mouse Mammary Gland Represent an Enriched Progenitor Cell Population, Developmental Biology 245(1) (2002) 42-56.

[86] M. Michaud, L. Balardy, G. Moulis, C. Gaudin, C. Peyrot, B. Vellas, M. Cesari, F. Nourhashemi, Proinflammatory Cytokines, Aging, and Age-Related Diseases, Journal of the American Medical Directors Association 14(12) (2013) 877-882.

[87] D. Wu, Z. Ren, M. Pae, W. Guo, X. Cui, A.H. Merrill, S.N. Meydani, Aging Up-Regulates Expression of Inflammatory Mediators in Mouse Adipose Tissue, The Journal of Immunology 179(7) (2007) 4829.

[88] K. Tsuruma, M. Yamauchi, S. Sugitani, T. Otsuka, Y. Ohno, Y. Nagahara, Y. Ikegame, M. Shimazawa, S. Yoshimura, T. Iwama, H. Hara, Progranulin, a Major Secreted Protein of Mouse Adipose-Derived Stem Cells, Inhibits Light-Induced Retinal Degeneration, STEM CELLS Translational Medicine 3(1) (2014) 42-53.

[89] F. Guo, Y. Lai, Q. Tian, E.A. Lin, L. Kong, C. Liu, Granulin-epithelin precursor binds directly to ADAMTS-7 and ADAMTS-12 and inhibits their degradation of cartilage oligomeric matrix protein, Arthritis & Rheumatism 62(7) (2010) 2023-2036.

[90] R.N. Jorissen, F. Walker, N. Pouliot, T.P.J. Garrett, C.W. Ward, A.W. Burgess, - Epidermal growth factor receptor: Mechanisms of activation and signalling, in: G. Carpenter (Ed.), The EGF

Receptor Family, Academic Press, Burlington, 2003, pp. 33-55.

[91] G. Ai, X. Shao, M. Meng, L. Song, J. Qiu, Y. Wu, J. Zhou, J. Cheng, X. Tong, Epidermal growth factor promotes proliferation and maintains multipotency of continuous cultured adipose stem cells via activating STAT signal pathway in vitro, Medicine 96(30) (2017).

[92] D.E. Maridas, V.E. DeMambro, P.T. Le, S. Mohan, C.J. Rosen, IGFBP4 Is Required for Adipogenesis and Influences the Distribution of Adipose Depots, Endocrinology 158(10) (2017) 3488-3500.

[93] G. Hutchings, K. Janowicz, L. Moncrieff, C. Dompe, E. Strauss, I. Kocherova, M.J. Nawrocki, Ł. Kruszyna, G. Wąsiatycz, P. Antosik, J.A. Shibli, P. Mozdziak, B. Perek, Z. Krasiński, B. Kempisty, M. Nowicki, The Proliferation and Differentiation of Adipose-Derived Stem Cells in Neovascularization and Angiogenesis, International Journal of Molecular Sciences 21(11) (2020).

[94] C.-H.L. Eng, M. Lawson, Q. Zhu, R. Dries, N. Koulena, Y. Takei, J. Yun, C. Cronin, C. Karp, G.-C. Yuan, L. Cai, Transcriptome-scale super-resolved imaging in tissues by RNA seqFISH+, Nature 568(7751) (2019) 235-239.

[95] C. Xia, J. Fan, G. Emanuel, J. Hao, X. Zhuang, Spatial transcriptome profiling by MERFISH reveals subcellular RNA compartmentalization and cell cycle-dependent gene expression, Proceedings of the National Academy of Sciences 116(39) (2019) 19490.

[96] I. Kukimoto, S. Elderkin, M. Grimaldi, T. Oelgeschläger, P.D. Varga-Weisz, The Histone-Fold Protein Complex CHRAC-15/17 Enhances Nucleosome Sliding and Assembly Mediated by ACF, Molecular Cell 13(2) (2004) 265-277.

[97] L. Lan, A. Ui, S. Nakajima, K. Hatakeyama, M. Hoshi, R. Watanabe, S.M. Janicki, H. Ogiwara, T. Kohno, S.-i. Kanno, A. Yasui, The ACF1 Complex Is Required for DNA Double-Strand Break Repair in Human Cells, Molecular Cell 40(6) (2010) 976-987.

[98] M. Narita, M. Narita, V. Krizhanovsky, S. Nuñez, A. Chicas, S.A. Hearn, M.P. Myers, S.W. Lowe, A Novel Role for High-Mobility Group A Proteins in Cellular Senescence and Heterochromatin Formation, Cell 126(3) (2006) 503-514.

[99] M. Ishii, Y. Suda, K. Kurokawa, A. Nakano, COPI is essential for Golgi cisternal maturation and dynamics, Journal of Cell Science 129(17) (2016) 3251-3261.

[100] P.J. Hornsby, Senescence As an Anticancer Mechanism, Journal of Clinical Oncology 25(14) (2007) 1852-1857.

[101] H.-F. Yuan, C. Zhai, X.-L. Yan, D.-D. Zhao, J.-X. Wang, Q. Zeng, L. Chen, X. Nan, L.-J. He, S.-T. Li, W. Yue, X.-T. Pei, SIRT1 is required for long-term growth of human mesenchymal stem cells, Journal of Molecular Medicine 90(4) (2012) 389-400.

[102] F. Wang, Q. Tong, SIRT2 suppresses adipocyte differentiation by deacetylating FOXO1 and enhancing FOXO1's repressive interaction with PPARgamma, Mol Biol Cell 20(3) (2009) 801-8.

[103] M. Zhao, R. Geng, X. Guo, R. Yuan, X. Zhou, Y. Zhong, Y. Huo, M. Zhou, Q. Shen, Y. Li, W. Zhu, J. Wang, PCAF/GCN5-Mediated Acetylation of RPA1 Promotes Nucleotide Excision Repair, Cell Reports 20(9) (2017) 1997-2009.

[104] J. Nakae, T. Kitamura, Y. Kitamura, W.H. Biggs, K.C. Arden, D. Accili, The Forkhead Transcription Factor Foxo1 Regulates Adipocyte Differentiation, Developmental Cell 4(1) (2003) 119-129.

[105] M. Higuchi, G.J. Dusting, H. Peshavariya, F. Jiang, S.T.-F. Hsiao, E.C. Chan, G.-S. Liu, Differentiation of Human Adipose-Derived Stem Cells into Fat Involves Reactive Oxygen Species and Forkhead Box O1 Mediated Upregulation of Antioxidant Enzymes, Stem Cells Dev 22(6) (2012) 878-888.

[106] F. Wang, C.B. Marshall, K. Yamamoto, G.-Y. Li, M.J. Plevin, H. You, T.W. Mak, M. Ikura, Biochemical and Structural Characterization of an Intramolecular Interaction in FOXO3a and Its

Binding with p53, Journal of Molecular Biology 384(3) (2008) 590-603.

[107] W. Yang, Y. Xia, X. Qian, M. Wang, X. Zhang, Y. Li, L. Li, Co-expression network analysis identified key genes in association with mesenchymal stem cell osteogenic differentiation, Cell and Tissue Research 378(3) (2019) 513-529.

[108] R.K. Khajuria, M. Munschauer, J.C. Ulirsch, C. Fiorini, L.S. Ludwig, S.K. McFarland, N.J. Abdulhay, H. Specht, H. Keshishian, D.R. Mani, M. Jovanovic, S.R. Ellis, C.P. Fulco, J.M. Engreitz, S. Schütz, J. Lian, K.W. Gripp, O.K. Weinberg, G.S. Pinkus, L. Gehrke, A. Regev, E.S. Lander, H.T. Gazda, W.Y. Lee, V.G. Panse, S.A. Carr, V.G. Sankaran, Ribosome Levels Selectively Regulate Translation and Lineage Commitment in Human Hematopoiesis, Cell 173(1) (2018) 90-103.e19.

[109] A. Divoux, K. Clément, Architecture and the extracellular matrix: the still unappreciated components of the adipose tissue, Obesity Reviews 12(5) (2011) e494-e503.

[110] T. Khan, E.S. Muise, P. Iyengar, Z.V. Wang, M. Chandalia, N. Abate, B.B. Zhang, P. Bonaldo, S. Chua, P.E. Scherer, Metabolic Dysregulation and Adipose Tissue Fibrosis: Role of Collagen VI, Molecular and Cellular Biology 29(6) (2009) 1575-1591.

[111] J. Honek, T. Seki, H. Iwamoto, C. Fischer, J. Li, S. Lim, N.J. Samani, J. Zang, Y. Cao, Modulation of age-related insulin sensitivity by VEGF-dependent vascular plasticity in adipose tissues, Proceedings of the National Academy of Sciences 111(41) (2014) 14906.

[112] J.L. Kirkland, T. Tchkonia, Senolytic drugs: from discovery to translation, J Intern Med 288(5) (2020) 518-536.

[113] M.P. Baar, R.M.C. Brandt, D.A. Putavet, J.D.D. Klein, K.W.J. Derks, B.R.M. Bourgeois, S. Stryeck, Y. Rijksen, H. van Willigenburg, D.A. Feijtel, I. van der Pluijm, J. Essers, W.A. van Cappellen, I.W.F. van, A.B. Houtsmuller, J. Pothof, R.W.F. de Bruin, T. Madl, J.H.J. Hoeijmakers, J. Campisi, P.L.J. de Keizer, Targeted Apoptosis of Senescent Cells Restores Tissue Homeostasis

in Response to Chemotoxicity and Aging, Cell 169(1) (2017) 132-147 e16.

[114] Y. Johmura, T. Yamanaka, S. Omori, T.-W. Wang, Y. Sugiura, M. Matsumoto, N. Suzuki, S. Kumamoto, K. Yamaguchi, S. Hatakeyama, T. Takami, R. Yamaguchi, E. Shimizu, K. Ikeda, N. Okahashi, R. Mikawa, M. Suematsu, M. Arita, M. Sugimoto, K.I. Nakayama, Y. Furukawa, S. Imoto, M. Nakanishi, Senolysis by glutaminolysis inhibition ameliorates various age-associated disorders, Science 371(6526) (2021) 265-270.

Supplementary information

Group	GO Term	*p*-value	Genes in the GO Term
0-2-4	negative regulation of T cell apoptotic process	0.015	*SERPINB9, CCL5*
	positive regulation of gene expression	0.015	*SERPINB9, ID2, CD3E, CCL5*
	negative regulation of neural precursor cell proliferation	0.018	*BTG2, ID2*
	aging	0.022	*ND4, COX1, ATP6*
	positive regulation of T cell activation	0.022	*CD3E, THY1*
	response to copper ion	0.024	*COX1, CYTB*
	response to hyperoxia	0.024	*CYTB, ATP6*
	transport	0.029	*RAMP3, ND1, ND4, COX1, VPS37B, CYTB, ATP6*
	response to electrical stimulus	0.039	*BTG2, COX1*
	negative regulation of viral genome replication	0.042	*ZC3HAV1, CCL5*
1-3-5	endodermal cell differentiation	<0.000	*COL6A1, MMP14, MMP2, FN1*
	astrocyte activation	<0.000	*EGFR, AGT, MT2*
	positive regulation of fibroblast proliferation	<0.000	*EGFR, AGT, SERPINE1, FN1*
	positive regulation of superoxide anion generation	<0.000	*EGFR, CXCL1, AGT*
	angiogenesis	<0.000	*SERPINE1, MMP14, TNFAIP2, MMP2, FN1*
	response to oxidative stress	0.001	*EGFR, GPX3, MMP14, MMP2*
	cellular response to amino acid stimulus	0.001	*EGFR, COL1A2, COL6A1, MMP2*
	positive regulation of cell migration	0.003	*EGFR, MMP14, MMP2, FN1*
	blood vessel development	0.005	*AGT, COL1A2, PLPP3*
	cellular response to drug	0.005	*EGFR, SERPINE1, DPEP1*
	cell-matrix adhesion	0.006	*AGT, NID1, FN1*
	wound healing	0.008	*EGFR, SERPINE1, FN1*
	proteolysis	0.009	*HP, HTRA3, MMP14, MMP2, DPEP1*

	extracellular matrix organization	0.012	*AGT, NID1, FN1*
	cellular response to cadmium ion	0.017	*GSN, MT2*
	positive regulation of gene expression	0.019	*GSN, AGT, SERPINE1, FN1*
	tissue remodeling	0.020	*MMP14, MMP2*
	positive regulation of vascular smooth muscle cell proliferation	0.020	*AGT, MMP2*
	protein heterotrimerization	0.027	*COL1A2, COL6A1*
	cell adhesion	0.032	*COL6A1, NID1, PLPP3, FN1*
	collagen catabolic process	0.034	*MMP14, MMP2*
	cellular response to estradiol stimulus	0.046	*EGFR, MMP2*
	acute-phase response	0.049	*HP, FN1*
6	microtubule-based movement	<0.000	*GM3417, GM3448, TCTE3*
	microtubule-based process	0.014	*TUBA3B, TUBA3A*
	transport	0.016	*FABP9, GM3417, GM3448, TCTE3*
7	activation of protein kinase B activity	0.011	*FGF1, GAS6*
	positive regulation of cell proliferation	0.028	*ENPP2, CLU, FGF1*
8	adaptive immune response	<0.000	*JCHAIN, CD79B, CD79A, CTSS, CD74*
	antigen processing and presentation	<0.000	*H2-AB1, CTSS, CD74*
	immune system process	0.001	*CD79B, H2-AB1, CD79A, CD74*
	antigen processing and presentation of peptide antigen	0.002	*H2-AB1, CTSS*
	antigen processing and presentation of exogenous peptide antigen via MHC class II	0.007	*H2-AB1, CD74*
	immune response	0.008	*H2-AB1, CTSS, CD74*
	B cell receptor signaling pathway	0.027	*CD79B, CD79A*
	B cell differentiation	0.040	*CD79B, CD79A*
9	protein processing	0.001	*MCPT4, CMA1, CMA2*
	regulation of angiotensin levels in blood	0.001	*MCPT4, CPA3*
	proteolysis	0.002	*MCPT4, CPA3, CMA1, TPSB2*
	immune response	0.008	*MCPT4, CMA1, CMA2*
	positive regulation of mast cell	0.008	*FCER1A, GATA2*

	degranulation		
10	immune response	<0.000	*CCL3, H2-EB1, IL1B, H2-AA, H2-AB1, CCL4, CCL6*
	cellular response to interferon-gamma	<0.000	*CCL3, H2-AB1, CCL4, CCL6*
	neutrophil chemotaxis	<0.000	*CCL3, IL1B, CCL4, CCL6*
	antigen processing and presentation of peptide or polysaccharide antigen via MHC class II	<0.000	*H2-EB1, H2-AA, H2-AB1*
	inflammatory response	<0.000	*CCL3, IL1B, CCL4, CD14, CCL6*
	antigen processing and presentation of exogenous peptide antigen via MHC class II	<0.000	*H2-EB1, H2-AA, H2-AB1*
	positive regulation of ERK1 and ERK2 cascade	<0.000	*CCL3, IL1B, CCL4, CCL6*
	lipopolysaccharide-mediated signaling pathway	<0.000	*CCL3, IL1B, CD14*
	lymphocyte chemotaxis	<0.000	*CCL3, CCL4, CCL6*
	monocyte chemotaxis	<0.000	*CCL3, CCL4, CCL6*
	antigen processing and presentation	<0.000	*H2-EB1, H2-AA, H2-AB1*
	chemokine-mediated signaling pathway	<0.000	*CCL3, CCL4, CCL6*
	positive regulation of tumor necrosis factor production	<0.000	*CCL3, CCL4, CD14*
	positive regulation of inflammatory response	<0.000	*CCL3, CCL4, CCL6*
	cell chemotaxis	0.001	*CCL3, CCL4, CCL6*
	cellular response to interleukin-1	0.001	*CCL3, CCL4, CCL6*
	immune system process	0.001	*H2-EB1, H2-AA, H2-AB1, CD14*
	cellular response to tumor necrosis factor	0.001	*CCL3, CCL4, CCL6*
	chemotaxis	0.001	*CCL3, CCL4, CCL6*
	antigen processing and presentation of peptide antigen	0.002	*H2-AA, H2-AB1*
	positive regulation of GTPase activity	0.002	*CCL3, CCL4, CCL6*
	positive regulation of natural killer cell	0.003	*CCL3, CCL4*

	chemotaxis		
	cell wall macromolecule catabolic process	0.005	*LYZ2, LYZ1*
	negative regulation by host of viral transcription	0.006	*CCL3, CCL4*
	leukocyte chemotaxis	0.011	*CCL3, CCL4*
	positive regulation of calcium-mediated signaling	0.012	*CCL3, CCL4*
	cytolysis	0.012	*LYZ2, LYZ1*
	response to interferon-gamma	0.013	*H2-EB1, H2-AA*
	positive regulation of calcium ion transport	0.015	*CCL3, CCL4*
	protein kinase B signaling	0.019	*CCL3, IL1B*
	negative regulation of T cell proliferation	0.020	*H2-AA, H2-AB1*
	positive regulation of interferon-gamma production	0.026	*IL1B, CD14*
	defense response to Gram-negative bacterium	0.028	*LYZ2, LYZ1*
	MAPK cascade	0.034	*CCL3, IL1B*
	positive regulation of neuron apoptotic process	0.034	*CCL3, IL1B*
	cellular response to organic cyclic compound	0.037	*CCL3, IL1B*
	cellular response to drug	0.037	*IL1B, CCL4*
	response to toxic substance	0.042	*CCL3, CCL4*
	defense response to Gram-positive bacterium	0.045	*LYZ2, LYZ1*

Supplemental table 1: GO analysis using the annotation information of the top 10 genes characteristically expressed in each group.

The functional annotation of DAVID version 6.8 was performed to search for GO Terms in each group. GO Terms with *p*-values less than 0.050 in the GOTERM_BP_DIRECT category were extracted.

Group	Gene symbol	Gene name	Predicted cell type
0-2-4	*Cxcr6*	*chemokine (C-X-C motif) receptor 6 (Cxcr6)*	HSCs
	Ctla2a	*cytotoxic T lymphocyte-associated protein 2 alpha (Ctla2a)*	
	Dgat1	*diacylglycerol O-acyltransferase 1 (Dgat1)*	
	Emb	*embigin (Emb)*	
	Il2rb	*interleukin 2 receptor, beta chain (Il2rb)*	
	Neurl3	*neuralized E3 ubiquitin protein ligase 3 (Neurl3)*	
	Ramp3	*receptor (calcitonin) activity modifying protein 3 (Ramp3)*	
	Thy1	*thymus cell antigen 1, theta (Thy1)*	
	Zc3hav1	*zinc finger CCCH type, antiviral 1 (Zc3hav1)*	
	D16Ertd472e	*DNA segment, Chr 16, ERATO Doi 472, expressed (D16Ertd472e)*	
	Cd3e	*CD3 antigen, epsilon polypeptide (Cd3e)*	
	Gimap3	*GTPase, IMAP family member 3 (Gimap3)*	
	Ccl5	*chemokine (C-C motif) ligand 5 (Ccl5)*	
	Rnf125	*ring finger protein 125 (Rnf125)*	
	Serpinb9	*serine (or cysteine) peptidase inhibitor, clade B, member 9 (Serpinb9)*	
	Vps37b	*vacuolar protein sorting 37B (Vps37b)*	
	Gimap4	*GTPase, IMAP family member 4 (Gimap4)*	
	Ms4a4b	*membrane-spanning 4-domains, subfamily A, member 4B (Ms4a4b)*	
	Nkg7	*natural killer cell group 7 sequence (Nkg7)*	
	Btg2	*B cell translocation gene 2, anti-proliferative (Btg2)*	
	Id2	*inhibitor of DNA binding 2 (Id2)*	

	Tnp2	*transition protein 2 (Tnp2)*	
	MT-Atp6	*ATP synthase F0 subunit 6 (ATP6, MT-Atp6)*	
	MT-Co1	*cytochrome c oxidase subunit I (COX1, MT-Co1)*	
	MT-Cytb	*cytochrome b (CYTB, MT-Cytb)*	
	MT-Nd1	*NADH dehydrogenase subunit 1 (ND1, MT-Nd1)*	
	MT-Nd4	*NADH dehydrogenase subunit 4 (ND4, MT-Nd4)*	
	MT-Rnr1	*s-rRNA (Rnr1)*	
	MT-Rnr2	*16S ribosomal RNA (Rnr2, MT-Rnr1)*	
1-3-5	*Clec3b*	*C-type lectin domain family 3, member b (Clec3b)*	ASCs
	Dpep1	*dipeptidase 1 (renal) (Dpep1)*	
	Fn1	*fibronectin 1 (Fn1)*	
	Fstl1	*follistatin-like 1 (Fstl1)*	
	Gsn	*gelsolin (Gsn)*	
	Gpx3	*glutathione peroxidase 3 (Gpx3)*	
	Hp	*haptoglobin (Hp)*	
	Pi16	*peptidase inhibitor 16 (Pi16)*	
	Tnfaip2	*tumor necrosis factor, alpha-induced protein 2 (Tnfaip2)*	
	Ppap2b	*phosphatidic acid phosphatase type 2B (Ppap2b)*	
	Htra3	*HtrA serine peptidase 3 (Htra3)*	
	Bgn	*biglycan (Bgn)*	
	Cxcl1	*chemokine (C-X-C motif) ligand 1 (Cxcl1)*	
	Col6a1	*collagen, type VI, alpha 1 (Col6a1)*	
	Gfpt2	*glutamine fructose-6-phosphate transaminase 2 (Gfpt2)*	
	Mt2	*metallothionein 2 (Mt2)*	
	Sult1e1	*sulfotransferase family 1E, member 1 (Sult1e1)*	

	Gm9780	*predicted gene 9780 (Gm9780)*	
	Cebpd	*CCAAT/enhancer binding protein (C/EBP), delta (Cebpd)*	
	Sparcl1	*SPARC-like 1 (Sparcl1)*	
	Agt	*angiotensinogen (serpin peptidase inhibitor, clade A, member 8) (Agt)*	
	Col1a2	*collagen, type I, alpha 2 (Col1a2)*	
	Egfr	*epidermal growth factor receptor (Egfr)*	
	Inmt	*indolethylamine N-methyltransferase (Inmt)*	
	Mmp14	*matrix metallopeptidase 14 (membrane-inserted) (Mmp14)*	
	Mmp2	*matrix metallopeptidase 2 (Mmp2)*	
	Nid1	*nidogen 1 (Nid1)*	
	Serpine1	*serine (or cysteine) peptidase inhibitor, clade E, member 1 (Serpine1)*	
6	*Fabp9*	*fatty acid binding protein 9, testis (Fabp9)*	Sperms
	Ldhc	*lactate dehydrogenase C (Ldhc)*	
	Gm3417	*predicted gene 3417 (Gm3417)*	
	Gm3448	*predicted gene 3448 (Gm3448)*	
	Tcte3	*t-complex-associated testis expressed 3 (Tcte3)*	
	Tuba3a	*tubulin, alpha 3A (Tuba3a)*	
	Tuba3b	*tubulin, alpha 3B (Tuba3b)*	
	Fhl4	*four and a half LIM domains 4 (Fhl4)*	
	Rbakdn	*RB-associated KRAB zinc finger downstream neighbor (non-protein coding) (Rbakdn)*	
	Spata4	*spermatogenesis associated 4 (Spata4)*	
7	*Nkain4*	*Na+/K+ transporting ATPase interacting 4 (Nkain4)*	Sertoli cells
	Clu	*clusterin (Clu)*	
	Cfb	*complement factor B (Cfb)*	

	Csrp2	*cysteine and glycine-rich protein 2 (Csrp2)*	
	Enpp2	*ectonucleotide pyrophosphatase/phosphodiesterase 2 (Enpp2)*	
	Fgf1	*fibroblast growth factor 1 (Fgf1)*	
	Gas6	*growth arrest specific 6 (Gas6)*	
	Slpi	*secretory leukocyte peptidase inhibitor (Slpi)*	
	Tmem119	*transmembrane protein 119 (Tmem119)*	
	Upk1b	*uroplakin 1B (Upk1b)*	
8	*Cd74*	*CD74 antigen (invariant polypeptide of major histocompatibility complex, class II antigen-associated) (Cd74)*	B cells
	Cd79a	*CD79A antigen (immunoglobulin-associated alpha) (Cd79a)*	
	Cd79b	*CD79B antigen (Cd79b)*	
	Pou2af1	*POU domain, class 2, associating factor 1 (Pou2af1)*	
	Ctss	*cathepsin S (Ctss)*	
	H2-Ab1	*histocompatibility 2, class II antigen A, beta 1 (H2-Ab1)*	
	Herpud1	*homocysteine-inducible, endoplasmic reticulum stress-inducible, ubiquitin-like domain member 1 (Herpud1)*	
	Ly6d	*lymphocyte antigen 6 complex, locus D (Ly6d)*	
	Mzb1	*marginal zone B and B1 cell-specific protein 1 (Mzb1)*	
	Igj	*immunoglobulin joining chain (Jchain, Igj)*	
9	*Fcer1a*	*Fc receptor, IgE, high affinity I, alpha polypeptide (Fcer1a)*	Mast cells
	Gata2	*GATA binding protein 2 (Gata2)*	

	Mrgprb1	*MAS-related GPR, member B1 (Mrgprb1)*	
	Cpa3	*carboxypeptidase A3, mast cell (Cpa3)*	
	Cma1	*chymase 1, mast cell (Cma1)*	
	Cma2	*chymase 2, mast cell (Cma2)*	
	Csf2rb	*colony stimulating factor 2 receptor, beta, low-affinity (granulocyte-macrophage) (Csf2rb)*	
	Hdc	*histidine decarboxylase (Hdc)*	
	Mcpt4	*mast cell protease 4 (Mcpt4)*	
	Tpsb2	*tryptase beta 2 (Tpsb2)*	
10	*Cd14*	*CD14 antigen (Cd14)*	Macrophages
	Ccl3	*chemokine (C-C motif) ligand 3 (Ccl3)*	
	Ccl4	*chemokine (C-C motif) ligand 4 (Ccl4)*	
	Ccl6	*chemokine (C-C motif) ligand 6 (Ccl6)*	
	H2-Aa	*histocompatibility 2, class II antigen A, alpha (H2-Aa)*	
	H2-Ab1	*histocompatibility 2, class II antigen A, beta 1 (H2-Ab1)*	
	H2-Eb1	*histocompatibility 2, class II antigen E beta (H2-Eb1)*	
	Il1b	*interleukin 1 beta (Il1b)*	
	Lyz1	*lysozyme 1 (Lyz1)*	
	Lyz2	*lysozyme 2 (Lyz2)*	

Supplemental table 2: Predicted cell types and genes characteristically expressed in each group.

Gene symbol	Gene name (from dataset)	RUNNING ES	*
HMGA1	*high mobility group AT-hook 1* [Source: HGNC Symbol; Acc: HGNC:5010]	0.153	**Yes**
MTHFR	*methylenetetrahydrofolate reductase* [Source: HGNC Symbol; Acc: HGNC:7436]	0.282	**Yes**
POLE3	*DNA polymerase epsilon 3, accessory subunit* [Source: HGNC Symbol; Acc: HGNC:13546]	0.329	**Yes**
AC016586.1	*sirtuin 6* [Source: NCBI gene; Acc:51548]	0.426	**Yes**
CHRAC1	*chromatin accessibility complex subunit 1* [Source: HGNC Symbol; Acc: HGNC:13544]	0.520	**Yes**
TPR	*translocated promoter region, nuclear basket protein* [Source: HGNC Symbol; Acc: HGNC:12017]	0.595	**Yes**
HP1BP3	*heterochromatin protein 1 binding protein 3* [Source: HGNC Symbol; Acc: HGNC:24973]	0.636	**Yes**
BAHD1	*bromo adjacent homology domain containing 1* [Source: HGNC Symbol; Acc: HGNC:29153]	0.689	**Yes**
MECOM	*MDS1 and EVI1 complex locus* [Source: HGNC Symbol; Acc: HGNC:3498]	0.682	**Yes**
LOXL2	*lysyl oxidase like 2* [Source: HGNC Symbol; Acc: HGNC:6666]	0.717	**Yes**
HELLS	*helicase, lymphoid specific* [Source: HGNC Symbol; Acc: HGNC:4861]	0.713	No
SNAI1	*snail family transcriptional repressor 1* [Source: HGNC Symbol; Acc: HGNC:11128]	0.646	No
CENPV	*centromere protein V* [Source: HGNC Symbol; Acc: HGNC:29920]	0.558	No
SETD7	*SET domain containing 7, histone lysine methyltransferase* [Source: HGNC Symbol; Acc: HGNC:30412]	0.494	No
SMCHD1	*structural maintenance of chromosomes flexible hinge domain containing 1* [Source: HGNC Symbol; Acc: HGNC:29090]	0.482	No

Supplemental table 3: Genes included in the "GO_HETEROCHROMATIN_ORGANIZATION" gene set.

When “Yes” is indicated in column of core enrichment gene, it shows that the gene contributed to the increase in the absolute enrichment score. RUNNING ES shows the enrichment score at that time point. *: core enrichment gene.

Gene symbol	Gene name (from dataset)	RUNNING ES	*
COPG1	*coatomer protein complex subunit gamma 1* [Source: HGNC Symbol; Acc: HGNC:2236]	0.100	**Yes**
KDELR1	*KDEL endoplasmic reticulum protein retention receptor 1* [Source: HGNC Symbol; Acc: HGNC:6304]	0.214	**Yes**
COPB2	*coatomer protein complex subunit beta 2* [Source: HGNC Symbol; Acc: HGNC:2232]	0.327	**Yes**
COPZ2	*coatomer protein complex subunit zeta 2* [Source: HGNC Symbol; Acc: HGNC:19356]	0.394	**Yes**
COPB1	*coatomer protein complex subunit beta 1* [Source: HGNC Symbol; Acc: HGNC:2231]	0.477	**Yes**
COPZ1	*coatomer protein complex subunit zeta 1* [Source: HGNC Symbol; Acc: HGNC:2243]	0.547	**Yes**
ARCN1	*archain 1* [Source: HGNC Symbol; Acc: HGNC:649]	0.618	**Yes**
ARFGAP3	*ADP ribosylation factor GTPase activating protein 3* [Source: HGNC Symbol; Acc: HGNC:661]	0.606	**Yes**
TMED7	*transmembrane p24 trafficking protein 7* [Source: HGNC Symbol; Acc: HGNC:24253]	0.666	**Yes**
COPA	*coatomer protein complex subunit alpha* [Source: HGNC Symbol; Acc: HGNC:2230]	0.639	No
COPG2	*coatomer protein complex subunit gamma 2* [Source: HGNC Symbol; Acc: HGNC:2237]	0.367	No
TMEM199	*transmembrane protein 199* [Source: HGNC Symbol; Acc: HGNC:18085]	0.350	No
ARFGAP2	*ADP ribosylation factor GTPase activating protein 2* [Source: HGNC Symbol; Acc: HGNC:13504]	0.282	No
SCYL1	*SCY1 like pseudokinase 1* [Source: HGNC Symbol; Acc: HGNC:14372]	0.242	No
TMED3	*transmembrane p24 trafficking protein 3* [Source: HGNC Symbol; Acc: HGNC:28889]	0.191	No
COPE	*coatomer protein complex subunit epsilon* [Source: HGNC Symbol; Acc: HGNC:2234]	0.160	No

Supplemental table 4: Genes included in the "GO_COPI_COATED_VESICLE_MEMBRANE" gene set.

When “Yes” is indicated in column of core enrichment gene, it shows that the gene contributed to the increase in the absolute enrichment score. RUNNING ES shows the enrichment score at that time point. *: core enrichment gene.

Gene symbol	Gene name (from dataset)	RUNNING ES	*
HDAC5	*histone deacetylase 5* [Source: HGNC Symbol; Acc: HGNC:14068]	0.146	**Yes**
HDAC1	*histone deacetylase 1* [Source: HGNC Symbol; Acc: HGNC:4852]	0.251	**Yes**
HDAC6	*histone deacetylase 6* [Source: HGNC Symbol; Acc: HGNC:14064]	0.239	**Yes**
AC016586.1	*sirtuin 6* [Source: NCBI gene; Acc:51548]	0.293	**Yes**
SIRT7	*sirtuin 7* [Source: HGNC Symbol; Acc: HGNC:14935]	0.348	**Yes**
HDAC8	*histone deacetylase 8* [Source: HGNC Symbol; Acc: HGNC:13315]	0.416	**Yes**
AC129492.1	*period circadian regulator 1* [Source: NCBI gene; Acc:5187]	0.467	**Yes**
HDAC9	*histone deacetylase 9* [Source: HGNC Symbol; Acc: HGNC:14065]	0.455	**Yes**
HDAC2	*histone deacetylase 2* [Source: HGNC Symbol; Acc: HGNC:4853]	0.491	**Yes**
HDAC4	*histone deacetylase 4* [Source: HGNC Symbol; Acc: HGNC:14063]	0.531	**Yes**
SIRT2	*sirtuin 2* [Source: HGNC Symbol; Acc: HGNC:10886]	0.567	**Yes**
ELK4	*ETS transcription factor ELK4* [Source: HGNC Symbol; Acc: HGNC:3326]	0.577	**Yes**
ATXN3L	*ataxin 3 like* [Source: HGNC Symbol; Acc: HGNC:24173]	0.592	**Yes**
SIRT1	*sirtuin 1* [Source: HGNC Symbol; Acc: HGNC:14929]	0.607	**Yes**
SFPQ	*splicing factor proline and glutamine rich* [Source: HGNC Symbol; Acc: HGNC:10774]	0.611	**Yes**
HDAC3	*histone deacetylase 3* [Source: HGNC Symbol; Acc: HGNC:4854]	0.581	No
HDAC11	*histone deacetylase 11* [Source: HGNC Symbol; Acc: HGNC:19086]	0.383	No
SMARCAD1	*SWI/SNF-related, matrix-associated actin-dependent regulator of chromatin, subfamily a, containing DEAD/H box 1* [Source: HGNC Symbol; Acc: HGNC:18398]	0.309	No

PER2	*period circadian regulator 2* [Source: HGNC Symbol; Acc: HGNC:8846]	0.269	No
HDAC7	*histone deacetylase 7* [Source: HGNC Symbol; Acc: HGNC:14067]	0.071	No

Supplemental table 5: Genes included in the "GO_HISTONE_H3_DEACETYLATION" gene set.

When "Yes" is indicated in column of core enrichment gene, it shows that the gene contributed to the increase in the absolute enrichment score. RUNNING ES shows the enrichment score at that time point. *: core enrichment gene.

Gene symbol	Gene name (from dataset)	RUNNING ES	*
ABCA6	*ATP binding cassette subfamily A member 6* [Source: HGNC Symbol; Acc: HGNC:36]	0.132	**Yes**
HDAC1	*histone deacetylase 1* [Source: HGNC Symbol; Acc: HGNC:4852]	0.260	**Yes**
SOD2	*superoxide dismutase 2* [Source: HGNC Symbol; Acc: HGNC:11180]	0.320	**Yes**
SIRT3	*sirtuin 3* [Source: HGNC Symbol; Acc: HGNC:14931]	0.360	**Yes**
FOXO4	*forkhead box O4* [Source: HGNC Symbol; Acc: HGNC:7139]	0.430	**Yes**
FOXO3	*forkhead box O3* [Source: HGNC Symbol; Acc: HGNC:3821]	0.503	**Yes**
FOXO1	*forkhead box O1* [Source: HGNC Symbol; Acc: HGNC:3819]	0.547	**Yes**
NR3C1	*nuclear receptor subfamily 3 group C member 1* [Source: HGNC Symbol; Acc: HGNC:7978]	0.591	**Yes**
G6PC	*glucose-6-phosphatase catalytic subunit* [Source: HGNC Symbol; Acc: HGNC:4056]	0.600	**Yes**
HDAC2	*histone deacetylase 2* [Source: HGNC Symbol; Acc: HGNC:4853]	0.649	**Yes**
SMAD3	*SMAD family member 3* [Source: HGNC Symbol; Acc: HGNC:6769]	0.666	**Yes**
CAT	*catalase* [Source: HGNC Symbol; Acc: HGNC:1516]	0.606	No
POMC	*proopiomelanocortin* [Source: HGNC Symbol; Acc: HGNC:9201]	0.565	No
SMAD2	*SMAD family member 2* [Source: HGNC Symbol; Acc: HGNC:6768]	0.519	No
SMAD4	*SMAD family member 4* [Source: HGNC Symbol; Acc: HGNC:6770]	0.519	No
PPARGC1A	*PPARG coactivator 1 alpha* [Source: HGNC Symbol; Acc: HGNC:9237]	0.492	No
FOXO6	*forkhead box O6* [Source: HGNC Symbol; Acc: HGNC:24814]	0.489	No
RETN	*resistin* [Source: HGNC Symbol; Acc: HGNC:20389]	0.357	No

PLXNA4	*plexin A4* [Source: HGNC Symbol; Acc: HGNC:9102]	0.352	No
TRIM63	*tripartite motif containing 63* [Source: HGNC Symbol; Acc: HGNC:16007]	0.313	No
SIN3A	*SIN3 transcription regulator family member A* [Source: HGNC Symbol; Acc: HGNC:19353]	0.227	No
SREBF1	*sterol regulatory element binding transcription factor 1* [Source: HGNC Symbol; Acc: HGNC:11289]	0.178	No

Supplemental table 6: Genes included in the "REACTOME_FOXO_MEDIATED_TRANSCRIPTION_OF_OXIDATIVE_STRESS_METABOLIC_AND_NEURONAL_GENES" gene set.

When "Yes" is indicated in column of core enrichment gene, it shows that the gene contributed to the increase in the absolute enrichment score. RUNNING ES shows the enrichment score at that time point. *: core enrichment gene.

Gene symbol	Gene name (from dataset)	RUNNING ES	*
MRPL23	*mitochondrial ribosomal protein L23* [Source: HGNC Symbol; Acc: HGNC:10322]	-0.022	No
MRPL4	*mitochondrial ribosomal protein L4* [Source: HGNC Symbol; Acc: HGNC:14276]	-0.022	No
MRPS18B	*mitochondrial ribosomal protein S18B* [Source: HGNC Symbol; Acc: HGNC:14516]	-0.020	No
MRPS24	*mitochondrial ribosomal protein S24* [Source: HGNC Symbol; Acc: HGNC:14510]	-0.014	No
MRPS9	*mitochondrial ribosomal protein S9* [Source: HGNC Symbol; Acc: HGNC:14501]	-0.034	No
MRPS18C	*mitochondrial ribosomal protein S18C* [Source: HGNC Symbol; Acc: HGNC:16633]	-0.033	No
MRPL24	*mitochondrial ribosomal protein L24* [Source: HGNC Symbol; Acc: HGNC:14037]	-0.039	No
MRPS12	*mitochondrial ribosomal protein S12* [Source: HGNC Symbol; Acc: HGNC:10380]	-0.047	No
MRPL11	*mitochondrial ribosomal protein L11* [Source: HGNC Symbol; Acc: HGNC:14042]	-0.047	No
MRPS2	*mitochondrial ribosomal protein S2* [Source: HGNC Symbol; Acc: HGNC:14495]	-0.053	No
MRPS25	*mitochondrial ribosomal protein S25* [Source: HGNC Symbol; Acc: HGNC:14511]	-0.050	No
MRPL12	*mitochondrial ribosomal protein L12* [Source: HGNC Symbol; Acc: HGNC:10378]	-0.044	No
MRPS17	*mitochondrial ribosomal protein S17* [Source: HGNC Symbol; Acc: HGNC:14047]	-0.042	No
MRPS35	*mitochondrial ribosomal protein S35* [Source: HGNC Symbol; Acc: HGNC:16635]	-0.045	No
RPL3	*ribosomal protein L3* [Source: HGNC Symbol; Acc: HGNC:10332]	-0.060	No
MRPS6	*mitochondrial ribosomal protein S6* [Source: HGNC Symbol; Acc: HGNC:14051]	-0.059	No
MRPS36	*mitochondrial ribosomal protein S36* [Source: HGNC Symbol; Acc: HGNC:16631]	-0.054	No

MRPL32	*mitochondrial ribosomal protein L32* [Source: HGNC Symbol; Acc: HGNC:14035]	-0.085	No
NDUFA7	*NADH: ubiquinone oxidoreductase subunit A7* [Source: HGNC Symbol; Acc: HGNC:7691]	-0.095	No
MRPS30	*mitochondrial ribosomal protein S30* [Source: HGNC Symbol; Acc: HGNC:8769]	-0.093	No
MRPL15	*mitochondrial ribosomal protein L15* [Source: HGNC Symbol; Acc: HGNC:14054]	-0.113	No
MRPL35	*mitochondrial ribosomal protein L35* [Source: HGNC Symbol; Acc: HGNC:14489]	-0.118	No
MRPS18A	*mitochondrial ribosomal protein S18A* [Source: HGNC Symbol; Acc: HGNC:14515]	-0.117	No
MRPL13	*mitochondrial ribosomal protein L13* [Source: HGNC Symbol; Acc: HGNC:14278]	-0.151	No
MRPL17	*mitochondrial ribosomal protein L17* [Source: HGNC Symbol; Acc: HGNC:14053]	-0.151	No
RPL7L1	*ribosomal protein L7 like 1* [Source: HGNC Symbol; Acc: HGNC:21370]	-0.151	No
MRPS22	*mitochondrial ribosomal protein S22* [Source: HGNC Symbol; Acc: HGNC:14508]	-0.160	No
MRPL30	*mitochondrial ribosomal protein L30* [Source: HGNC Symbol; Acc: HGNC:14036]	-0.163	No
MRPL3	*mitochondrial ribosomal protein L3* [Source: HGNC Symbol; Acc: HGNC:10379]	-0.196	No
MRPL2	*mitochondrial ribosomal protein L2* [Source: HGNC Symbol; Acc: HGNC:14056]	-0.196	No
MRPS7	*mitochondrial ribosomal protein S7* [Source: HGNC Symbol; Acc: HGNC:14499]	-0.198	No
MRPS5	*mitochondrial ribosomal protein S5* [Source: HGNC Symbol; Acc: HGNC:14498]	-0.198	No
MRPL18	*mitochondrial ribosomal protein L18* [Source: HGNC Symbol; Acc: HGNC:14477]	-0.340	No
MRPL16	*mitochondrial ribosomal protein L16* [Source: HGNC Symbol; Acc: HGNC:14476]	-0.340	No
MRPL28	*mitochondrial ribosomal protein L28* [Source: HGNC Symbol; Acc: HGNC:14484]	-0.341	No

MRPL22	*mitochondrial ribosomal protein L22* [Source: HGNC Symbol; Acc: HGNC:14480]	-0.341	No
MRPL36	*mitochondrial ribosomal protein L36* [Source: HGNC Symbol; Acc: HGNC:14490]	-0.342	No
MRPL37	*mitochondrial ribosomal protein L37* [Source: HGNC Symbol; Acc: HGNC:14034]	-0.342	No
MRPL34	*mitochondrial ribosomal protein L34* [Source: HGNC Symbol; Acc: HGNC:14488]	-0.342	No
MRPL41	*mitochondrial ribosomal protein L41* [Source: HGNC Symbol; Acc: HGNC:14492]	-0.343	No
MRPL42	*mitochondrial ribosomal protein L42* [Source: HGNC Symbol; Acc: HGNC:14493]	-0.343	No
MRPL49	*mitochondrial ribosomal protein L49* [Source: HGNC Symbol; Acc: HGNC:1176]	-0.343	No
MRPL47	*mitochondrial ribosomal protein L47* [Source: HGNC Symbol; Acc: HGNC:16652]	-0.343	No
MRPL57	*mitochondrial ribosomal protein L57* [Source: HGNC Symbol; Acc: HGNC:14514]	-0.344	No
MRPL55	*mitochondrial ribosomal protein L55* [Source: HGNC Symbol; Acc: HGNC:16686]	-0.344	No
MRPS16	*mitochondrial ribosomal protein S16* [Source: HGNC Symbol; Acc: HGNC:14048]	-0.373	No
MRPS34	*mitochondrial ribosomal protein S34* [Source: HGNC Symbol; Acc: HGNC:16618]	-0.373	No
SRBD1	*S1 RNA binding domain 1* [Source: HGNC Symbol; Acc: HGNC:25521]	-0.471	No
MRPS21	*mitochondrial ribosomal protein S21* [Source: HGNC Symbol; Acc: HGNC:14046]	-0.577	No
RPL4	*ribosomal protein L4* [Source: HGNC Symbol; Acc: HGNC:10353]	-0.594	No
MRPL43	*mitochondrial ribosomal protein L43* [Source: HGNC Symbol; Acc: HGNC:14517]	-0.595	No
RSL24D1	*ribosomal L24 domain containing 1* [Source: HGNC Symbol; Acc: HGNC:18479]	-0.618	No
MRPL9	*mitochondrial ribosomal protein L9* [Source: HGNC Symbol; Acc: HGNC:14277]	-0.617	No

RPS7	*ribosomal protein S7* [Source: HGNC Symbol; Acc: HGNC:10440]	-0.625	No
MRPS14	*mitochondrial ribosomal protein S14* [Source: HGNC Symbol; Acc: HGNC:14049]	-0.627	No
RPL22	*ribosomal protein L22* [Source: HGNC Symbol; Acc: HGNC:10315]	-0.627	No
MRPL27	*mitochondrial ribosomal protein L27* [Source: HGNC Symbol; Acc: HGNC:14483]	-0.645	No
MRPL52	*mitochondrial ribosomal protein L52* [Source: HGNC Symbol; Acc: HGNC:16655]	-0.648	No
MRPL21	*mitochondrial ribosomal protein L21* [Source: HGNC Symbol; Acc: HGNC:14479]	-0.650	No
RPL21	*ribosomal protein L21* [Source: HGNC Symbol; Acc: HGNC:10313]	-0.658	No
MRPL1	*mitochondrial ribosomal protein L1* [Source: HGNC Symbol; Acc: HGNC:14275]	-0.657	No
RPL38	*ribosomal protein L38* [Source: HGNC Symbol; Acc: HGNC:10349]	-0.655	No
RPL12	*ribosomal protein L12* [Source: HGNC Symbol; Acc: HGNC:10302]	-0.664	No
MRPS33	*mitochondrial ribosomal protein S33* [Source: HGNC Symbol; Acc: HGNC:16634]	-0.658	No
MRPS11	*mitochondrial ribosomal protein S11* [Source: HGNC Symbol; Acc: HGNC:14050]	-0.657	No
MRPS15	*mitochondrial ribosomal protein S15* [Source: HGNC Symbol; Acc: HGNC:14504]	-0.651	No
MRPS31	*mitochondrial ribosomal protein S31* [Source: HGNC Symbol; Acc: HGNC:16632]	-0.651	No
MRPL54	*mitochondrial ribosomal protein L54* [Source: HGNC Symbol; Acc: HGNC:16685]	-0.654	No
MRPL10	*mitochondrial ribosomal protein L10* [Source: HGNC Symbol; Acc: HGNC:14055]	-0.671	**Yes**
MRPL19	*mitochondrial ribosomal protein L19* [Source: HGNC Symbol; Acc: HGNC:14052]	-0.667	**Yes**
RPS27L	*ribosomal protein S27 like* [Source: HGNC Symbol; Acc: HGNC:18476]	-0.660	**Yes**

DAP3	*death associated protein 3* [Source: HGNC Symbol; Acc: HGNC:2673]	-0.657	**Yes**
RPL23A	*ribosomal protein L23a* [Source: HGNC Symbol; Acc: HGNC:10317]	-0.653	**Yes**
RPL35	*ribosomal protein L35* [Source: HGNC Symbol; Acc: HGNC:10344]	-0.654	**Yes**
RPL39	*ribosomal protein L39* [Source: HGNC Symbol; Acc: HGNC:10350]	-0.648	**Yes**
RPL36	*ribosomal protein L36* [Source: HGNC Symbol; Acc: HGNC:13631]	-0.645	**Yes**
AC004086.1	*ribosomal protein L6* [Source: NCBI gene; Acc:6128]	-0.641	**Yes**
RPL14	*ribosomal protein L14* [Source: HGNC Symbol; Acc: HGNC:10305]	-0.631	**Yes**
RPL11	*ribosomal protein L11* [Source: HGNC Symbol; Acc: HGNC:10301]	-0.622	**Yes**
RPL15	*ribosomal protein L15* [Source: HGNC Symbol; Acc: HGNC:10306]	-0.615	**Yes**
MRPL20	*mitochondrial ribosomal protein L20* [Source: HGNC Symbol; Acc: HGNC:14478]	-0.607	**Yes**
RPS3	*ribosomal protein S3* [Source: HGNC Symbol; Acc: HGNC:10420]	-0.599	**Yes**
RPL29	*ribosomal protein L29* [Source: HGNC Symbol; Acc: HGNC:10331]	-0.590	**Yes**
MRPL51	*mitochondrial ribosomal protein L51* [Source: HGNC Symbol; Acc: HGNC:14044]	-0.581	**Yes**
RPL28	*ribosomal protein L28* [Source: HGNC Symbol; Acc: HGNC:10330]	-0.574	**Yes**
RPL19	*ribosomal protein L19* [Source: HGNC Symbol; Acc: HGNC:10312]	-0.568	**Yes**
RPL18	*ribosomal protein L18* [Source: HGNC Symbol; Acc: HGNC:10310]	-0.558	**Yes**
RPS5	*ribosomal protein S5* [Source: HGNC Symbol; Acc: HGNC:10426]	-0.553	**Yes**
RPL30	*ribosomal protein L30* [Source: HGNC Symbol; Acc: HGNC:10333]	-0.540	**Yes**

RPL22L1	*ribosomal protein L22 like 1* [Source: HGNC Symbol; Acc: HGNC:27610]	-0.528	**Yes**
RPS28	*ribosomal protein S28* [Source: HGNC Symbol; Acc: HGNC:10418]	-0.515	**Yes**
RPL10A	*ribosomal protein L10a* [Source: HGNC Symbol; Acc: HGNC:10299]	-0.501	**Yes**
MRPL33	*mitochondrial ribosomal protein L33* [Source: HGNC Symbol; Acc: HGNC:14487]	-0.488	**Yes**
RPS17	*ribosomal protein S17* [Source: HGNC Symbol; Acc: HGNC:10397]	-0.475	**Yes**
RPL24	*ribosomal protein L24* [Source: HGNC Symbol; Acc: HGNC:10325]	-0.461	**Yes**
RPS26	*ribosomal protein S26* [Source: HGNC Symbol; Acc: HGNC:10414]	-0.447	**Yes**
RPL36A	*ribosomal protein L36a* [Source: HGNC Symbol; Acc: HGNC:10359]	-0.433	**Yes**
RPS19	*ribosomal protein S19* [Source: HGNC Symbol; Acc: HGNC:10402]	-0.419	**Yes**
RPL8	*ribosomal protein L8* [Source: HGNC Symbol; Acc: HGNC:10368]	-0.405	**Yes**
RPS13	*ribosomal protein S13* [Source: HGNC Symbol; Acc: HGNC:10386]	-0.390	**Yes**
RPS11	*ribosomal protein S11* [Source: HGNC Symbol; Acc: HGNC:10384]	-0.376	**Yes**
RPS15A	*ribosomal protein S15a* [Source: HGNC Symbol; Acc: HGNC:10389]	-0.359	**Yes**
RPS27	*ribosomal protein S27* [Source: HGNC Symbol; Acc: HGNC:10416]	-0.343	**Yes**
MRPL14	*mitochondrial ribosomal protein L14* [Source: HGNC Symbol; Acc: HGNC:14279]	-0.325	**Yes**
RPS9	*ribosomal protein S9* [Source: HGNC Symbol; Acc: HGNC:10442]	-0.308	**Yes**
RPS14	*ribosomal protein S14* [Source: HGNC Symbol; Acc: HGNC:10387]	-0.291	**Yes**
RPL10L	*ribosomal protein L10 like* [Source: HGNC Symbol; Acc: HGNC:17976]	-0.273	**Yes**

RPS24	*ribosomal protein S24* [Source: HGNC Symbol; Acc: HGNC:10411]	-0.256	**Yes**
RPS23	*ribosomal protein S23* [Source: HGNC Symbol; Acc: HGNC:10410]	-0.238	**Yes**
RPS15	*ribosomal protein S15* [Source: HGNC Symbol; Acc: HGNC:10388]	-0.219	**Yes**
RPL35A	*ribosomal protein L35a* [Source: HGNC Symbol; Acc: HGNC:10345]	-0.198	**Yes**
RPL13	*ribosomal protein L13* [Source: HGNC Symbol; Acc: HGNC:10303]	-0.176	**Yes**
RPS4X	*ribosomal protein S4 X-linked* [Source: HGNC Symbol; Acc: HGNC:10424]	-0.154	**Yes**
RPS16	*ribosomal protein S16* [Source: HGNC Symbol; Acc: HGNC:10396]	-0.132	**Yes**
RPLP2	*ribosomal protein lateral stalk subunit P2* [Source: HGNC Symbol; Acc: HGNC:10377]	-0.109	**Yes**
RPL37A	*ribosomal protein L37a* [Source: HGNC Symbol; Acc: HGNC:10348]	-0.084	**Yes**
RPLP1	*ribosomal protein lateral stalk subunit P1* [Source: HGNC Symbol; Acc: HGNC:10372]	-0.058	**Yes**
MRPL46	*mitochondrial ribosomal protein L46* [Source: HGNC Symbol; Acc: HGNC:1192]	-0.030	**Yes**
RPS21	*ribosomal protein S21* [Source: HGNC Symbol; Acc: HGNC:10409]	0.000	**Yes**

Supplemental table 7: Genes included in the "GO_STRUCTURAL_CONSTITUENT_OF_RIBOSOME" gene set.

When "Yes" is indicated in column of core enrichment gene, it shows that the gene contributed to the increase in the absolute enrichment score. RUNNING ES shows the enrichment score at that time point. *: core enrichment gene.

Gene symbol	Gene name (from dataset)	RUNNING ES	*
APOD	*apolipoprotein D* [Source: HGNC Symbol; Acc: HGNC:612]	0.007	No
EIF2AK3	*eukaryotic translation initiation factor 2 alpha kinase 3* [Source: HGNC Symbol; Acc: HGNC:3255]	-0.090	No
RPL3	*ribosomal protein L3* [Source: HGNC Symbol; Acc: HGNC:10332]	-0.125	No
SURF6	*surfeit 6* [Source: HGNC Symbol; Acc: HGNC:11478]	-0.144	No
MCTS1	*MCTS1 re-initiation and release factor* [Source: HGNC Symbol; Acc: HGNC:23357]	-0.185	No
EIF2AK4	*eukaryotic translation initiation factor 2 alpha kinase 4* [Source: HGNC Symbol; Acc: HGNC:19687]	-0.197	No
HBA2	*hemoglobin subunit alpha 2* [Source: HGNC Symbol; Acc: HGNC:4824]	-0.211	No
RPL7L1	*ribosomal protein L7 like 1* [Source: HGNC Symbol; Acc: HGNC:21370]	-0.235	No
EIF2D	*eukaryotic translation initiation factor 2D* [Source: HGNC Symbol; Acc: HGNC:6583]	-0.306	No
EIF2A	*eukaryotic translation initiation factor 2A* [Source: HGNC Symbol; Acc: HGNC:3254]	-0.306	No
PPARGC1A	*PPARG coactivator 1 alpha* [Source: HGNC Symbol; Acc: HGNC:9237]	-0.374	No
HBA1	*hemoglobin subunit alpha 1* [Source: HGNC Symbol; Acc: HGNC:4823]	-0.433	No
GEMIN5	*gem nuclear organelle associated protein 5* [Source: HGNC Symbol; Acc: HGNC:20043]	-0.632	No
ZNF622	*zinc finger protein 622* [Source: HGNC Symbol; Acc: HGNC:30958]	-0.671	No
RPL4	*ribosomal protein L4* [Source: HGNC Symbol; Acc: HGNC:10353]	-0.676	No
RSL24D1	*ribosomal L24 domain containing 1* [Source: HGNC Symbol; Acc: HGNC:18479]	-0.702	No
RPS7	*ribosomal protein S7* [Source: HGNC Symbol; Acc: HGNC:10440]	-0.711	No

RPL22	*ribosomal protein L22* [Source: HGNC Symbol; Acc: HGNC:10315]	-0.717	No
NUFIP1	*nuclear FMR1 interacting protein 1* [Source: HGNC Symbol; Acc: HGNC:8057]	-0.739	No
FXR2	*FMR1 autosomal homolog 2* [Source: HGNC Symbol; Acc: HGNC:4024]	-0.738	No
RPL21	*ribosomal protein L21* [Source: HGNC Symbol; Acc: HGNC:10313]	-0.748	No
MRPL1	*mitochondrial ribosomal protein L1* [Source: HGNC Symbol; Acc: HGNC:14275]	-0.746	No
RPL38	*ribosomal protein L38* [Source: HGNC Symbol; Acc: HGNC:10349]	-0.742	No
LARP4	*La ribonucleoprotein domain family member 4* [Source: HGNC Symbol; Acc: HGNC:24320]	-0.742	No
RPL12	*ribosomal protein L12* [Source: HGNC Symbol; Acc: HGNC:10302]	-0.740	No
EIF4G1	*eukaryotic translation initiation factor 4 gamma 1* [Source: HGNC Symbol; Acc: HGNC:3296]	-0.755	No
RPS27L	*ribosomal protein S27 like* [Source: HGNC Symbol; Acc: HGNC:18476]	-0.775	**Yes**
RPL23A	*ribosomal protein L23a* [Source: HGNC Symbol; Acc: HGNC:10317]	-0.774	**Yes**
DDX3X	*DEAD-box helicase 3 X-linked* [Source: HGNC Symbol; Acc: HGNC:2745]	-0.769	**Yes**
RPL35	*ribosomal protein L35* [Source: HGNC Symbol; Acc: HGNC:10344]	-0.762	**Yes**
RPL39	*ribosomal protein L39* [Source: HGNC Symbol; Acc: HGNC:10350]	-0.753	**Yes**
RPL36	*ribosomal protein L36* [Source: HGNC Symbol; Acc: HGNC:13631]	-0.748	**Yes**
EIF2AK2	*eukaryotic translation initiation factor 2 alpha kinase 2* [Source: HGNC Symbol; Acc: HGNC:9437]	-0.738	**Yes**
AC004086.1	*ribosomal protein L6* [Source: NCBI gene; Acc:6128]	-0.729	**Yes**
RPL14	*ribosomal protein L14* [Source: HGNC Symbol; Acc: HGNC:10305]	-0.717	**Yes**

RPL11	*ribosomal protein L11* [Source: HGNC Symbol; Acc: HGNC:10301]	-0.705	**Yes**
RPL15	*ribosomal protein L15* [Source: HGNC Symbol; Acc: HGNC:10306]	-0.695	**Yes**
RPS3	*ribosomal protein S3* [Source: HGNC Symbol; Acc: HGNC:10420]	-0.687	**Yes**
RPL29	*ribosomal protein L29* [Source: HGNC Symbol; Acc: HGNC:10331]	-0.675	**Yes**
RPL28	*ribosomal protein L28* [Source: HGNC Symbol; Acc: HGNC:10330]	-0.666	**Yes**
RPL19	*ribosomal protein L19* [Source: HGNC Symbol; Acc: HGNC:10312]	-0.657	**Yes**
RPL18	*ribosomal protein L18* [Source: HGNC Symbol; Acc: HGNC:10310]	-0.643	**Yes**
RPS5	*ribosomal protein S5* [Source: HGNC Symbol; Acc: HGNC:10426]	-0.636	**Yes**
RPL30	*ribosomal protein L30* [Source: HGNC Symbol; Acc: HGNC:10333]	-0.619	**Yes**
RPL22L1	*ribosomal protein L22 like 1* [Source: HGNC Symbol; Acc: HGNC:27610]	-0.603	**Yes**
RPS28	*ribosomal protein S28* [Source: HGNC Symbol; Acc: HGNC:10418]	-0.586	**Yes**
RPL10A	*ribosomal protein L10a* [Source: HGNC Symbol; Acc: HGNC:10299]	-0.569	**Yes**
RPS17	*ribosomal protein S17* [Source: HGNC Symbol; Acc: HGNC:10397]	-0.552	**Yes**
RPL24	*ribosomal protein L24* [Source: HGNC Symbol; Acc: HGNC:10325]	-0.534	**Yes**
RPS26	*ribosomal protein S26* [Source: HGNC Symbol; Acc: HGNC:10414]	-0.517	**Yes**
RPL36A	*ribosomal protein L36a* [Source: HGNC Symbol; Acc: HGNC:10359]	-0.498	**Yes**
RPS19	*ribosomal protein S19* [Source: HGNC Symbol; Acc: HGNC:10402]	-0.480	**Yes**
RPL8	*ribosomal protein L8* [Source: HGNC Symbol; Acc: HGNC:10368]	-0.462	**Yes**

RPS13	*ribosomal protein S13* [Source: HGNC Symbol; Acc: HGNC:10386]	-0.443	**Yes**
RPS11	*ribosomal protein S11* [Source: HGNC Symbol; Acc: HGNC:10384]	-0.424	**Yes**
RPS15A	*ribosomal protein S15a* [Source: HGNC Symbol; Acc: HGNC:10389]	-0.403	**Yes**
RPS27	*ribosomal protein S27* [Source: HGNC Symbol; Acc: HGNC:10416]	-0.382	**Yes**
RPS9	*ribosomal protein S9* [Source: HGNC Symbol; Acc: HGNC:10442]	-0.359	**Yes**
RPS14	*ribosomal protein S14* [Source: HGNC Symbol; Acc: HGNC:10387]	-0.337	**Yes**
RPL10L	*ribosomal protein L10 like* [Source: HGNC Symbol; Acc: HGNC:17976]	-0.315	**Yes**
RPS24	*ribosomal protein S24* [Source: HGNC Symbol; Acc: HGNC:10411]	-0.293	**Yes**
RPS23	*ribosomal protein S23* [Source: HGNC Symbol; Acc: HGNC:10410]	-0.269	**Yes**
RPS15	*ribosomal protein S15* [Source: HGNC Symbol; Acc: HGNC:10388]	-0.245	**Yes**
RPL35A	*ribosomal protein L35a* [Source: HGNC Symbol; Acc: HGNC:10345]	-0.217	**Yes**
RPL13	*ribosomal protein L13* [Source: HGNC Symbol; Acc: HGNC:10303]	-0.190	**Yes**
RPS4X	*ribosomal protein S4 X-linked* [Source: HGNC Symbol; Acc: HGNC:10424]	-0.162	**Yes**
RPS16	*ribosomal protein S16* [Source: HGNC Symbol; Acc: HGNC:10396]	-0.133	**Yes**
RPLP2	*ribosomal protein lateral stalk subunit P2* [Source: HGNC Symbol; Acc: HGNC:10377]	-0.103	**Yes**
RPL37A	*ribosomal protein L37a* [Source: HGNC Symbol; Acc: HGNC:10348]	-0.072	**Yes**
RPLP1	*ribosomal protein lateral stalk subunit P1* [Source: HGNC Symbol; Acc: HGNC:10372]	-0.038	**Yes**
RPS21	*ribosomal protein S21* [Source: HGNC Symbol; Acc: HGNC:10409]	0.000	**Yes**

Supplemental table 8: Genes included in the "GO_CYTOSOLIC_RIBOSOME" gene set. When "Yes" is indicated in column of core enrichment gene, it shows that the gene contributed to the increase in the absolute enrichment score. RUNNING ES shows the enrichment score at that time point. *: core enrichment gene.

Gene symbol	Gene name (from dataset)	RUNNING ES	*
COL28A1	*collagen type XXVIII alpha 1 chain* [Source: HGNC Symbol; Acc: HGNC:22442]	-0.090	No
COL4A5	*collagen type IV alpha 5 chain* [Source: HGNC Symbol; Acc: HGNC:2207]	-0.142	No
COL16A1	*collagen type XVI alpha 1 chain* [Source: HGNC Symbol; Acc: HGNC:2193]	-0.152	No
COL27A1	*collagen type XXVII alpha 1 chain* [Source: HGNC Symbol; Acc: HGNC:22986]	-0.231	No
COL8A2	*collagen type VIII alpha 2 chain* [Source: HGNC Symbol; Acc: HGNC:2216]	-0.359	No
COL23A1	*collagen type XXIII alpha 1 chain* [Source: HGNC Symbol; Acc: HGNC:22990]	-0.377	No
COL11A2	*collagen type XI alpha 2 chain* [Source: HGNC Symbol; Acc: HGNC:2187]	-0.394	No
COL12A1	*collagen type XII alpha 1 chain* [Source: HGNC Symbol; Acc: HGNC:2188]	-0.402	No
COL4A4	*collagen type IV alpha 4 chain* [Source: HGNC Symbol; Acc: HGNC:2206]	-0.411	No
COL14A1	*collagen type XIV alpha 1 chain* [Source: HGNC Symbol; Acc: HGNC:2191]	-0.615	No
COL5A1	*collagen type V alpha 1 chain* [Source: HGNC Symbol; Acc: HGNC:2209]	-0.675	**Yes**
COL18A1	*collagen type XVIII alpha 1 chain* [Source: HGNC Symbol; Acc: HGNC:2195]	-0.645	**Yes**
COL5A2	*collagen type V alpha 2 chain* [Source: HGNC Symbol; Acc: HGNC:2210]	-0.646	**Yes**
COL6A6	*collagen type VI alpha 6 chain* [Source: HGNC Symbol; Acc: HGNC:27023]	-0.608	**Yes**
COL3A1	*collagen type III alpha 1 chain* [Source: HGNC Symbol; Acc: HGNC:2201]	-0.644	**Yes**
COL8A1	*collagen type VIII alpha 1 chain* [Source: HGNC Symbol; Acc: HGNC:2215]	-0.610	**Yes**
COL1A1	*collagen type I alpha 1 chain* [Source: HGNC Symbol; Acc: HGNC:2197]	-0.563	**Yes**

COL15A1	*collagen type XV alpha 1 chain* [Source: HGNC Symbol; Acc: HGNC:2192]	-0.524	**Yes**
COL6A3	*collagen type VI alpha 3 chain* [Source: HGNC Symbol; Acc: HGNC:2213]	-0.468	**Yes**
COL1A2	*collagen type I alpha 2 chain* [Source: HGNC Symbol; Acc: HGNC:2198]	-0.418	**Yes**
COL6A1	*collagen type VI alpha 1 chain* [Source: HGNC Symbol; Acc: HGNC:2211]	-0.352	**Yes**
COL4A1	*collagen type IV alpha 1 chain* [Source: HGNC Symbol; Acc: HGNC:2202]	-0.282	**Yes**
COL6A2	*collagen type VI alpha 2 chain* [Source: HGNC Symbol; Acc: HGNC:2212]	-0.210	**Yes**
COL6A5	*collagen type VI alpha 5 chain* [Source: HGNC Symbol; Acc: HGNC:26674]	-0.137	**Yes**
COL5A3	*collagen type V alpha 3 chain* [Source: HGNC Symbol; Acc: HGNC:14864]	-0.062	**Yes**
COL4A2	*collagen type IV alpha 2 chain* [Source: HGNC Symbol; Acc: HGNC:2203]	0.018	**Yes**

Supplemental table 9: Genes included in the "GO_EXTRACELLULAR_MATRIX_STRUCTURAL_CONSTITUENT_CONFERRING_TENSILE_STRENGTH" gene set.

When "Yes" is indicated in column of core enrichment gene, it shows that the gene contributed to the increase in the absolute enrichment score. RUNNING ES shows the enrichment score at that time point. *: core enrichment gene.

Acknowledgments

I'm most grateful to Professor Akihito Ishigami at Tokyo metropolitan institute of gerontology (TMIG) for continuous support on my research.

I would like to express my profound gratitude to Professor Toshiro Aigaki at Tokyo metropolitan university for many discussions on the research and for providing me with many opportunities and wisdom.

I would deeply appreciate Professor Shinichi Hashimoto and Assistant Professor Sadahiro Iwabuchi at Wakayama Medical University supporting in conducting and analyzing the scRNA-seq.

I give a special thanks to Ms. Haruka Sano at Tokyo Medical and Dental University for her great contribution to the preparation and publication of the paper as a co-author.

I also thank to all members of the Department of Molecular Aging Regulation at TMIG for their great guidance and support.